Structural Engineering Report No. 112

ULTIMATE STRENGTH OF TIMBER BEAM COLUMNS

by

T. M. OLATUNJI

J. LONGWORTH

November 1983

THE UNIVERSITY OF ALBERTA

ULTIMATE STRENGTH OF TIMBER BEAM COLUMNS

by

T.M. Olatunji,[1] and J. Longworth[2]

November 1983

Department of Civil Engineering

Edmonton, Alberta

---

[1]Graduate Student, Dept. of Civil Engineering, University of Alberta, Edmonton, Canada. On study leave from University of Ilorin, Nigeria.
[2]Professor of Civil Engineering, University of Alberta, Edmonton, Canada, T6G 2G7.

Acknowledgements

This investigation was made possible through a grant provided by the National Sciences and Engineering Research Council of Canada. The test specimens were donated by Western Archrib Ltd., Edmonton. Testing facilities were provided by the Department of Civil Engineering at the University of Alberta.

This report was originally prepared as a Master of Science thesis under the supervision of Prof. J. Longworth at the University of Alberta.

ABSTRACT

As timber design codes move from allowable stress design methods to limit states design, there is need to define the behaviour of timber members up to ultimate conditions. The present study is an investigation into the behaviour and ultimate strength of commercial grade Douglas-fir glued laminated timber beam-columns.

Approximate analytical procedures, based on an elasto-plastic compression and linear tension stress-strain distribution in tension, are used to predict ultimate strength. Interaction curves based on material properties obtained from small-scale tests are developed from the analyses.

The experimental program consisted of testing nine full-scale factory manufactured beam-columns, ten compression specimens and ten standard small-scale tension specimens. Variables investigated in the beam-column tests included slenderness ratio and magnitude of axial load. The behaviour of the beam-column specimens was monitored by measurements of lateral loads, cross-section strain distribution and lateral deflections.

Interaction curves derived from Newmark's numerical analysis procedure and modiified by an undercapacity factor of 0.7 are in good agreement with test results.

Table of Contents

List of Tables

List of Figures

List of Plates

List of Symbols

a	= depth of yielding from extreme compression fibre
a'	= depth of compression part still elastic(ac)
A	= cross sectional area
b	= width of rectangular cross-section
c	= distance to cendroidal axis
c'	=distance from extreme compression fibre to neutral axis
d	= depth
E	= modulus of elasticity of wood
I	= moment of inertia
L	= clear span of beam-column
L/d	= slenderness ratio
M	= moment
Mext	= external moment
Mint	= internal moment
M_o	= applied moment
$(M_o)max$	= maximum applied moment
M_y	= yield moment
P	= axial load
P_e	= Euler critical load
P_y	= yield load
Q	= lateral load
S	= section modulus
w	= deflection

α = ratio of yield strain to ultimate strain

δ = deflection at midspan

ϵ_c = compression strain

ϵ_t = tension strain

ϵ_{yc} = compression yield strain

ϵ_{uc} = ultimate compression strain

ϵ_{ut} = ultimate tension strain

θ = rotation about z-axis

θ_o = end rotation

λ = ratio of ultimate compression stress to ultimate tension stress

σ = axial or bending stress

σ_{yc} = compression yield stress

σ_{ut} = ultimate compression stress

σ = ultimate tension stress

ϕ = curvature

ϕ_m = maximum curvature

ϕ_y = yield curvature

1. INTRODUCTION

1.1 General Remarks

Glued-laminated timber columns are frequently subjected to situations where continuity conditions and effects of lateral forces such as wind impose significant moment in addition to axial loads. Presently in Canada, timber beam-columns are designed according to the Code for Engineering Design in Wood, CAN3-086-M80', which is an allowable stress code. The current move towards a limit states code requires an understanding of the behaviour of these members up to ultimate conditions.

A number of investigators have focussed on the strength of timber columns subjected to axial load with small eccentricities. Relatively few studies have related to the interaction diagram approach to design of beam-columns based on ultimate conditions.

1.2 Object and Scope

The main objectives of this investigation are:

1. To develop analytical procedures which predict ultimate strength of timber beam-columns.
2. To carry out preliminary testing on commercial grade glued-laminated timber beam-columns to observe their behaviour and ultimate capacity.
3. To establish a basis for further studies on ultimate strength of timber beam-columns.

2. LITERATURE REVIEW

2.1 Previous Research

Comparatively little research has been conducted on timber members subjected to combined axial load and bending moment. In 1954, Pearson[2] investigated the effects of species, slenderness ratio, eccentricity of load and orientation of growth rings on the strength of solid timber columns. Over 400 specimens were tested, including more than 250 eccentrically loaded columns. Slenderness ratio (L/d) ranged from 5 to 50 with eccentricity to depth ratio of 0 to 0.5. Based on the test results, a modification of Jezek's formula (through Pearson, 1954) was proposed for calculating the maximum strength of eccentrically loaded columns. Pearson also compared his test results with the predictions based on the modified secant formula. The test results were found to be in much closer agreement with the modified secant formula when the eccentricities were small than when they were large.

Wood[3], in 1961, presented formulae for calculating the safe capacity of timber columns with lateral loads and eccentric axial load. The formulae were essentially those developed by Newlin (through Wood, 1961), but included some extensions and applications to design problems. Wood assumed that the maximum stress developed under combined load was equal to the flexural strength. For columns having a slenderness ratio, L/d, of 11 or less (short members), an

interaction equation for the general case of eccentric axial load and lateral load was derived. For long columns, having L/d of 20 or more, a model column with initial cosine wave curvature was used. By assuming a small curvature, a general interaction equation for this case was also derived. It was then suggested that a linear interpolation be used for calculating the capacities of columns in the intermediate slenderness range i.e. L/d between 11 and 20.

In 1970, Hammond, Curtis, Sidebottom and Benjamin[5] studied the effect of eccentricity and end restraints on the strength of timber columns. The stress-strain diagram obtained from simple tension and compression as shown in Figure 2.1(a) was idealized as elasto-plastic in compression and linear in tension as in Figure 2.1(b). Expressions were derived for the axial load P, and bending moment M, expressed as functions of the cross-section and the depth of yielding. Interaction curves were then obtained for various depths of yielding. Curvature at a given section was determined from the strain distribution in terms of bending moment and depth of yielding. By assuming the deflected shape as a sine curve, and linear elastic end restraints, the expression for the eccentricity was obtained. The collapse load was then obtained by trial and error, given the eccentricity and the depth of yielding as shown in Fig. 2.2. Theoretical curves relating end constraint, column eccentricity to depth ratio, column length to depth ratio, and average fibre stress were derived from the analysis,

thus simplifying the design of such columns. Hammond et al tested 54 solid timber columns with eccentricity to depth ratio of 0.1 to 10, three different elastic end restraints, and slenderness ratio of about 80 to 200. The test results were reported to be in good agreement with the theoretical curves.

Zakic[9], in 1975, provided mathematical solutions for timber members subjected to bending moment plus compressive axial force and bending moment plus tensile axial force. He derived interaction equations for elastic and inelastic behaviour in both cases. Parabolic compression and linear tension stress-strain curves shown in Figure 2.3, derived in his earlier research[4], were used. Zakic made use of certain limiting stresses at impending yield, i.e. $\sigma_{yc}=0.5\sigma_{uc}$ where σ_{yc} is the compression stress at yield and σ_{uc} is the ultimate compression stress. Adopting the mathematical equations for the stress diagram proposed by Moe (through Zakic, 1979), non-linear interaction equations were developed for inelastic beam-column behaviour. Zakic reported 15 full-scale glue-laminated beam-column tests. The test specimens were simply supported, and two symmetrically placed concentrated lateral loads were applied. The interaction curve obtained from the test results was in good agreement with the theoretically predicted curve.

In 1979, Larsen and Theiglaard[10] derived theoretical capacities for the general case of beam-columns subjected to equal end moments, with initial double curvature and initial

torsion. The initial curvature and torsion were assumed to be represented by cosine functions; and the failure condition was assumed to be a linear interaction of compression and bending stresses. These assumptions were used to solve the general differential equations, leading to an expression for the total loading capacity. The general expression was later specialized for cases of combined axial load and in-plane bending moment or pure in-plane bending alone. Larsen and Theiglaard's experimental program consisted of tests of 39 specimens employing different material grades, cross-sections and lengths. For the case of in-plane bending and axial load, plumb-line measurements of initial displacement and stress ratios from the Danish Code (through Larsen et al, 1979) were used to obtain the ultimate moment. Close agreement between the measured and calculated ultimate moments was reported. Approximate expressions and design curves were presented for use in designing members for the cases investigated. It was noted that column capacity was not only affected by the slenderness ratio, but also by the depth to breadth ratio; and that the capacity was least for square columns.

Malhotra'', in 1982, developed a mathematical model for the analysis of timber members subjected to compression loads with small eccentricities. The analysis was based on Jezek's simplification of an ideal elasto-plastic stress-strain relationship in compression and a linear relationship in tension. The axis of the deflected column

was assumed to take the form of a half sine wave . Equilibrium conditions were established at the column mid-height to obtain the critical column stress as a function of slenderness ratio and eccentricity to depth ratio. Malhotra's test program involved over 350 columns with eccentricity to depth ratio from 0.1 to 0.3, and slenderness ratios ranging from 40 to 160. Most columns were pin-ended, but a few were flat-ended. The test results were compared with the modified secant equation and the Perry-Robertson's formula. It was found that the experimental results were in good agreement with Malhotra's model based on Jezek's approach and also with the modified secant formula. Malhotra proposed a semi-rational approach for the design of columns subjected to axial load and small eccentricities.

2.2 Present Code Requirements and General Comments

CAN3-086-M80 Code for Engineering Design in Wood' is a working stress design code. Its requirements for members subjected to combined axial load and bending moment are based on a linear interaction equation given by:

$$\frac{P/A}{a} + \frac{M/S}{F} \leq 1 \qquad (2.1)$$

where P is the concentrated axial load, A is the area of cross-section, a is the allowable unit stress in tension or compression that would be permitted if axial load only

existed, taking into account the slenderness ratio and the duration of load factor. M is the total bending moment, including the moment due to axial load, S is the section modulus; F is the allowable unit stress in bending that would be permitted if bending only existed, and modified for the duration of load.

Some researchers[3,9,11], have suggested that a linear interaction equation, based on the ultimate strength of timber beam-columns, is conservative. Larsen and Theiglaard [10] reported slightly unconservative results when comparing the linear interaction diagram with strength based on assumed initial displacements. However, considering the variation in the properties of structural timber, the linear interaction was considered acceptable.

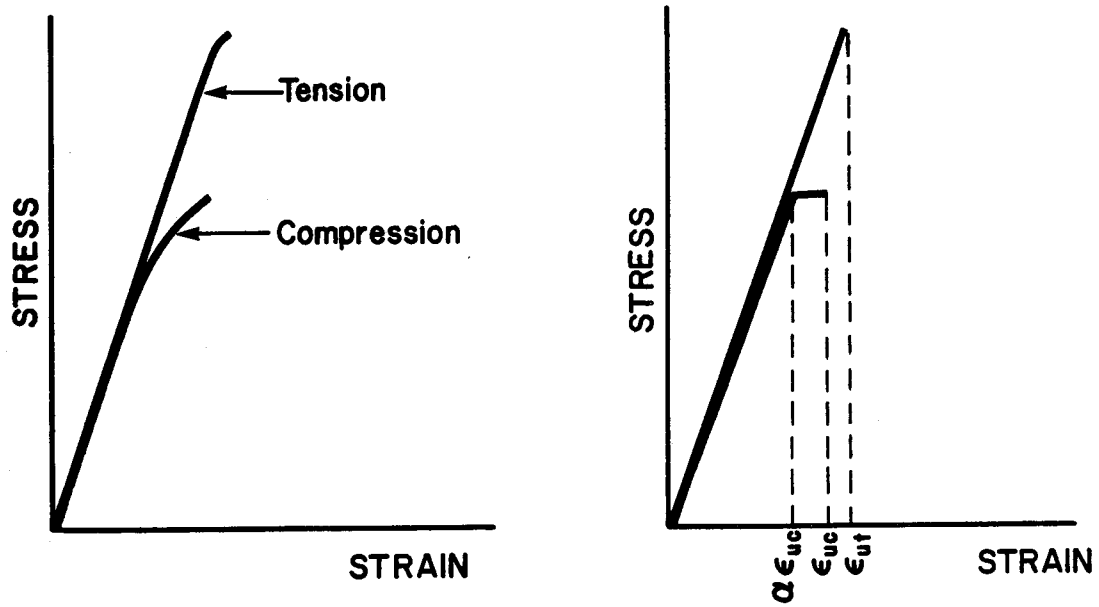

Figure 2.1 Stress-Strain Diagrams in Direct Tension and Compression

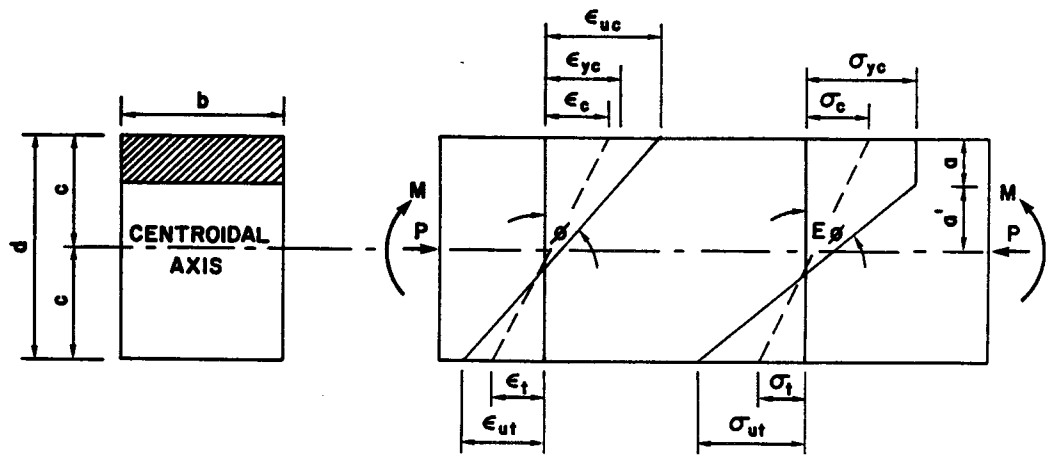

Figure 2.2 Strain and Stress Distributions

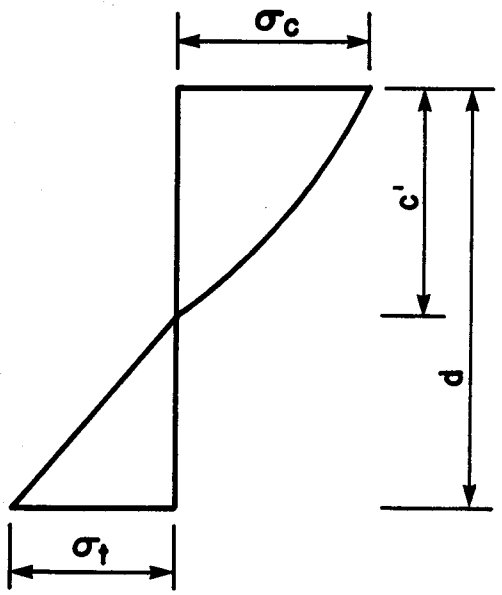

Figure 2.3 Parabolic Compression Linear Tension Stress Distribution

3. ANALYSIS

3.1 Introduction

Three analytical procedures may be adapted to the case of timber beam-columns of rectangular cross-section; namely the method of assumed deflected shape of beam-column, Newmark's numerical integration procedure, and the moment magnifier method. The following assumptions are common to the the first two methods:

1. Strains are linearly distributed across a section subjected to bending moment and compressive axial load.
2. The stress-strain characteristics for wood in direct compression and tension are available for a given moisture content.
3. The stress-strain diagram in compression is idealised as elatic-perfectly plastic.
4. Modulus of elasticity is the same in tension and compression.
5. Failure criterion is based on attainment of the ultimate strain in compression at the extreme compression fibre of the section. Thus the failure sequence is plastic compression-splitting tension.
6. The behaviour of the beam-column is not affected by strength reducing defects.
7. Axial load and bending moments are in the plane of bending.
8. Shear forces are neglected.

9. Columns are initially straight.

Figures 2.1 shows typical stress-strain diagrams in tension and compression, and the idealization of the compression stress-strain diagram. The stress-strain distribution, and the nomenclature used are shown in Figure 2.2.

Based on the above assumptions and a suitable deflected shape, interaction diagrams for any depth of yielding, slenderness ratio, and ultimate strains in compression and tension can be generated.

3.2 Method of Assumed Deflected Shape (Method 1)

To derive the interaction equation by this method[5], it is further assumed that the beam-column deflects in the form of a portion of a sine curve. Referring to Figure 2.2, if the axial thrust acting on the member is P, then

$$P = \int_A \sigma dA$$

or

$$P = b[\sigma_{yc} + 1/2\ \sigma_{ut}(d-a-a')]$$
$$= bd\sigma_{yc} + 0.5b(d-a)(\sigma_{yc}+\sigma_{ut})$$

where σ_{yc} is the yield stress in compression, σ_{ut} is the ultimate tensile stress, a' is the depth of yielding, a is the depth of the elastic portion in compression, b and d are the width and depth of the section respectively.

Equation (3.1) can be transformed into dimensionless form by dividing by the yield load in direct compression, P_y which is equal to $bd\sigma_{yc}$ to give

$$P/P_y = 1 - 0.5(1-a/d)(1+\sigma_{ut}/\sigma_{yc}) \qquad (3.1)$$

The bending moment M, on the cross-section is given by

$$\begin{aligned} M &= \int_A \sigma w dA \\ &= 0.5\sigma_{yc} ab(d-a) + 0.5\sigma_{yc} a'(d/2-a-a'/3) \\ &\quad + 0.5\sigma_{ut} b(d-a-a')[d/2-(d-a-a')/3] \end{aligned}$$

Simplifying and substituting $M_y = bd^2\sigma_{yc}/6$, the yield moment in pure compression, results in

$$M/M_y = (1-a/d)(1+\sigma_{ut}/\sigma_{yc})(0.5+a/d) \qquad (3.2)$$

Curvature

Since strains are small, from the stress diagram of Fig. 2.2,

$$\tan E\phi \simeq E\phi = \frac{(\sigma_{yc}+\sigma_{ut})}{(d-a)} \qquad (3.3)$$

The limiting curvature for elastic conditions, ϕ_y, is

$$\phi_y = \frac{M_y}{EI} = \frac{2\sigma_y}{Ed} \qquad (3.4)$$

From Equations (3.3) and (3.4)

$$\frac{\phi}{\phi_y} = \frac{(1+\sigma_{ut}/\sigma_{yc})}{(1-a/d)} \tag{3.5}$$

Substituting Equations (3.1) and (3.2) in (3.5) gives the following M-P-ϕ relationship:

$$\frac{\phi}{\phi_y} = \frac{4(1-P/P_y)^3}{[3(1-P/P_y)-M/M_y]^2} \tag{3.6}$$

Load Curvature Relationship

Based on a sine curve, the equation of the deflected shape is

$$y = \delta \sin \pi x/L$$

where y is the deflection at any given distance x from one end of the member of length L; and δ is the maximum deflection at midspan as shown in Figure 3.1. The curvature at midspan is defined as

$$\phi\ (L/2) = -y''(L/2) = \delta\pi^2/L^2$$

Using the expression for ϕ_y given in equation (3.4), gives

$$\frac{\phi_m}{\phi_y} = \frac{\pi^2 EI\ \delta}{L^2\ M_y}$$

where ϕ_m is the maximum curvature occurring at column midspan. Since $M_y=bd^2\sigma_y/6=P_yd/6$, and the Euler critical

load, $P = \pi^2 EI/L^2$, then

$$\frac{\phi_m}{\phi_y} = \frac{P_e 6\delta}{P_y d} \tag{3.7}$$

Equilibrium

From Equation (3.6), the internal moment can be written as

$$\frac{Mint}{M_y} = 3(1-P/P_y) - \frac{2(1-P/P_y)^{3/2}}{(\phi/\phi_y)^{1/2}} \tag{3.8}$$

The external moment at the maximum moment section (column midspan) can be written as

$$\frac{Mext}{M_y} = \frac{M_o + P\delta}{M_y} \tag{3.9}$$

where M_o is the moment due to applied loads. Substituting Equation (3.7) into Equation (3.8), and equating Mext=Mint yields

$$\frac{M_o + 6\delta\ P}{d\ P_y} = 3(1-P/P_y) - \frac{2(1-P/P_y)^{3/2}}{[6(\delta/d)(P_e/P_y)]^{1/2}} \tag{3.10}$$

Equation (3.10) defines the failure criterion.

Expression for δ/d

Equating Equations (3.5) and (3.7), for $\phi=\phi_m$ yields

$$\frac{(1+\sigma_{ut}/\sigma_{yc})}{2(1-a/d)} = \frac{6\delta\ P_e}{d\ P_y} \tag{3.11}$$

From equation (3.1)

$$1-a/d = \frac{2(1-P/P_y)}{(1+\sigma_t/\sigma_y)} \tag{3.12}$$

Thus

$$\frac{6\delta}{d} = \frac{(1+\sigma_t/\sigma_y)^2 P_y}{4(1-P/P_y)\ P_e} \tag{3.13}$$

Substituting Equation (3.13) into Equation (3.10) and simplifying yields the following interaction equation at midspan

$$\frac{M}{M_y} = 3(1-P/P_y) - \frac{4(1-P/P_y)^2}{(1+\sigma_t/\sigma_y)} - \frac{(1+\sigma_t/\sigma_y)^2 P}{4(1-P/P_y)\ P_e} \tag{3.14}$$

Again from equation (3.1),

$$\frac{\sigma_t}{\sigma_y} = \frac{2(1-P/P_y)}{(1-a/d)} - 1 \tag{3.15}$$

From the strain distribution of Fig. 2.2

$$\frac{a}{d} = \frac{\epsilon_{uc}(1-\alpha)}{\epsilon_{uc}+\epsilon_{ut}} = \frac{\sigma_{yc}(1-\alpha)}{\sigma_{yc}+\alpha\sigma_{ut}} \tag{3.16}$$

where ϵ_{uc} is the ultimate strain in compression ϵ_{ut} is the ultimate tension strain and α is the ratio of yield strain to ultimate strain. Substituting Equation (3.16) into

Equation (3.15) and setting $A=(1-P/P_y)$ and $\lambda=\sigma_{ut}/\sigma_{yc}$

$$a\lambda^2 + 2a(1-A)\lambda + (a-2A) = 0$$

from which

$$\lambda = (A-1) \pm \frac{a^2(A-1)^2 + a(2A-a)}{a} \qquad (3.17)$$

Noting that

$$\frac{P}{P} = \frac{P/P_y}{P_e/P_y}$$

and using $P_y=bda\epsilon$ E and $P=\pi^2EI/L^2$ and $I=bd^3/12$ then

$$P/P_y = \pi^2/[12(l/d)^2 a\epsilon_{yc}] \qquad (3.18)$$

Subtitution of equation (3.18) into equation (3.14) yields the final interaction equation as

$$\frac{M}{M_y} = 3(1-P/P_y) - \frac{4(1-P/P_y)}{(1+\sigma_{ut}/\sigma_{yc})} - \frac{(1+\sigma_{ut}/\sigma_{yc})}{4(1-P/P_y)} \times \frac{12P/P_y}{\pi^2}(L/d)^2 a\epsilon_{yc} \qquad (3.19)$$

Equations (3.17) and (3.19) can be used to generate interaction diagrams for any slenderness ratio and material properties.

3.3 Newmark's Numerical Integration Procedure (Method 2)

This method[5,9] uses a more precise deflection curve than the simple sine wave assumed in Method 1. It is, however, necessary to have a moment-thrust-curvature (M-P-ϕ)

relationship for the type of material and cross-section being analysed. The procedure is as follows:

1. The beam-column is divided into a number of equal segments.
2. Values of L/d and P are selected for investigation.
3. A low value of M_o is assumed.
4. A trial deflected shape is assumed.
5. Using P from Step (2), and M_o from Step (3), and the deflections from Step (4), bending moment is computed at the intermediate points in the span.
6. From an M-P-ϕ curve of the material and cross-section, curvature corresponding to the total moment is obtained.
7. A new deflected shape is computed by integrating the curvature twice, using Newmark's method as shown in Figure 3.2.
8. Steps (5), (6) and (7) are repeated with the new deflected shape until convergence to a fixed shape is obtained. Fig. 3.1 shows the computation procedure. If M_o does not exceed the maximum moment the member can carry, a satisfactory answer is obtained after 3 or 4 cycles.
9. Steps (3) through (8) are repeated with a new value of M_o
10. End slope θ_o, is computed for each M_o:

$$\theta_o = 4w_2/L \text{ ,}$$

where w_2 is the deflection at the second intermediate position in the span as shown in Figure 3.2.

11. The M_o-θ_o curve can then be drawn; or the highest value of M_o can be made as close to, but yet still somewhat below the actual value of $(M_o)max.$ desired. Fig. 3.3 shows a typical M_o-θ_o curve.

The above procedure was applied in this study with the following peculiarities:

1. A beam-column with four point lateral loading system was analysed as shown in Figure 3.1.
2. The beam-column was divided into eight equal segments.
3. The deflected shape for an elastic beam-column with equal end moments was used as a first approximation to the true deflected shape.
4. The axial load capacity for each slenderness ratio was obtained from the column curve.
5. M-P-ϕ curves obtained from material properties based on small-scale tests were employed, as shown in Figure 3.4.
6. The criterion for maximum moment was either the exceeding of ultimate moment or curvature, or divergence of deflection after 5 iterations.
7. The final deflected shape was obtained to an accuracy of about 5%.

3.4 Moment Magnifier Procedure (Method 3)

The moment magnifier method[5] is an approximate equation for the design of beam-columns. It is based on a linear interaction of axial load and moment accounting for additional moment due to axial load by a amplification

factor $1/(1-P/P_e)$. It is adapted to predict the ultimate strength of timber beam-column in the following form:

$$\frac{P}{P_y} + \frac{C_m M_o}{(1-P/P_e)M_y} = 1 \qquad (3.20)$$

where the various terms are as defined earlier, and C_m is a factor dependent on the distribution of the applied moment. For the type of loading investigated in this study C_m was taken as 1.0, as it was close to a uniformly distributed loading.

3.5 Computer Codings and Interaction Diagrams

In order to facilitate the tracing of the interaction curves, computer programs were written for each of the methods described above. These programs are placed in Appendices A1 through A3, corresponding respectively to Methods 1 through 3. Various values of material properties and slenderness ratios can be used to generate as many interaction diagrams as desired.

Interaction curves based on ultimate compression and tension strains of 0.0028mm/mm and 0.0032mm/mm respectively, a value of α of 0.864 and slenderness ratios of 10, 20, 30, and 40 for analysis Method 2 are shown in Figure 3.5. However, the material may possess more or less plasticity in compression and/or a different tensile strain limit at failure[8]. Analysis Method 2 is therefore examined for values

of a of 0.7, 0.8 and 0.9; and for tensile strains of 30%, 50%, 70% and 100% of ultimate, at a slenderness ratio of 20. Figure 3.6 indicate reduction in moment capacity as a decreases from 0.7 to 0.9. Figure 3.7 show decrease in moment capacity for P/P_y less than 0.3 as the tensile strain at failure is reduced from ultimate.

3.6 Comparison of Analysis Methods

Figure 3.8 shows interaction curves based on the three analysis methods for slenderness ratios of 10, 20 and 30. It is observed from the curves that Method 1 gives the highest predictions. Method 3 gives the least moment values. Method 2 seems to give moment values intermediate between the other two methods.

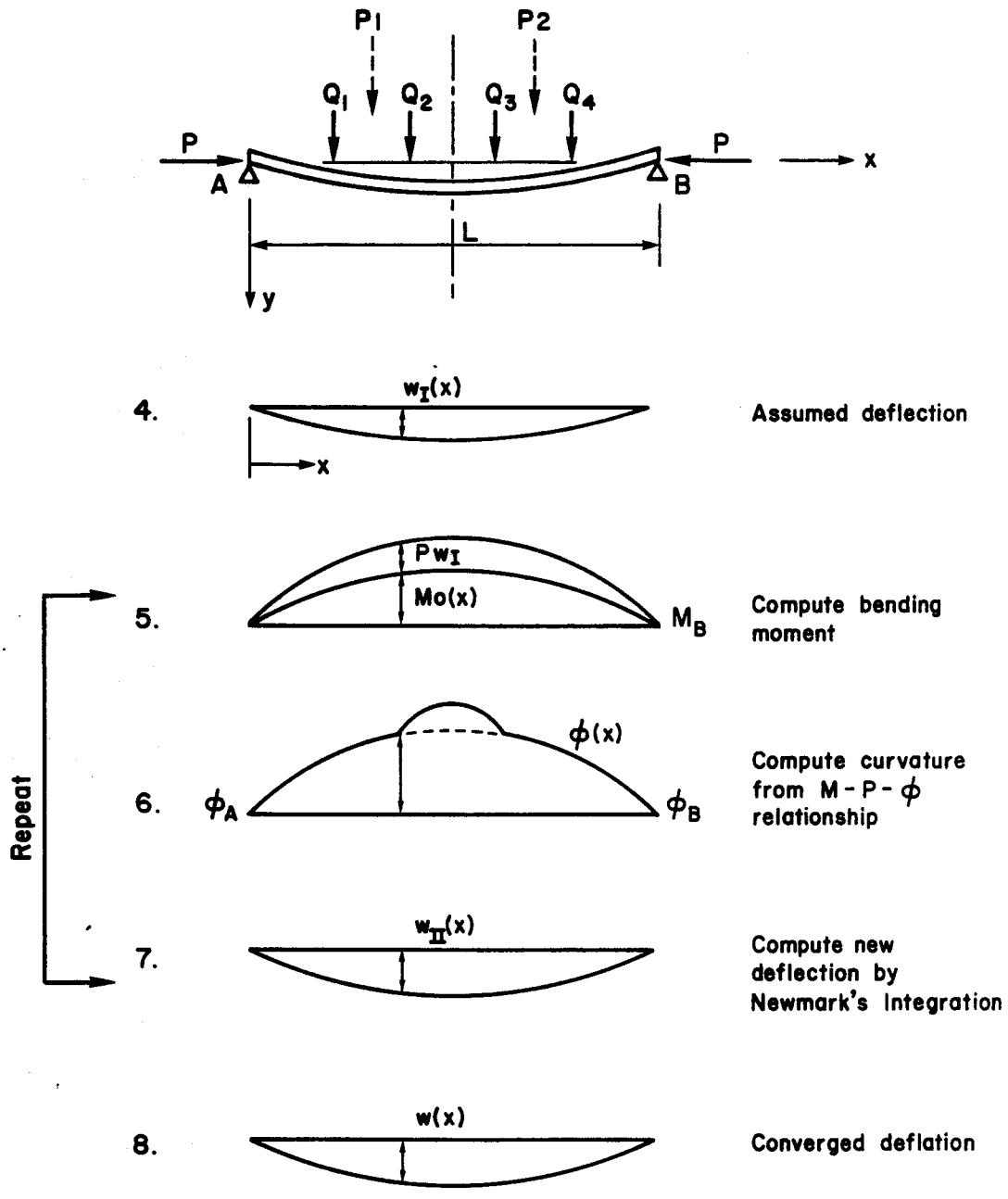

Figure 3.1 Computation Procedure for Beam-Column Deflection

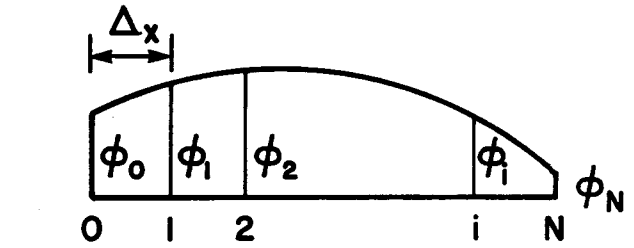

Curvature

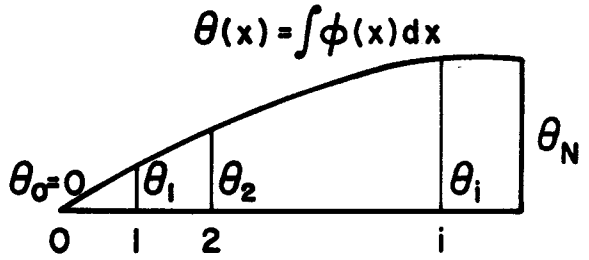

Slope

$$\theta_i = \sum_{k=\Delta}^{i} (\phi_k \Delta_x)$$

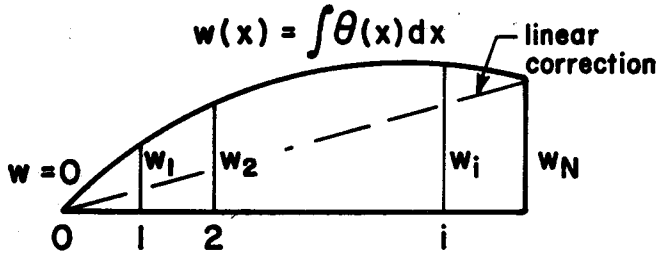

Deflection

$$w_i = \sum_{k=\Delta}^{i} (\theta_k \Delta_x)$$

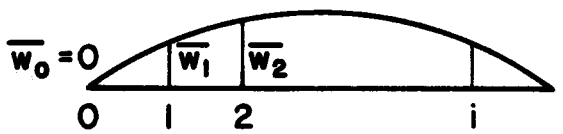

Corrected Deflection

$$\overline{w_i} = w_i - \frac{i}{N} w_N$$

Figure 3.2 Newmark's Integration Technique

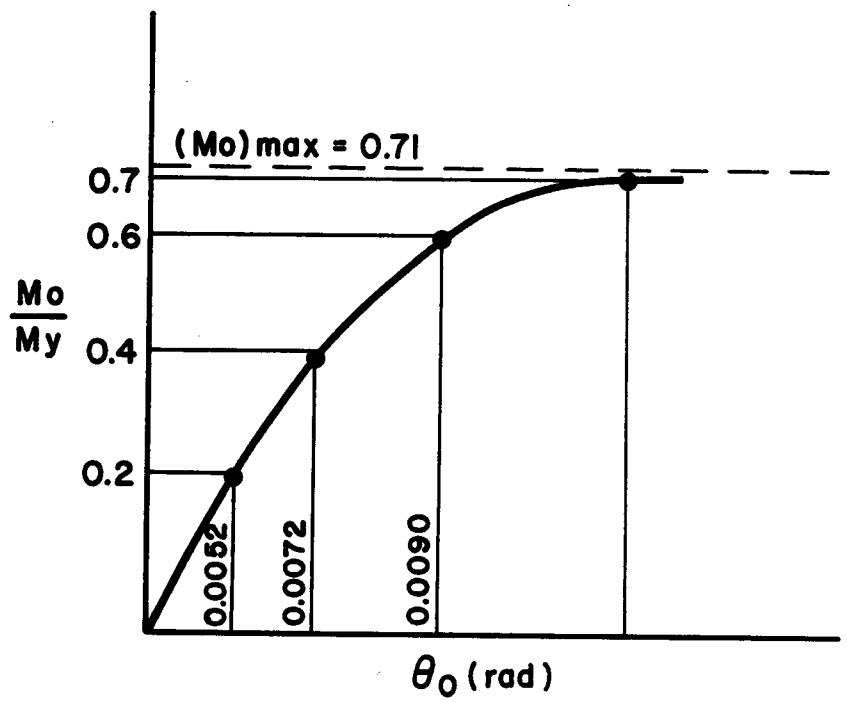

Figure 3.3 Sample Moment-Rotation Curve

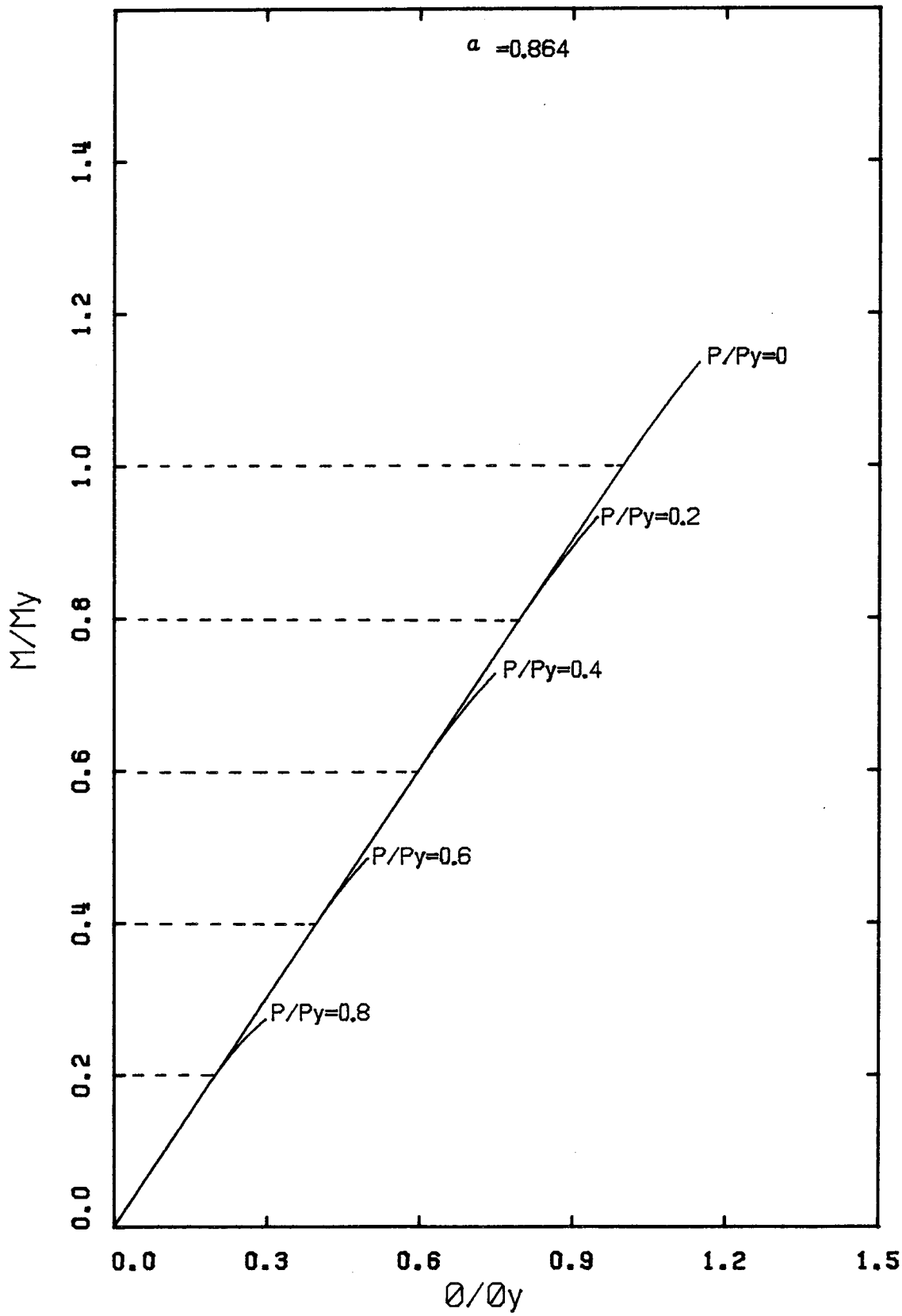

Figure 3.4 Moment-Curvature Curves for Timber Beam-Columns

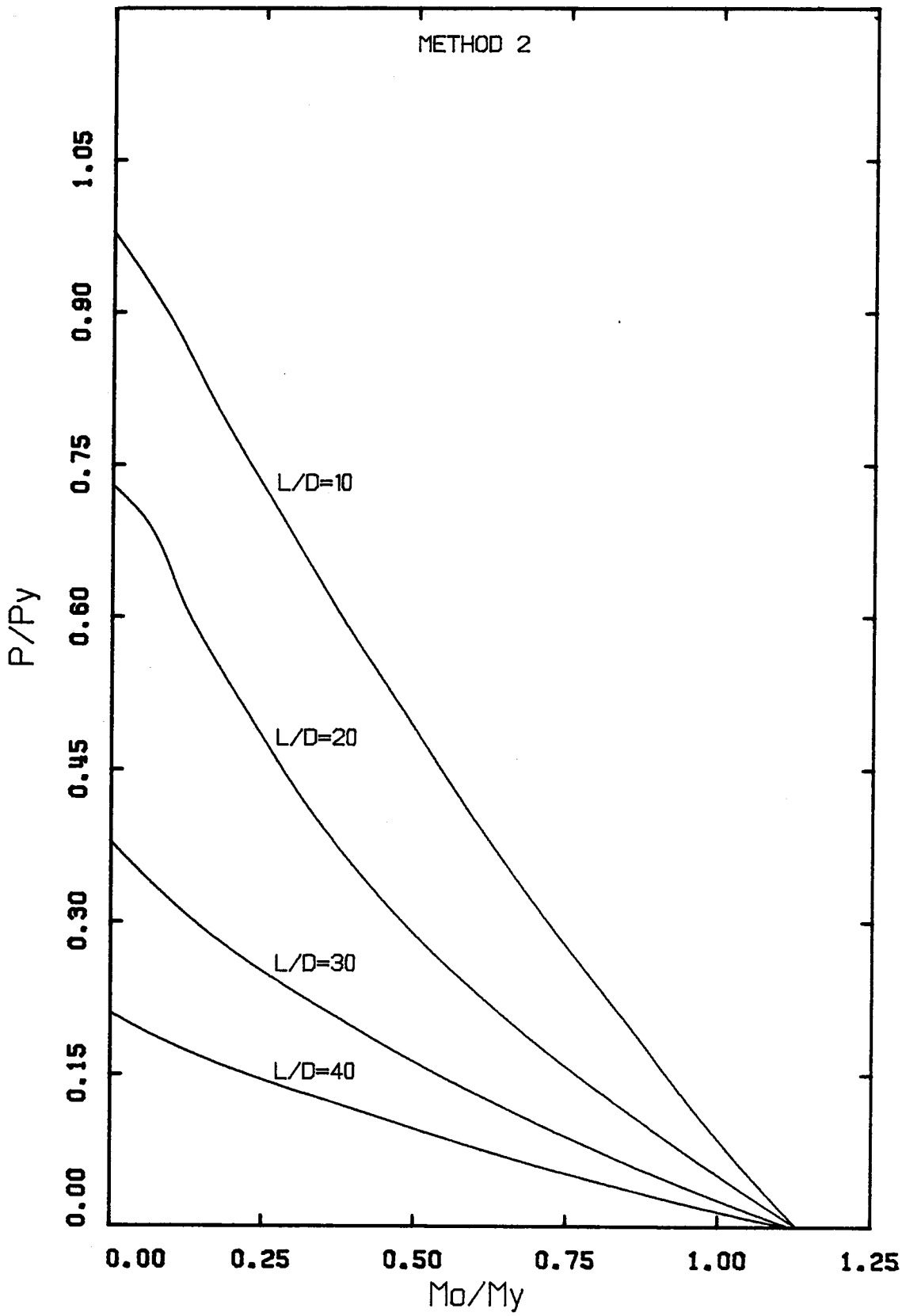

Figure 3.5 Interaction Curves for Timber Beam-Columns

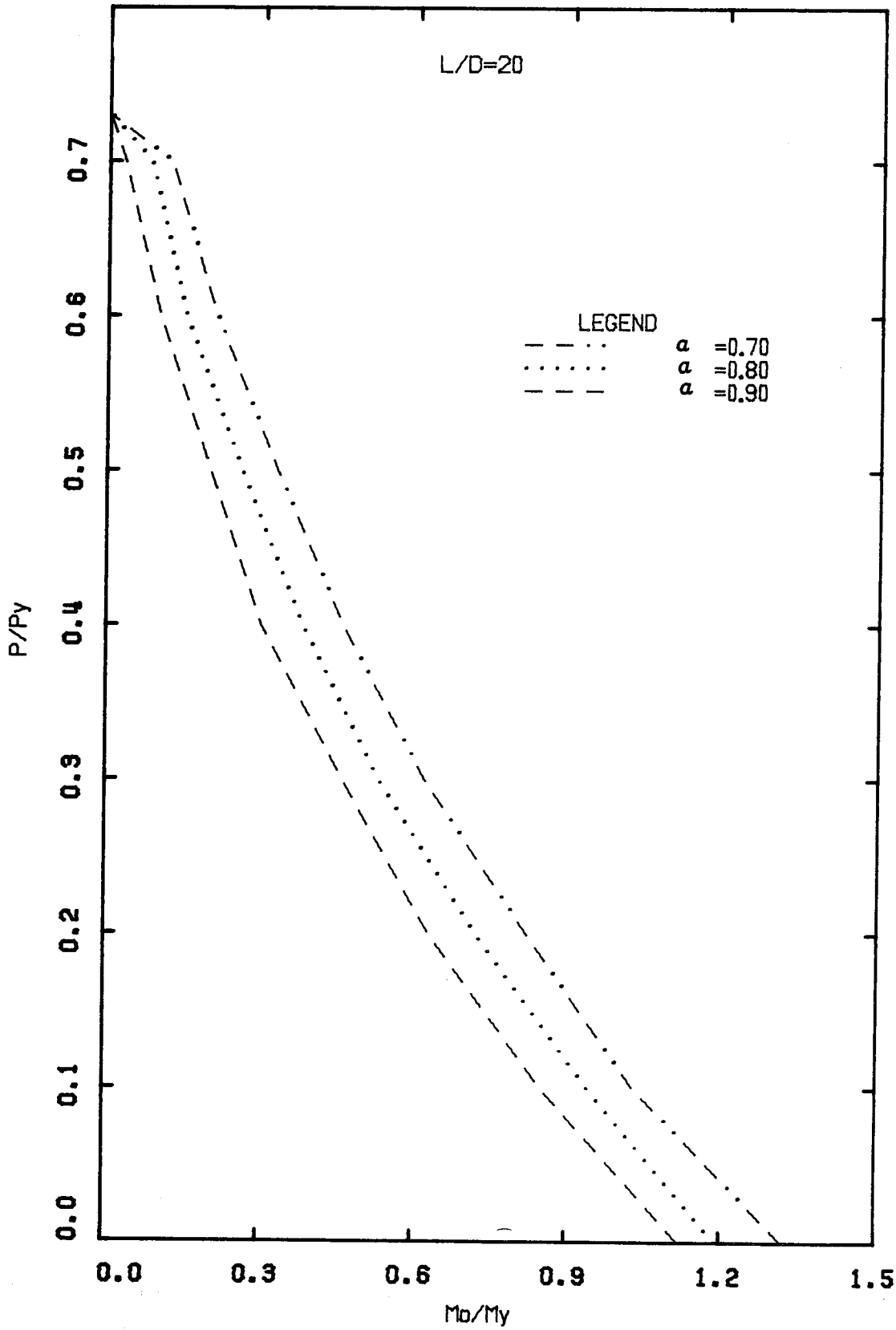

Figure 3.6 Interaction Curves for Various Depth of Yielding (Method 2)

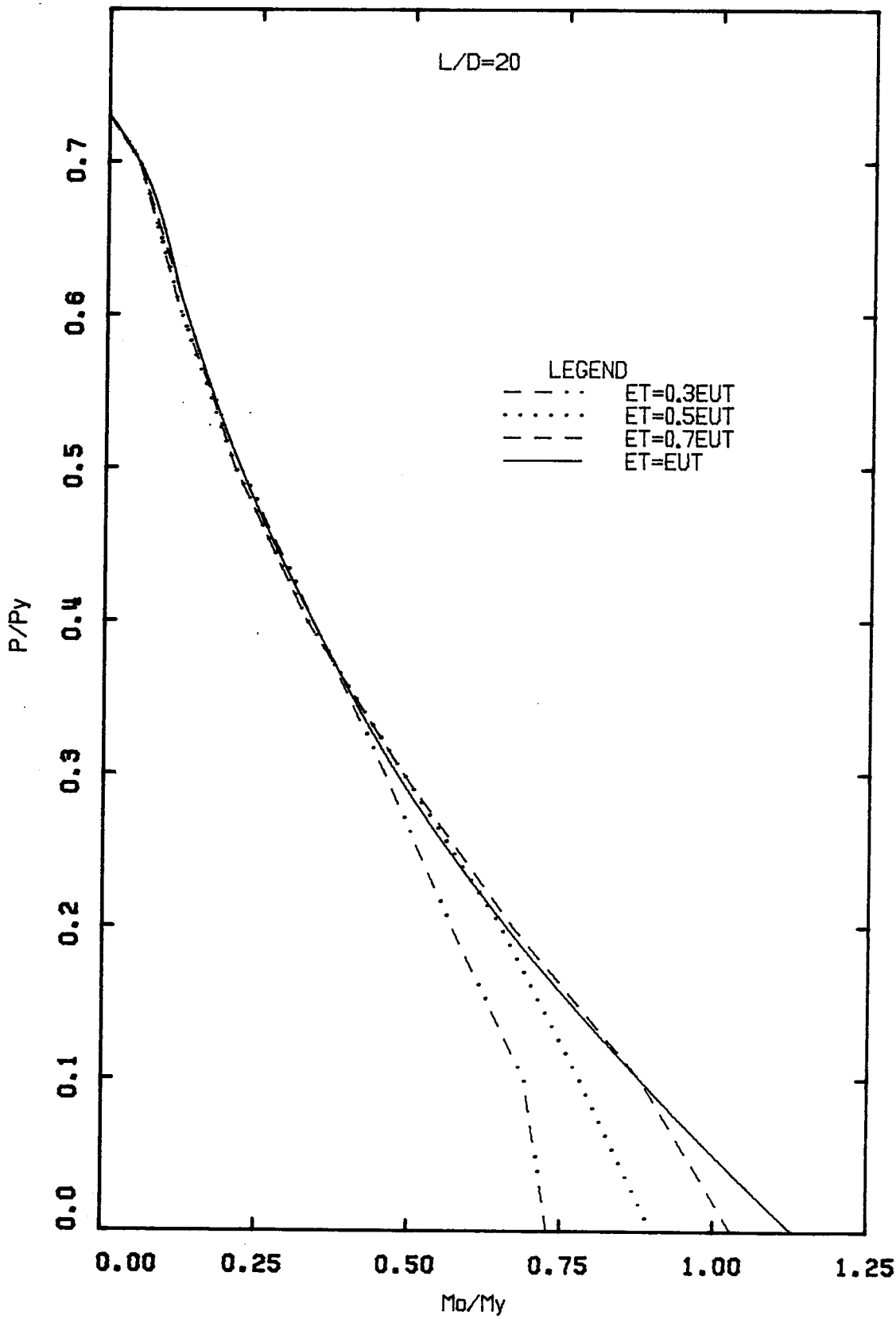

Figure 3.7 Interaction Curves for Various Tensile Strains (Method 2)

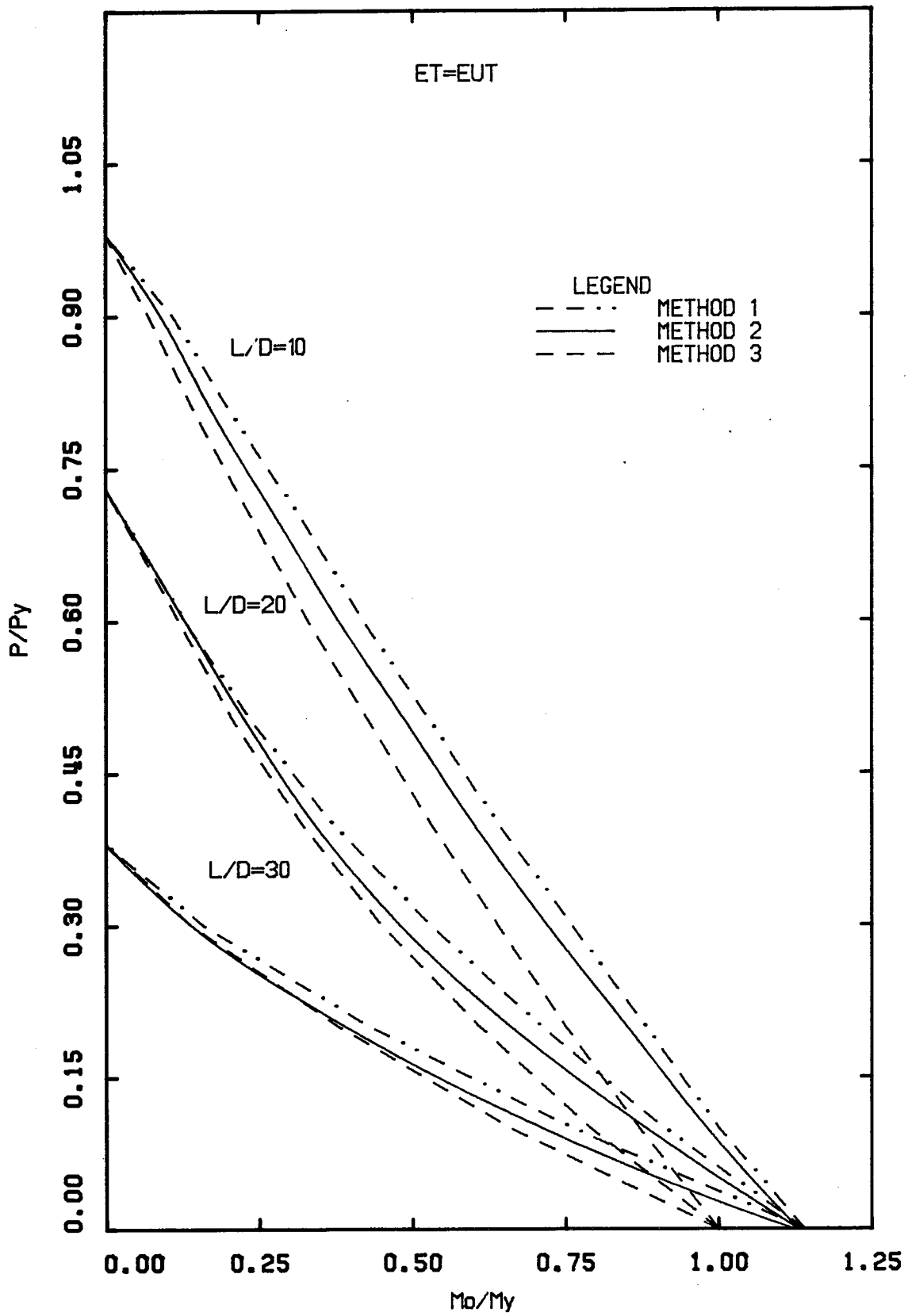

Figure 3.8 Interaction Curves Using Various Methods

4. EXPERIMENTAL PROGRAM

4.1 Test Specimens

4.1.1 Full Scale Specimens

A total of nine full-scale, factory manufactured beam-column specimens were tested. The test specimens were categorized into three series - A, B and C corresponding to three cross-section sizes: 175x152, 175x228 and 130x380. The resulting slenderness ratios (L/d) were 13, 22, and 33. Three specimens were tested in each series. Table 4.1 summarizes the properties of the specimens.

The specimens were fabricated in a plant certified under CSA Standard 0177-M81[13]. The specimens were 4990mm long. The laminations were 38mm thick and were of sufficient length so that no end jointing was required. Casco 1909 cold-setting casein glue, was used in glueing the laminations together. Shear block tests were performed to confirm the adequacy of the glue bond.

The material used in the beam-columns was Douglas fir-Larch, 16c-E grade in accordance with the requirements of CSA Standard 0122-M80[12]. The average modulus of elasticity, E, for all laminations equalled or exceeded the minimum of 12,400MPa required by the CSA Standard. Average moisture content for all laminations ranged from 7% to 12%.

4.1.2 Small Scale Specimens

Small scale specimens for establishing tension and compression strengths were fabricated from material cut from three pieces selected at random from the stock used for the beam-column specimens. Figure 4.1 shows the cutting pattern used to obtain the pieces required for 10 compression and 10 tension specimens. The details of the specimens, based on CSA and ASTM standards [12,14], are shown in Figures 4.2(a) and (b). The moisture content for all the small scale specimens ranged between 6% and 9%.

4.2 Test Set-Up

The beam-column specimens were tested in a horizontal test frame designed to provide reactions for the concentric axial load applied through a hydraulic jack, rated at 4,450kN maximum load. The test frame, shown in Figures 4.3 and 4.4, consisted of rolled wide flange sections in the longitudinal direction and built-up I-sections as cross members.

Transverse loads were applied at four points, symmetrically positioned with respect to the midspan of the specimen. The lateral loading system consisted of two HSS sections and high strength steel rods. These formed a yoke for applying pressure through load cells placed at positions P1 and P2 shown in Plate 4.1. Additional HSS sections were used as distributing beams to produce a four-point loading system on the specimen. 90kN capacity hydraulic jacks,

reacting against the laboratory floor slab at positions P1 and P2 applied loads to the loading yokes.

Two end support fixtures held the ends of the specimen in position. These fixtures transmitted axial load to the specimen through large capacity high strength steel rotation rollers, enclosed by machined steel plates. Reaction rollers placed under one of the steel plates allowed horizontal movement of the end of the specimen. Because of the positioning of the reaction rollers, temporary adjustable supports were provided; and also used as levelling devices for the specimen.

To prevent lateral-torsional buckling about the weak axis, lateral bracing was provided close to positions P1 and P2. The bracing system consisted of adjustable HSS sections acting as vertical guides to the specimen. These HSS sections were in turn braced against the main testing frame. Figure 4.5 shows a diagram of the loads acting on the specimen.

4.3 Instrumentation

Most measurements recorded during the tests were obtained by means of electronic equipment. Only the strain distribution on the cross-section was measured manually.

An electronic load cell calibrated to a maximum load of 2,600kN was used to measure the axial load. 160kN capacity load cells were used for measuring lateral loads. The accuracy of the load measurement is considered to be ±1%.

Deflections were measured by seven electronic linear, variable differential transformer (LVDT) transducers. A transducer was placed at each of the four lateral load points, one was placed at the midspan, and the remaining two were placed as close as possible to the end supports. These end transducers were used to monitor the effectiveness of the end supports and provided a means of measuring the end rotations by measurement of deflections.

Strains at midspan were obtained by means of a calibrated 125mm Demec gauge. Demec points were spaced at 25mm for the A and B series and at 40mm for the C series. Figure 4.6 shows a typical arrangement. Demec gauge readings were recorded manually. All the data from the load cells and transducers were fed directly into the NOVA Computer in the laboratory.

4.4 Test Procedure

The specimen was positioned in the end support fixture, and filler boards were placed at the ends to ensure full contact. Due attention was paid to proper alignment of the specimen to ensure concentric axial loading. Wood shims were used as necessary to bring the specimen to the required elevation.

The specimen was supported temporarily at midspan while the vertical loading apparatus was positioned. The LVDT's were positioned and Demec points were installed.

To ensure that the loading equipment was functioning properly, pre-test loads of approximately 10% of the maximum axial or estimated lateral loads were applied. The pre-test loads were then removed and any necessary adjustments were made. The test was then ready to begin.

An axial load of about 20kN was applied in order to hold the specimen in place while all temporary supports and keeper bars were removed. A set of readings was then taken.

The axial load was increased in increments of approximately one-fifth of the total axial load, with readings, except Demec readings, being taken at each increment. When the full axial load was reached, it was maintained for the remainder of the test. A complete set of readings was taken at this point. The lateral loads were then applied, also in increments of one-fifth their expected maximum value.

At each increment, the loads were allowed to stabilize before a set of readings was taken. However, due to the nature of the loading equipment (air driven motor hydraulic pumps) and specimen behaviour, it was difficult to maintain the load at a precisely constant level.

The behaviour of the specimen was monitored by plotting a lateral load versus midspan deflection curve as the test progressed. As soon as the specimen began to show significant non-linear behaviour, readings were taken more frequently. The Demec readings were discontinued at this stage. All specimens were tested to complete failure.

The test data were transmitted from the NOVA computer to the AMDAHL 470 computer for further processing.

Table 4.1 Properties of Beam-Column Specimens

Specimen No.	Nominal Size (mm)	Actual Size (mm)	Slenderness Ratio (L/d)	Cross Sectional Area $(mm^2)\times10^4$	Moment of Inertia $(mm^4)\times10^7$	Yield Load (kN)	Yield Moment (kN.m)	Euler Load (kN)
BCA1	175x152	171.0x152.5	33	2.61	5.05	1252	32.3	370
BCA2	175x152	170.5x151.5	33	2.58	4.94	1240	31.8	362
BCA3	175x152	170.8x151.2	33	2.58	4.92	1240	31.7	360
BCB1	175x228	170.6x227.8	22	3.89	16.81	1865	71.8	1231
BCB2	175x228	170.1x227.8	22	3.87	16.76	1860	71.8	1228
BCB3	175x228	170.5x228.8	22	3.90	17.02	1873	72.4	1247
BCC1	130x380	132.5x382.8	13	5.07	61.94	2435	157.6	4538
BCC2	130x380	126.8x381.6	13	4.84	58.72	2323	149.8	4302
BCC3	130x380	126.7x383.6	13	4.86	59.60	2333	151.3	4366

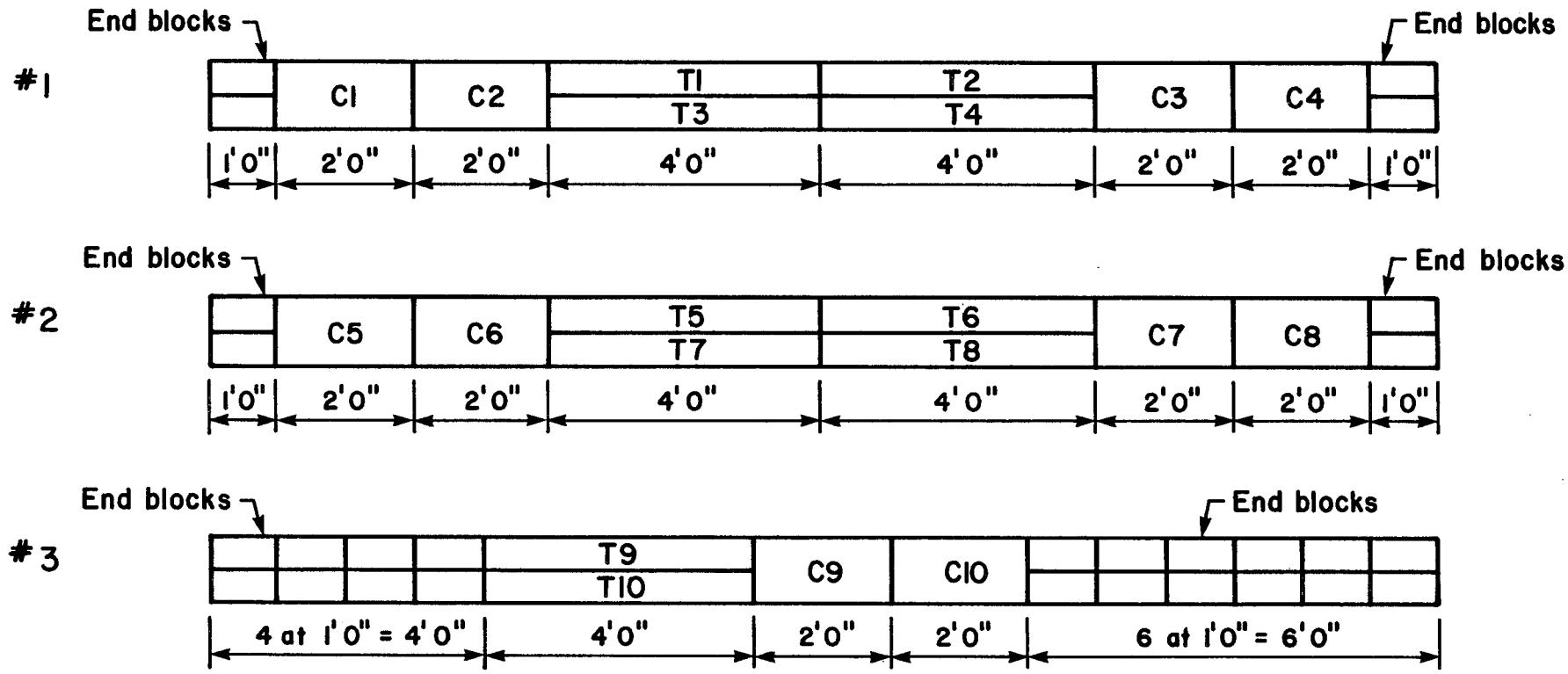

Figure 4.1 Cutting Pattern for Tension and Compression Specimens

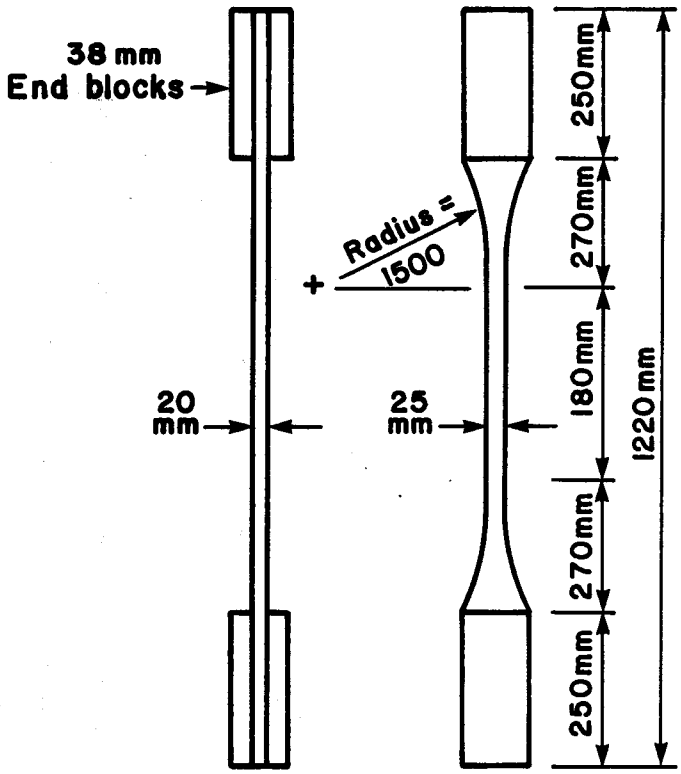

(a) Tension Specimen

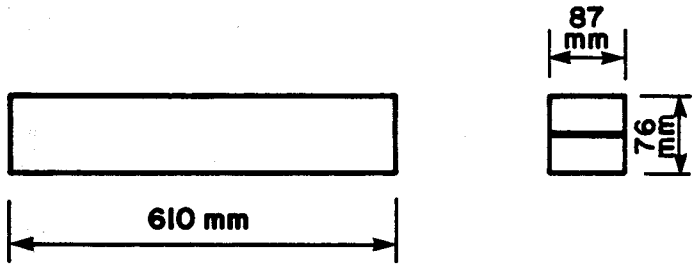

(b) Compression Specimen

Figure 4.2 Small-Scale Specimens

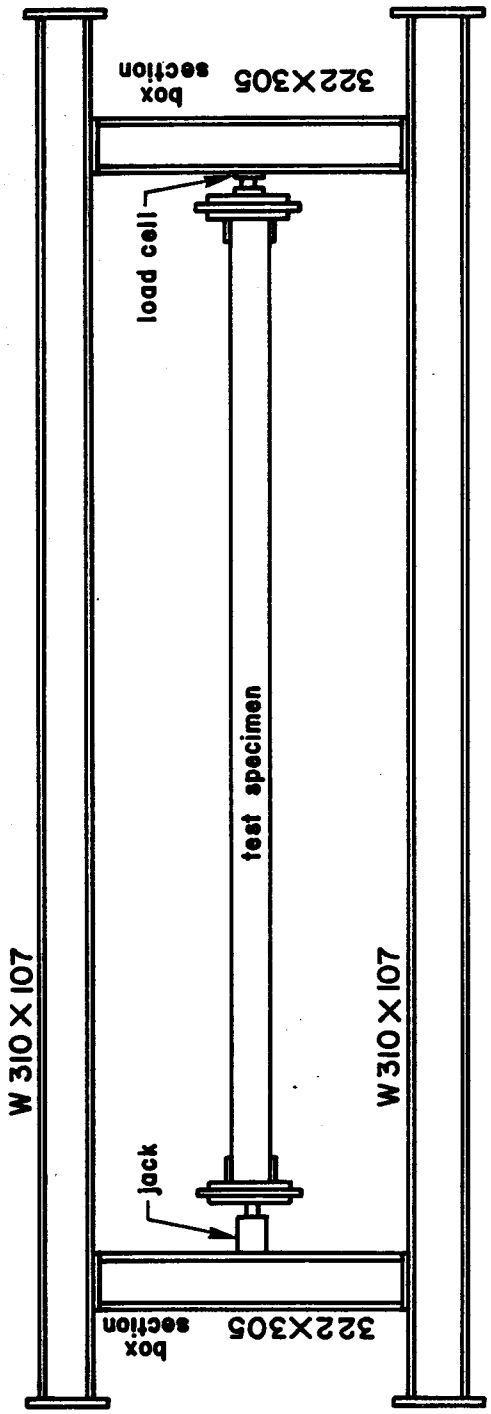

Figure 4.3 Plan View of Testing Frame

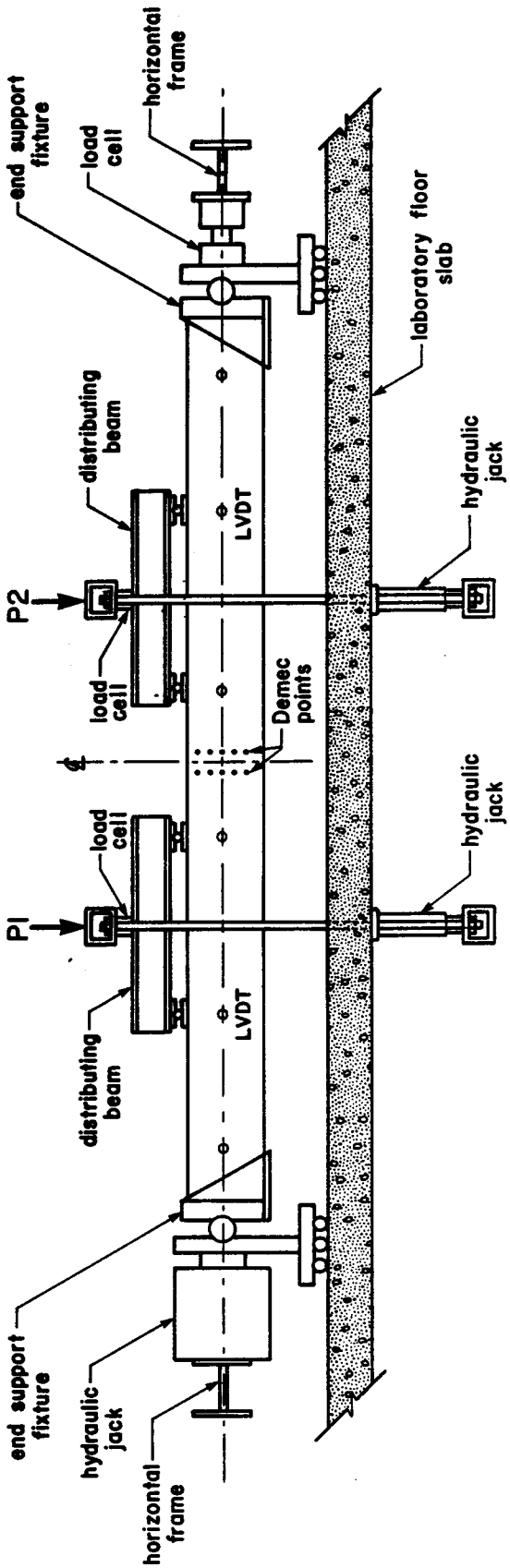

Figure 4.4 Idealized Test Set-Up and Instrumentation

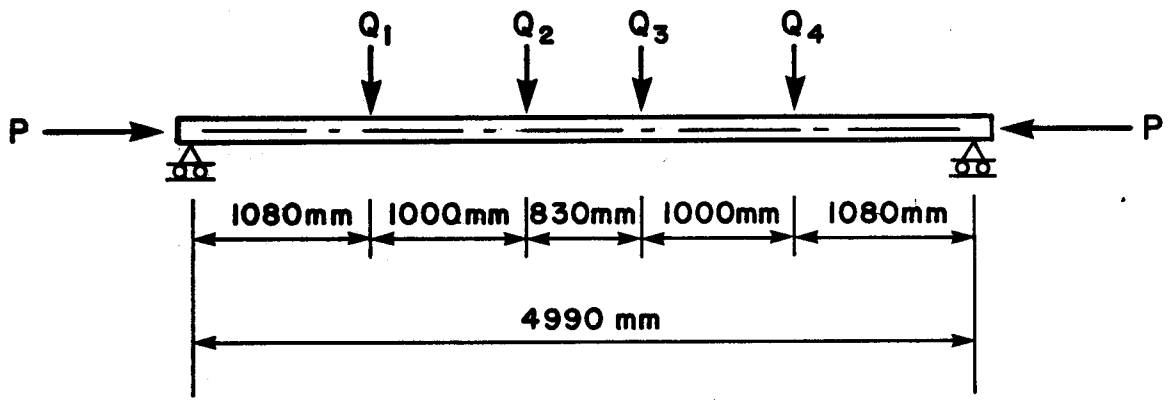

Figure 4.5 Beam-Column Loading

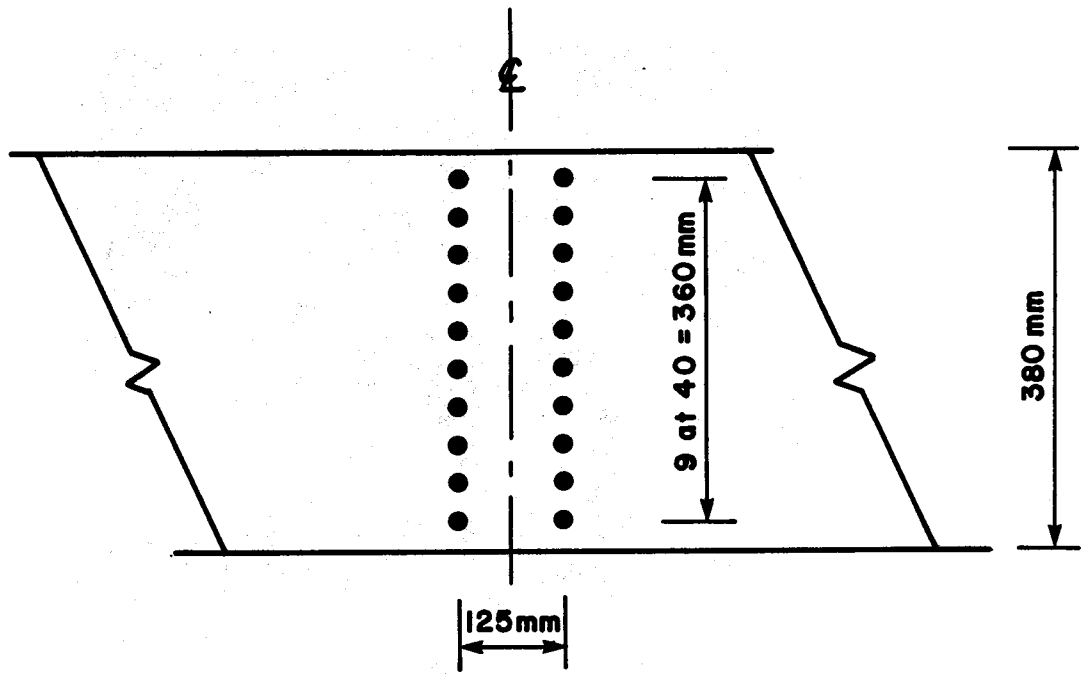

Figure 4.6 Demec Point Spacing on Series C Specimens

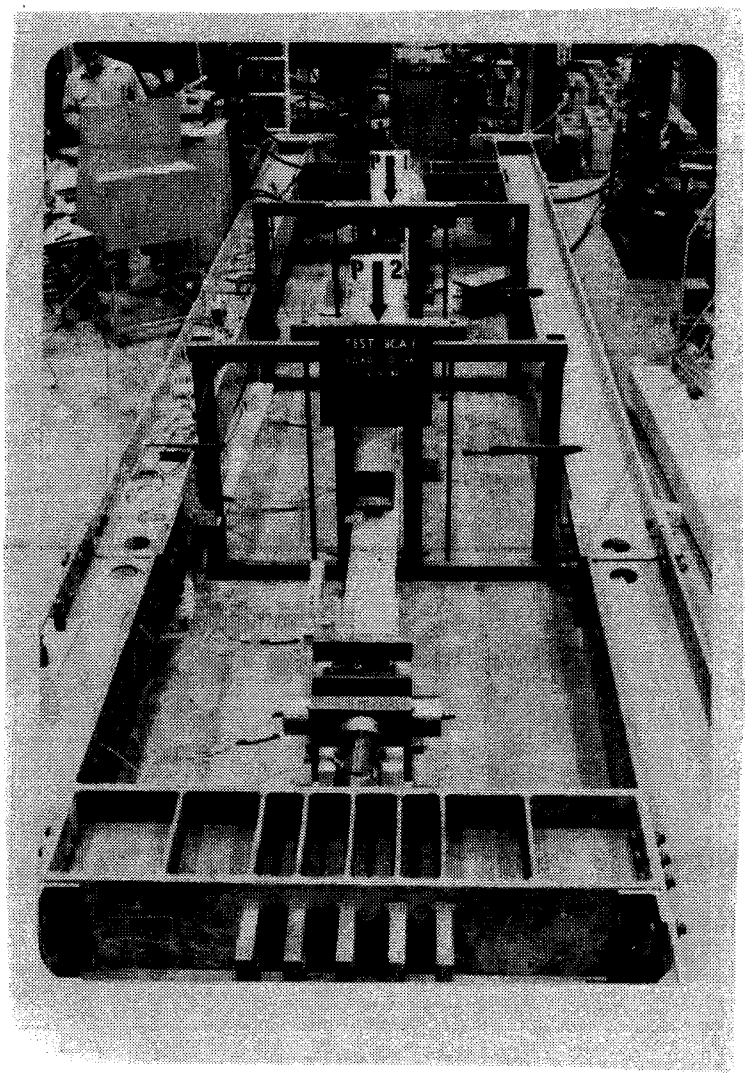

Plate 4.1 Test Set-Up

5. TEST RESULTS AND DISCUSSION

5.1 Introduction

Tables 5.1 and 5.2 summarize the results of compression and tension tests on the small-scale specimens. Tables 5.3 and 5.4 give corresponding summaries for the full-scale tests.

For the purpose of plotting lateral load versus midspan deflection graphs, the average of the loads read from load-cells at positions P1 and P2 was used. The equipment load amounted to a total of 1.1kN at each load position. The load-deflection curves for all specimens are shown in Figures 5.1 to 5.3. The moment-end rotation curves are given in Figures 5.4 to 5.6; while the strain distribution on the cross-sections are shown in Figures 5.7 to 5.13. Figures 5.15 to 5.22 show the deflected shapes. Figure 5.23 show test results together with analytical predictions for 33 percent ultimate tension strain, using method 2.

During the tests, the laboratory temperature varied between 71°F and 74°F. The relative humidity varied between 26% and 30%. The average moisture content of all specimens was approximately 7%.

5.2 Small-Scale Tests

The results shown in Table 5.1 and 5.2 were obtained from the 10 compression and 10 tension tests performed on standard specimens as described in Chapter 4.

In compression, the average yield stress was 48MPa. This is also the ultimate strength, using an elasto-plastic stress strain curve. The average ultimate strain was 0.0028mm/mm, while the modulus of elasticity averaged 19,800MPa. The value of α obtained was 0.864. The average values in tension were 62MPa for ultimate stress, 0.0032mm/mm for ultimate strain and 20,800MPa for the modulus of elasticity.

The average of the moduli of elasticity in tension and compression, 20,300MPa, was used in all computations. Coefficients of variation for all calculated averages varied between 10% and 22%.

5.3 Full-Scale Tests

5.3.1 General Behaviour

Specimen BCA1

Some fine cracks were observed on the compression face before the test. These cracks did not seem to have any significant effect on the behaviour of the specimen.

At a lateral load of 4kN, a cracking sound was heard. at a load of 7kN, crack openings around knots and knot-holes close to the tension face initiated failure. At a load of 8kN, splitting in the tension zone was becoming common. The beam-column finally failed when a large sloping crack formed through the bottom two laminations. Plates 5.1(a) and (b) show the crack patterns.

Specimen BCA2

When the lateral load due to the equipment was applied, this specimen deflected significantly at midspan. At a lateral load of 2kN, a wide crack developed suddenly from a knot in the second lamination from the bottom face, close to load position P1. This crack quickly propagated to both sides of the knot, and the beam-column became very sensitive to the lateral load adjustments. An attempt to increase the load caused increasing deflection, resulting in final collapse of the specimen. Plates 5.2(a) and (b) show the observed crack patterns at failure.

Specimen BCA3

A number of knots were observed throughout this specimen. As for BCA2, significant deflection at a lateral load of 1kN was observed. At a load of 4kN, cracks started to open up around some of the knots close to midspan. At a load of 6kN, a large crack opened up at a knot in the bottom lamination close to load position P1. This crack penetrated three bottom laminations along a sloping grain, to cause the final failure. Plates 5.3(a) and (b) show the condition of the specimen at failure.

Specimen BCB1

Initial fine cracks were observed around knots at a lateral load of 10kN, close to load position P1. Other fine cracks formed at a load of 15kN, while the initial cracks

opened up. Multiple cracks formed at midspan and propagated in a slightly sloping grain to cause final failure at a load of 27kN. Plates 5.4(a) and (b) show the condition of the specimen at failure

Specimen BCB2

The behaviour of this specimen was similar to that of specimen BCB1. At a lateral load of 13kN, a knot on the compression face initiated cracking. The specimen failed at a load of 14kN when large inclined cracks, initiated at small knots on the bottom lamination, opened up significantly. Plates 5.5(a) and (b) show the final failure condition.

Specimen BCB3

This specimen behaved similar to BCB1 and BCB2. Initial cracks observed prior to testing on one side of the specimen proved of no significant consequence. At a load of 6kN, the beam-column suddenly cracked around two knots on the compression face. As a load of 7kN was reached, compression failure coupled with a minor edge split in the tension zone caused the final failure. The failure cracks are shown in Plates 5.6(a) and (b).

Specimen BCC1

At a lateral load of 30kN, minute cracks started to open up. Compression failure occurred close to load position

P1 at a lateral load of 40kN and near load position P2 at a load of 45kN. The beam-column failed essentially in compression, with minor splitting in the tension zone at a load of 54kN. The crack patterns are shown in plates 5.7(a) and (b).

Specimen BCC2

The behaviour of this specimen was somewhat similar to that of BCC1. As a result of the large axial load, minute cracks opened up before application of any lateral load. At a lateral load of 17kN, more cracks formed in the compression zone. These cracks widened at a load of 30kN. At a load of 35kN, the beam-column failed by crushing in the compression zone, confined essentially to the top two laminations. Plates 5.8(a) and (b) show the crack patterns.

Specimen BCC3

This specimen carried the largest axial load, which caused small cracks to open up at zero lateral load. At a lateral load of 15kN, the cracks widened around knots close to the compression face. At a load of 24kN, crushing in the compression zone, coupled with some tensile cracks at a knot caused the final failure. Plates 5.9(a) and (b) show the conditions at failure.

5.3.2 Load Deflection Curves

Series A Specimens

The load-deflection curves obtained for the series A specimens are shown in Fig. 5.1. As was expected, the lateral load at failure decreased as the concentric axial load was increased. A general non-linear but relatively smooth plot for specimen BCA1 was perhaps due to the light axial load. The behaviour of specimen BCA3 was irregular due to the significant number of knots present, and perhaps the higher level of axial load. Specimen BCA2 with the largest axial load in this series (67 percent of the Euler load), failed in an instability mode as indicated by the load deflection curve.

Series B Specimens

The behaviour of Series B specimens was similar to that observed for the series A specimens. The stockier nature of these specimens is however reflected in the relatively smoother load-deflection curves as shown in Fig. 5.2. For specimen BCB3, significant deflection occurred when the lateral load due to the equipment was applied. Also at a lateral load of approximately 4kN, an apparent defect caused a significant increase in deflection.

Series C Specimens

Series C specimens which were the stockiest specimens produced the smoothest load-deflection curves as shown in

Fig. 5.3. However, the effects of knots and knotholes were still evident. Specimen BCC3 showed some upward deflection after the introduction of full axial load. This, however, did not significantly affect its final failure.

5.3.3 Moment-End Rotation Curves

Figures 5.4 to 5.6 show the moment versus end rotation curves for all specimens. As expected the shapes of these curves are similar to those of the load-deflection curves.

5.3.4 Strain Distribution

The measured strains across the cross-section for specimen BCA1, series B and C specimens are shown in Figures 5.7 to 5.13. It was difficult to measure strains on the cross-section of specimens BCA2 and BCA3 because of unstable behaviour. The effect of knots and knotholes on the linear distribution of strain could be observed in some of the figures.

5.3.5 Deflected Shapes

Figures 5.15 to 5.22 show the deflected shape for all specimens. It is observed that these shapes are similar to a portion of sine wave in most cases, especially at loads close to failure. Effects of knots or knotholes sometimes affected the shapes as evident in some of the figures.

5.4 Typical Failure Modes

Tensile splitting produced by sloping grain was the common failure mode of the series A specimens. This was perhaps due to the high slenderness ratio and presence of knots and knotholes. Strain measurements on the cross-section of specimen BCA1 indicated compression failure preceding tensile splitting. Because of unstable behaviour of specimens BCA2 and BCA3, this failure mode could not be confirmed.

Specimens BCB1 and BCB2 were the best examples of the assumed failure criterion employed in the analyses. Crushing close to the compression face followed by tensile splitting was observed for both specimens.

Specimens BCB3 and all series C specimens failed essentially in compression, usually around knots and knotholes. However, it was interesting to observe slight splitting in the tension zone, except for specimen BCC2 which showed no sign of any tensile splitting (See Plate 5.8). The cross-section of specimen BCC3 was in compression up to 70% of its failure load, as indicated in Fig. 5.13.

5.5 Ultimate Strength of Beam-Columns

Table 5.3 shows the maximum strengths of the beam-column specimens based on properties listed in Table 4.1. The mean value of the axial force (Col. 2), which was maintained practically constant during a given test, was used in estimating the bending moment due to axial load

(Col. 7). The maximum value of the total bending moment (Col. 8) is then the sum of the moment due to transverse load (Col. 5) and the moment from Col. 7.

5.6 Comparison of Test Results With Analytical Predictions

Table 5.4 shows the measured and predicted strength for all beam-columns, using all analyses Methods (Cols. 6 and 7). The predictions based on Method 1 (Col. 3) are observed to be generally within 10% of those based on Method 2 (Col. 4). This is not surprising since for most specimens, measured deflected shapes were similar to the sine waveform assumed in analysis Method 1. It is also observed that analysis Method 3 (Col. 3) gives predicted moments close but generally conservative compared to those from Method 2. It thus has potential for use as a method of design because of its simplicity. The result for specimen BCA2 is questioned because of its instability failure. Also, Specimen BCB3 failed prematurely in compression, limiting its capacity compared to the other two Series B specimens. This result is also questioned. The difference between predicted and test moments may be attributed to:

1. The influence on ultimate strength of natural defects such as knots, knotholes and sloping grain. This is evident from the strain distribution on the cross-section of the various specimens. Only Series B specimens attained an average of about 40% ultimate tension strain at failure.

2. The usual scatter in results from timber tests, which does not allow for much confidence in the use of average values. It is observed that the average ultimate strains used in the prediction curves have a coefficient of variation of more than 20%. Perhaps matched small-scale specimens, from an increased number of full-scale tests, may give closer agreement between analysis and test results.
3. The relatively small number of tests reported in this investigation.

To account for the above effects the analyses may be modified by applying an undercapacity factor. To illustrate this approach an undercapacity factor of 0.7 has been applied to analysis Method 2 (Col. 6 of Table 5.4). The resulting modified interaction diagrams are shown in Figure 5.23 together with test results. With the exception of the questioned test results, a good correlation is observed.

Table 5.1 Compression Test Results

Specimen No.	Cross-Sectional Area (mm^2)	Maximum Load (kN)	Ultimate Stress (MPa)	Ultimate Strain (mm/mm)	Modulus of Elasticity (mPa)	Alpha
C1	6474	314	48.5	0.0022	22,598	1.000
C2	6411	290	45.2	0.0028	19,259	0.843
C3	6501	300	46.2	0.0031	18,567	0.794
C4	6421	275			20,715	
C5	5732	317	55.3	0.0023	26,881	0.912
C6	6221	285	45.8	0.0033	19,248	0.716
C7	6125	301	49.1	0.0024	22,249	0.929
C8	6300	287	45.6		18,571	
C9	6299	179			16,200	
C10	6336	342	54.0	0.0037	16,529	0.855

Table 5.2 Tension Test Results

Specimen No.	Cross-Sectional Area (mm^2)	Maximum Load (kN)	Ultimate Stress (mPa)	Ultimate* Strain (mm/mm)	Modulus of Elasticity (mPa)
T1	559	33.5	59.8	0.0030	18,724
T2	548	38.5	70.2	0.0029	24,331
T3	582	34.8	59.8	0.0033	18,409
T4	554	39.0	70.4	0.0037	19.295
T5	566	42.3	74.7	0.0030	24,776
T6	581	43.4	74.7	0.0032	23,662
T7	598	29.7	49.8	0.0021	24,174
T8	609	42.9	70.4	0.0035	20,086
T9	627	37.4	59.6	0.0041	17,222
T10**	624	19.1	30.6	0.0020	17,180

* Curves extrapolated to failure load
** Premature failure

Table 5.3 Beam-Column Test Results

Test Specimen	Mean Value of Axial Load (kN)	Axial Load Ratio, P/Py	Lateral Load at Failure (kN)	Transverse Bending Moment (kN.m)	Maximum Deflection (mm)	Axial Load Moment (kN.m)	Total Bending Moment (kN.m)
1	2	3	4	5	6	7	8
BCA1	125	0.10	8.33	84	90	10.50	23.67
BCA2	245	0.20	1.95	43	43	10.75	13.83
BCA3	158	0.15	6.83	72	111	11.38	31.66
BCB1	195	0.10	27.60	80	80	15.52	59.13
BCB2	481	0.25	16.16	77	75	37.26	64.25
BCB3	770	0.40	6.72	44	67	34.10	62.50
BCC1	545	0.20	54.64	50	50	27.50	113.83
BCC2	1067	0.40	35.76	40	40	42.80	99.30
BCC3	1610	0.60	24.00	38	20	32.16	70.16

Table 5.4 Measured and Predicted Values

Test Specimen	Test M/My	Theoretical M/My			Theoretical M/My
		Method 1	Method 2	Method 3	Modified Method 2*
1	2	3	4	5	6
BCA1	0.41	0.70	0.65	0.62	0.46
BCA2	0.10**	0.32	0.27	0.29	0.19
BCA3	0.34	0.50	0.45	0.44	0.32
BCB1	0.61	0.89	0.85	0.77	0.60
BCB2	0.36	0.56	0.51	0.48	0.36
BCB3	0.15**	0.30	0.27	0.26	0.19
BCC1	0.55	0.84	0.79	0.71	0.55
BCC2	0.38	0.58	0.48	0.42	0.34
BCC3	0.25	0.35	0.22	0.20	0.15

* Method 2 modified by an undercapacity factor of 0.7
** Premature failure

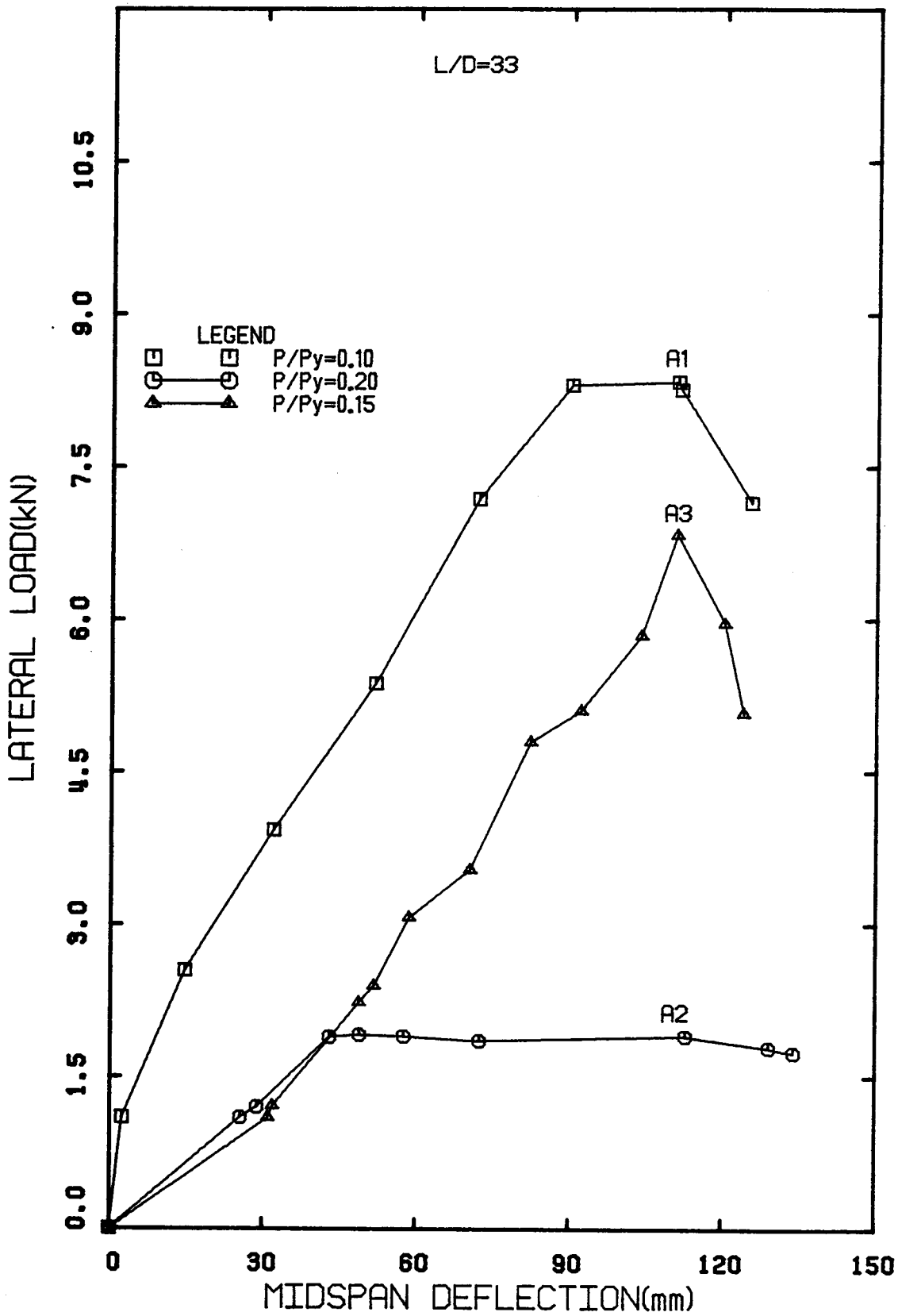

Figure 5.1 Load-Deflection Curves for Series A Specimens

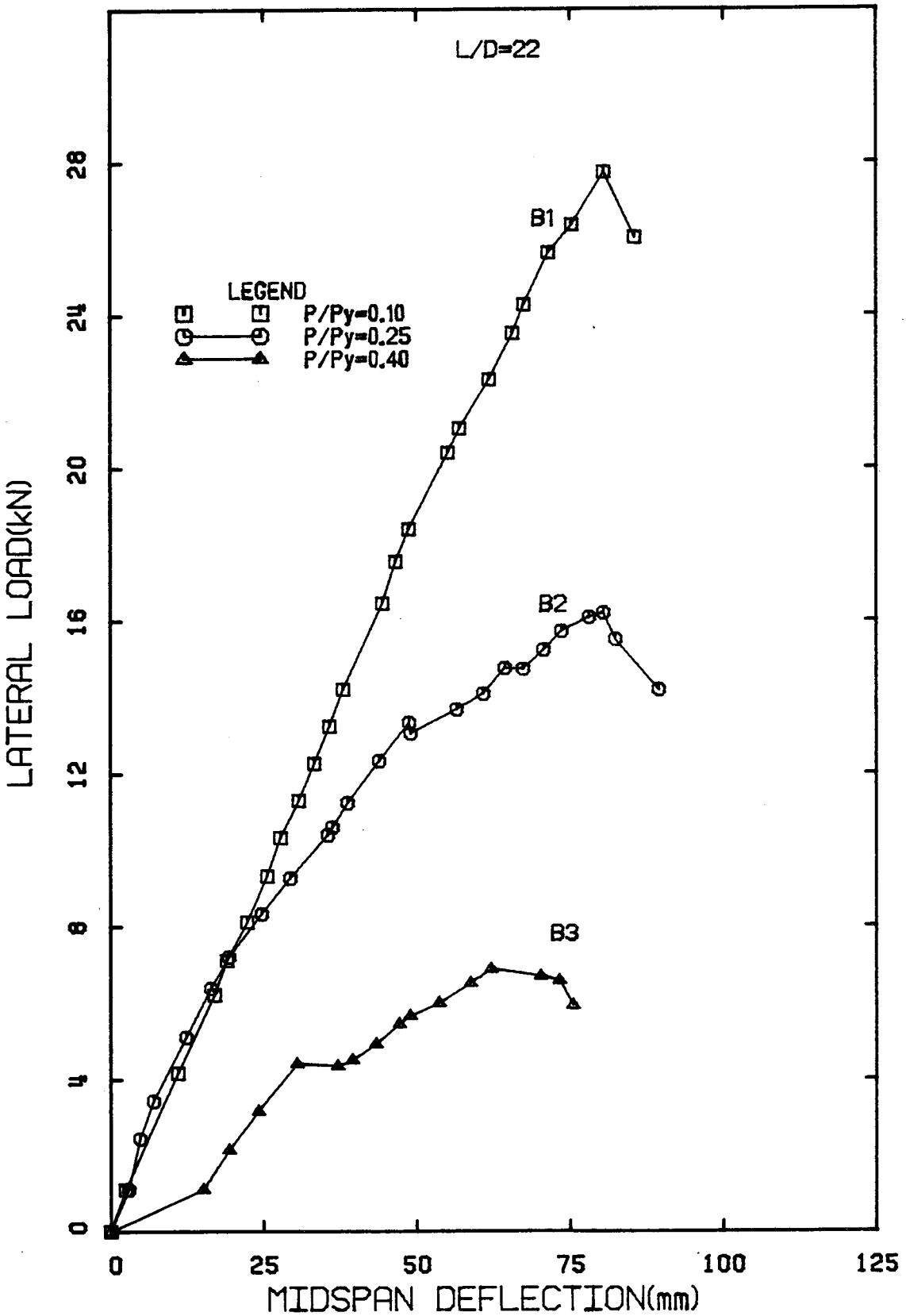

Figure 5.2 Load-Deflection Curves for Series B Specimens

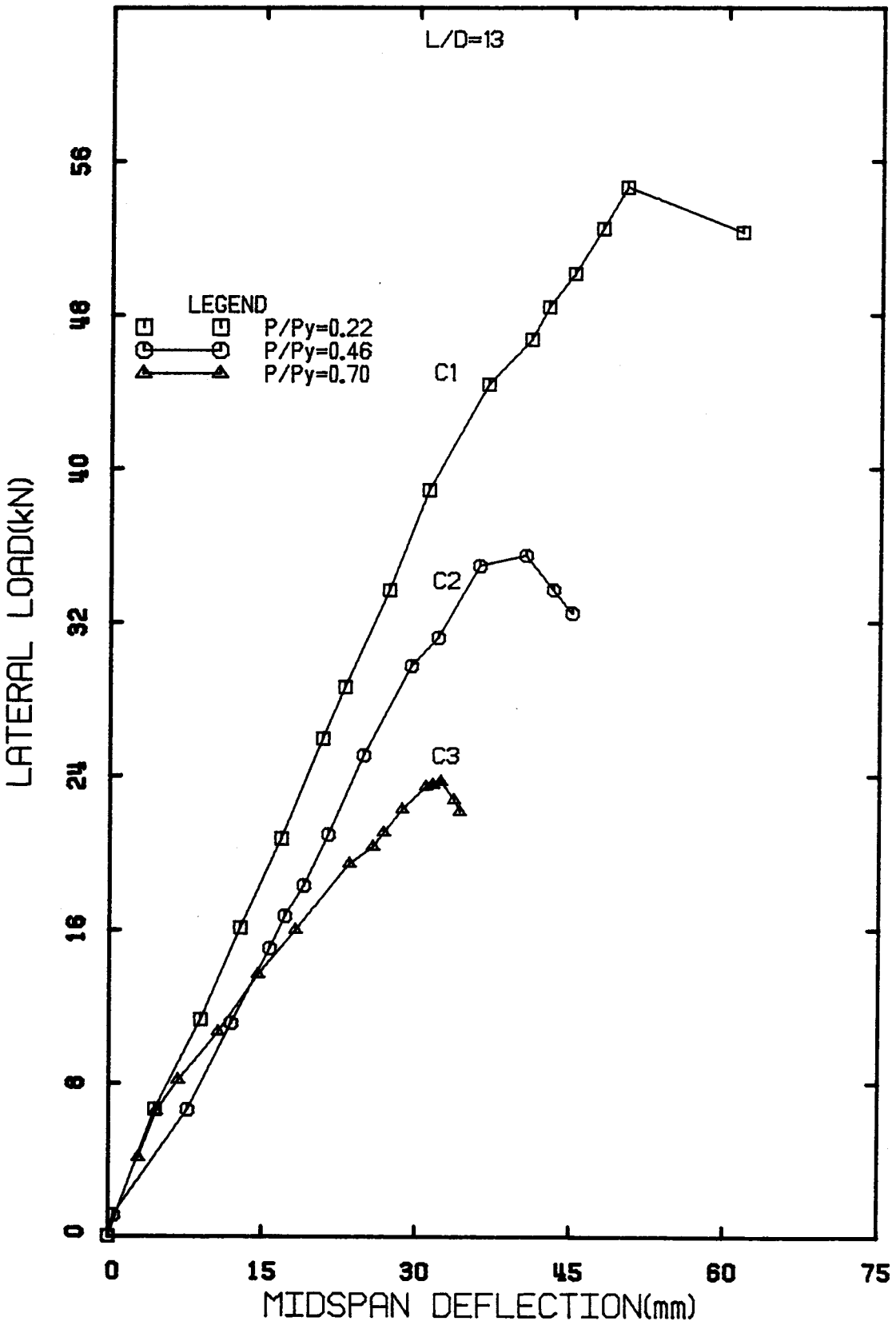

Figure 5.3 Load-Deflection Curves for Series C Specimens

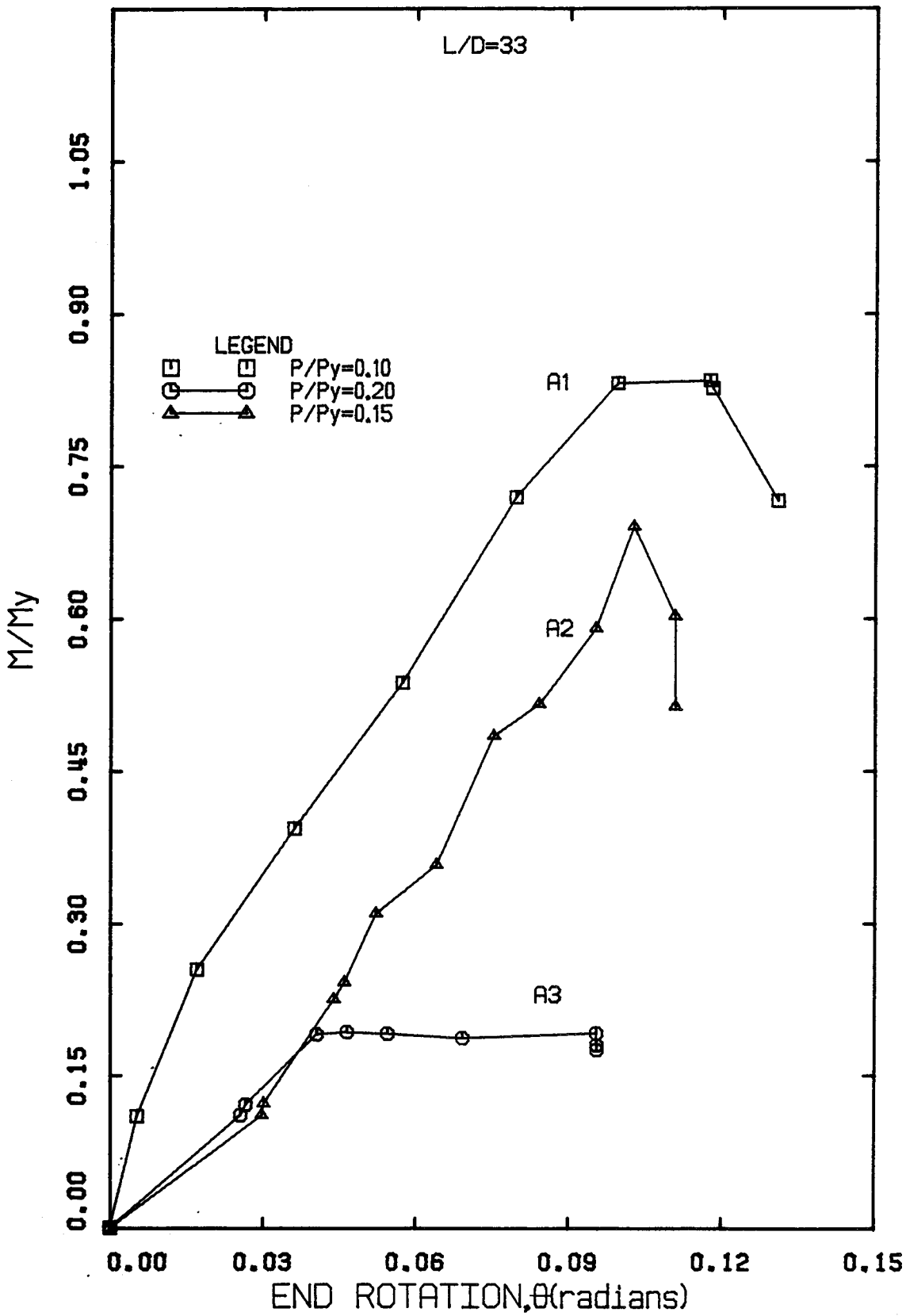

Figure 5.4 Moment-Rotation Curves for Series A Specimens

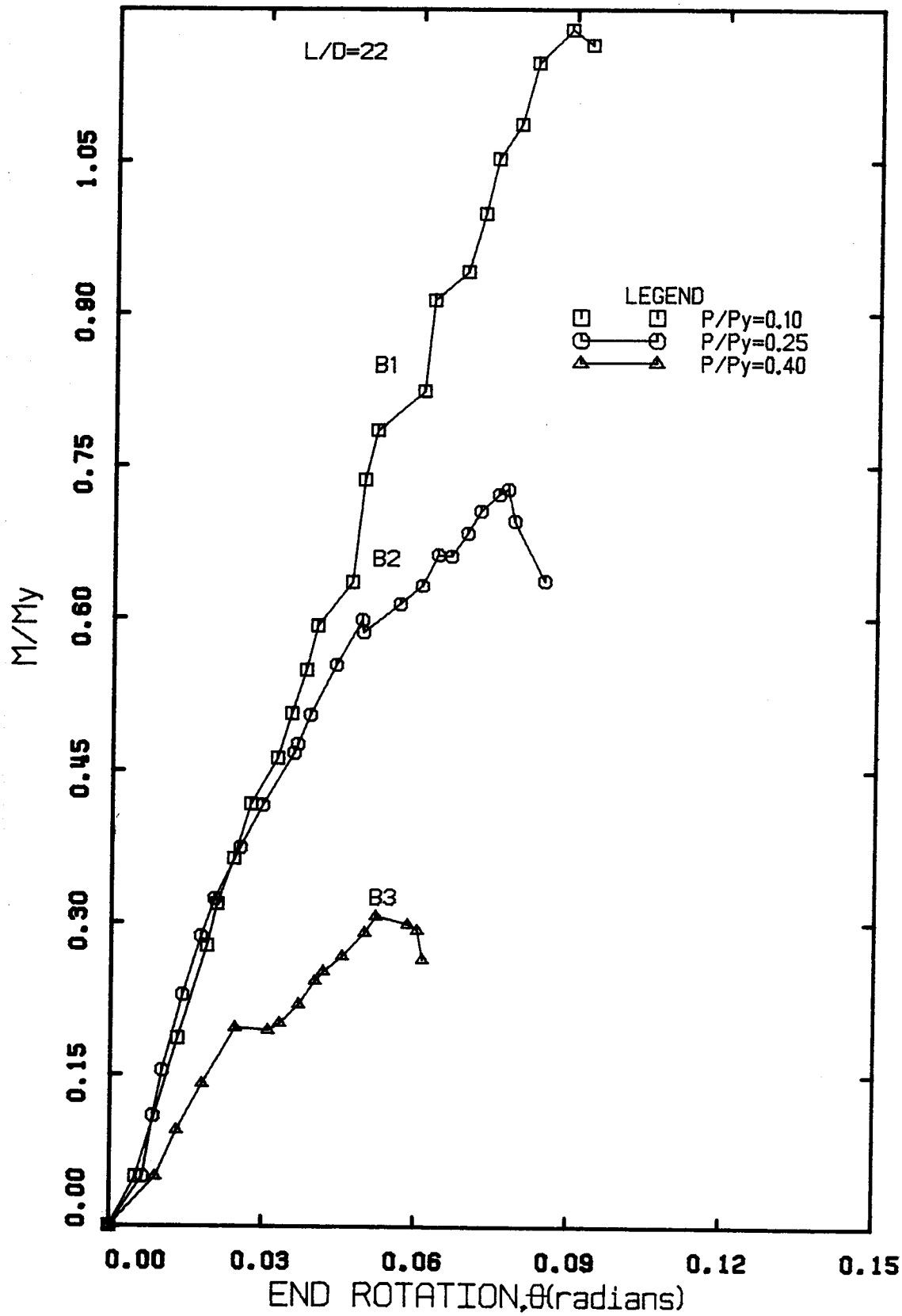

Figure 5.5 Moment-Rotation Curves for Series B Specimens

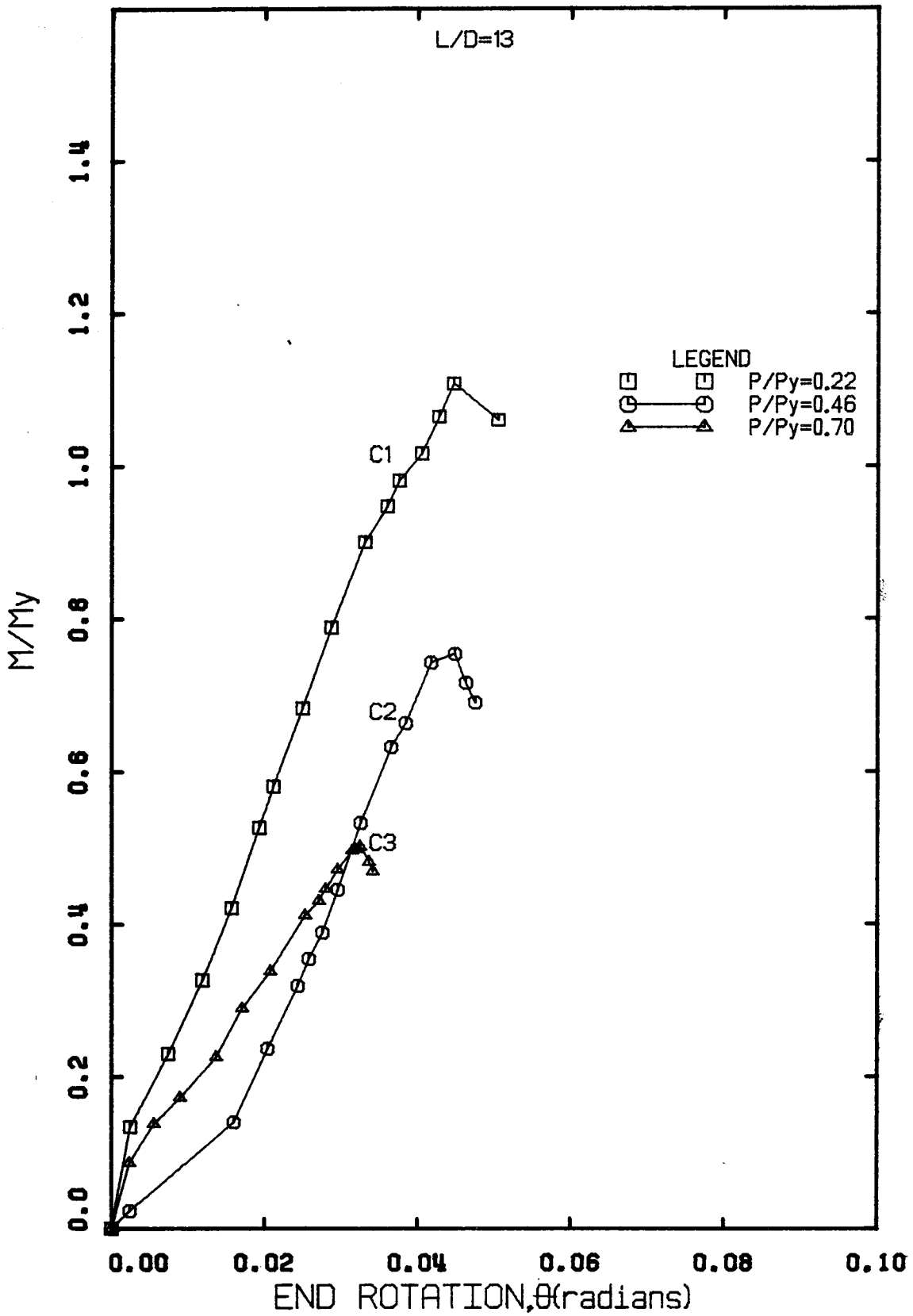

Figure 5.6 Moment-Rotation Curves for Series C Specimens

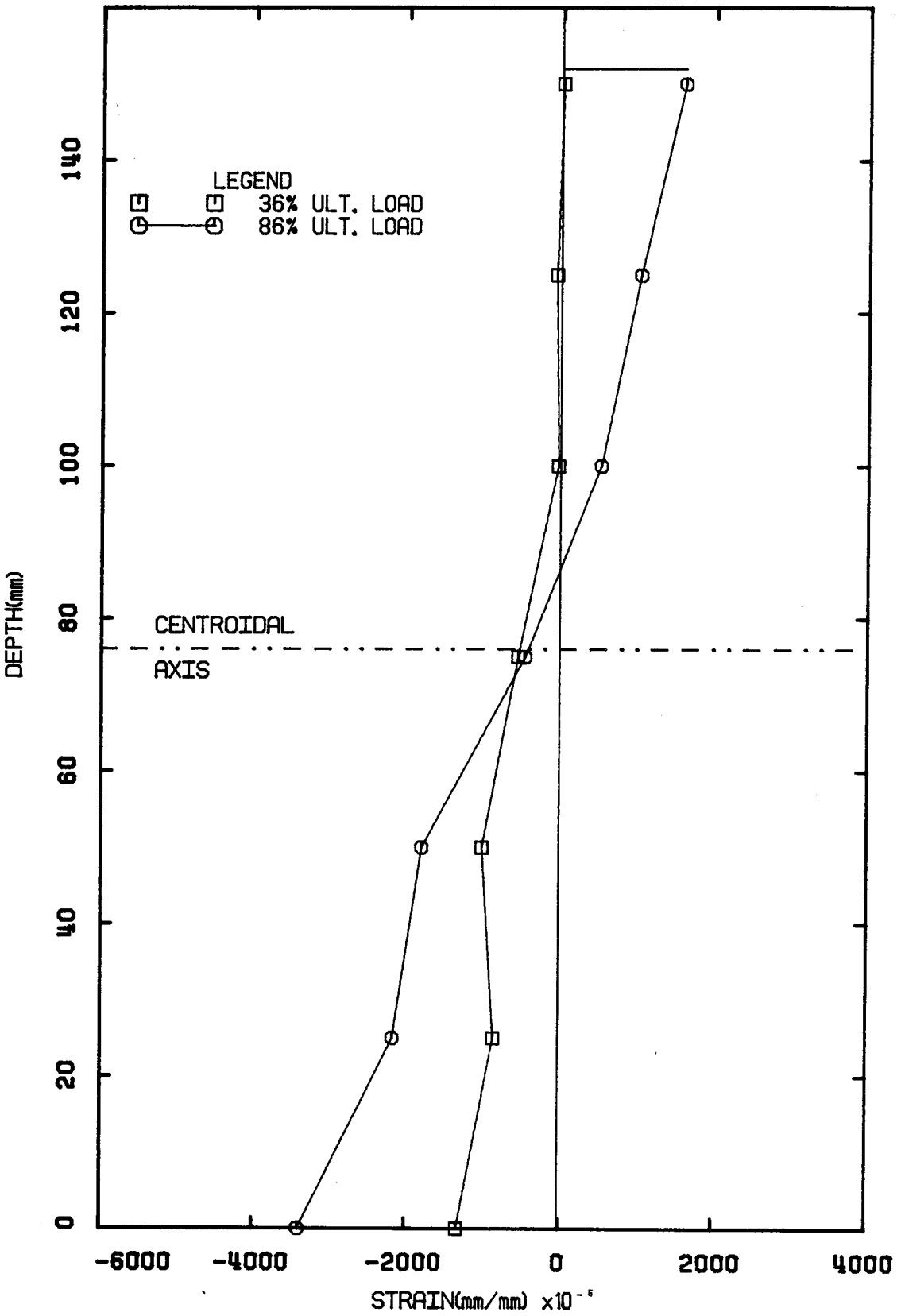

Figure 5.7 Strain Distribution on Specimen BCA1

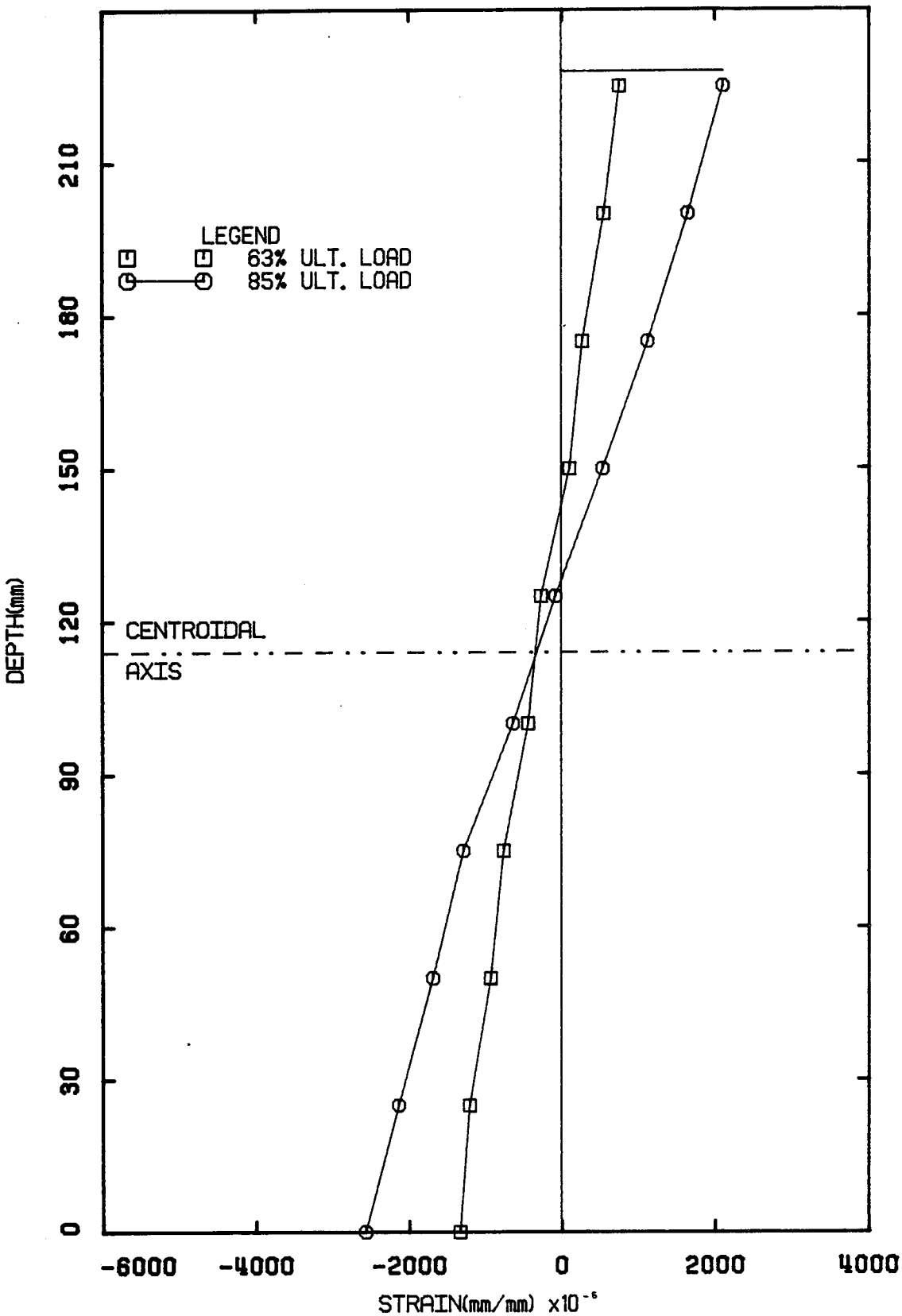

Figure 5.8 Strain Distribution on Specimen BCB1

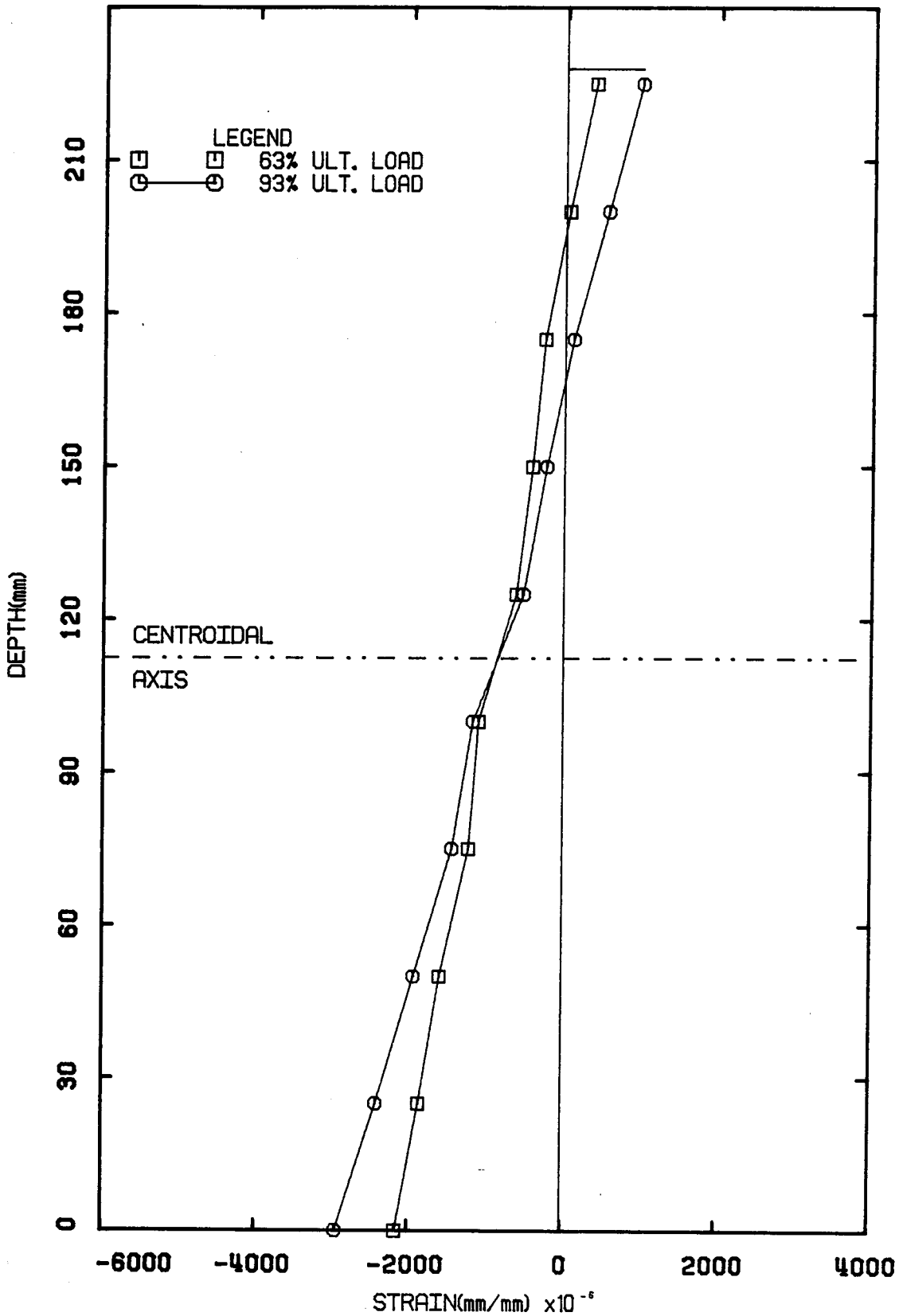

Figure 5.9 Strain Distribution on Specimen BCB2

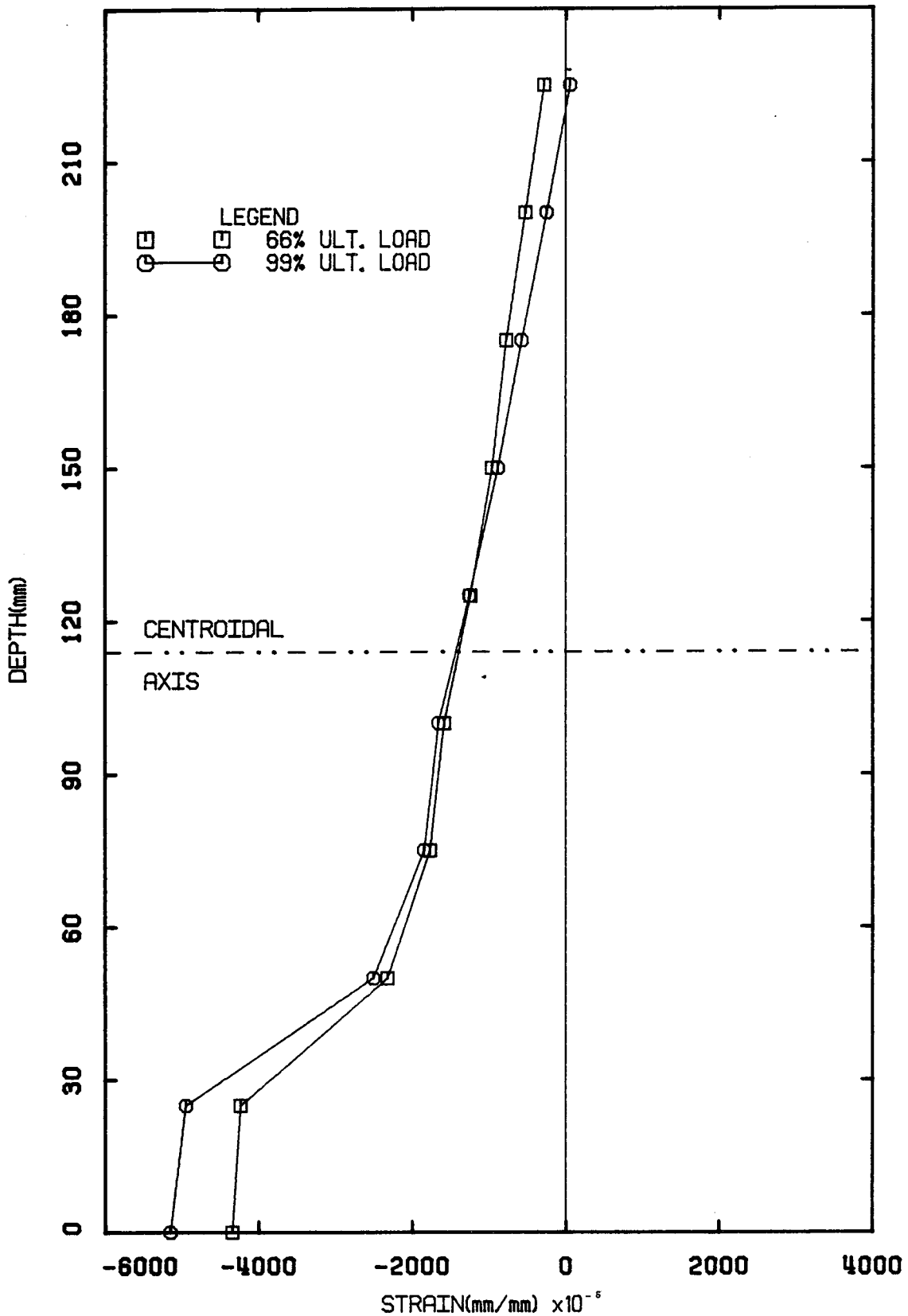

Figure 5.10 Strain Distribution on Specimen BCB3

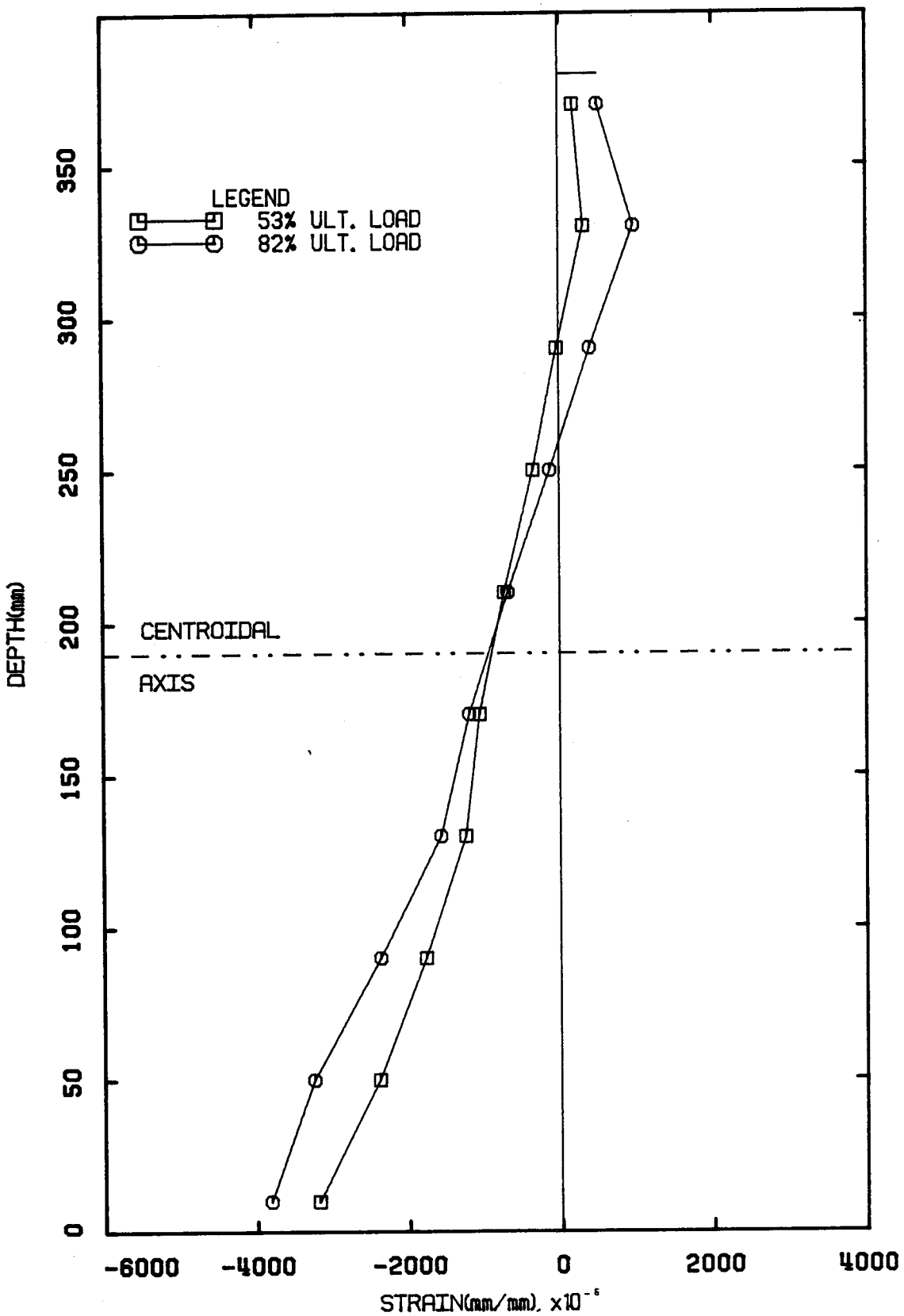

Figure 5.11 Strain Distribution on Specimen BCC1

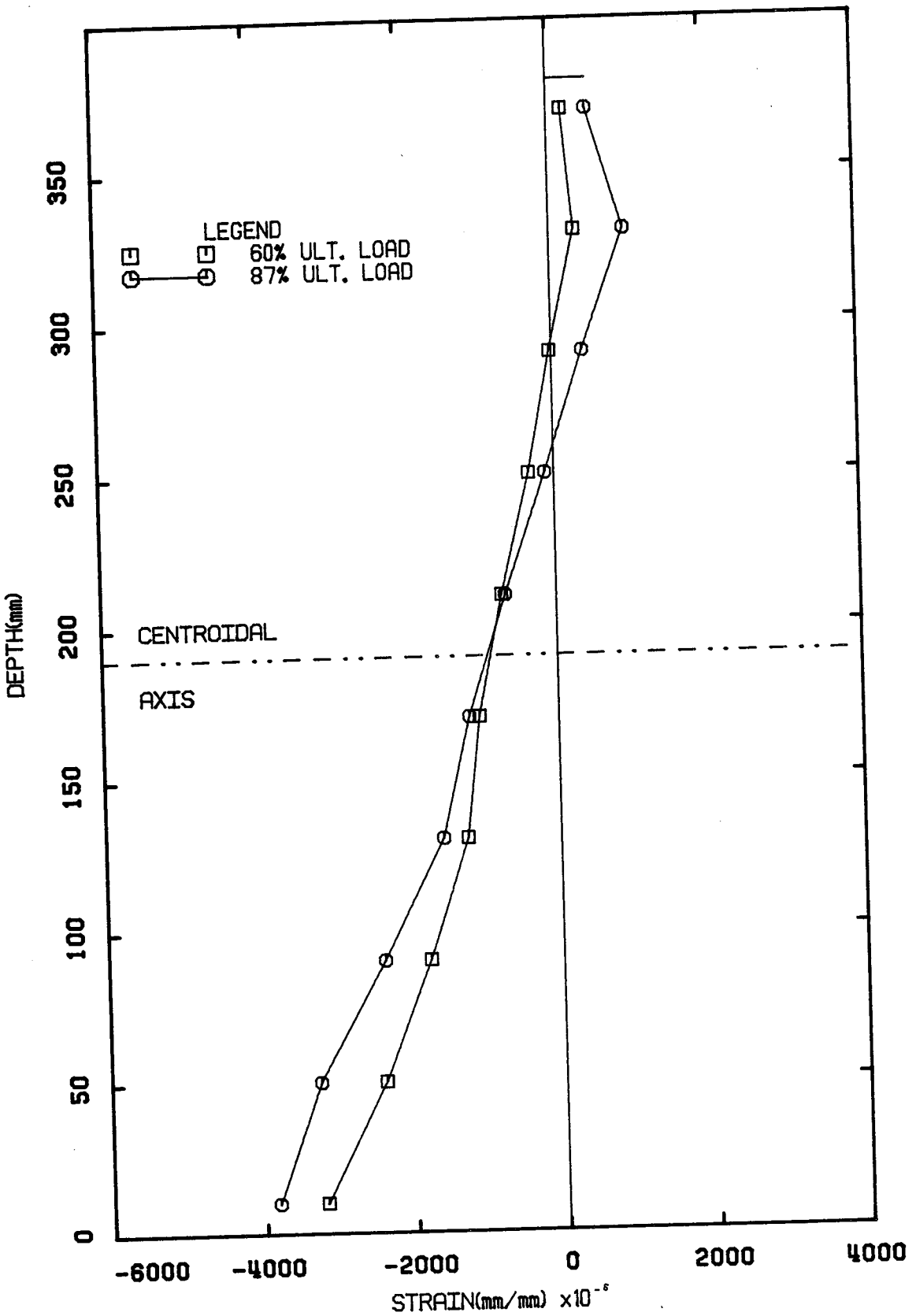

Figure 5.12 Strain Distribution on Specimen BCC2

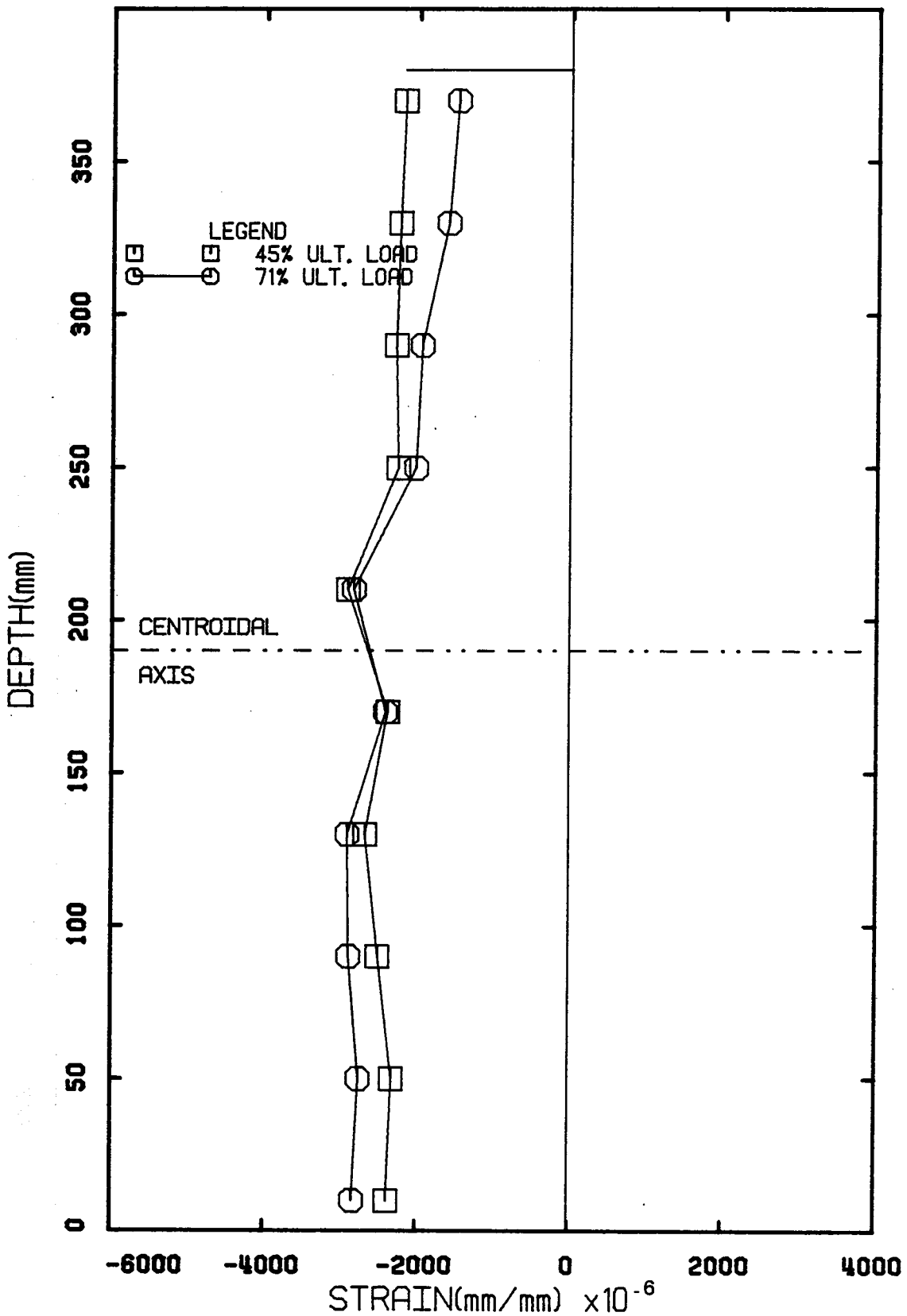

Figure 5.13 Strain Distribution on Specimen BCC3

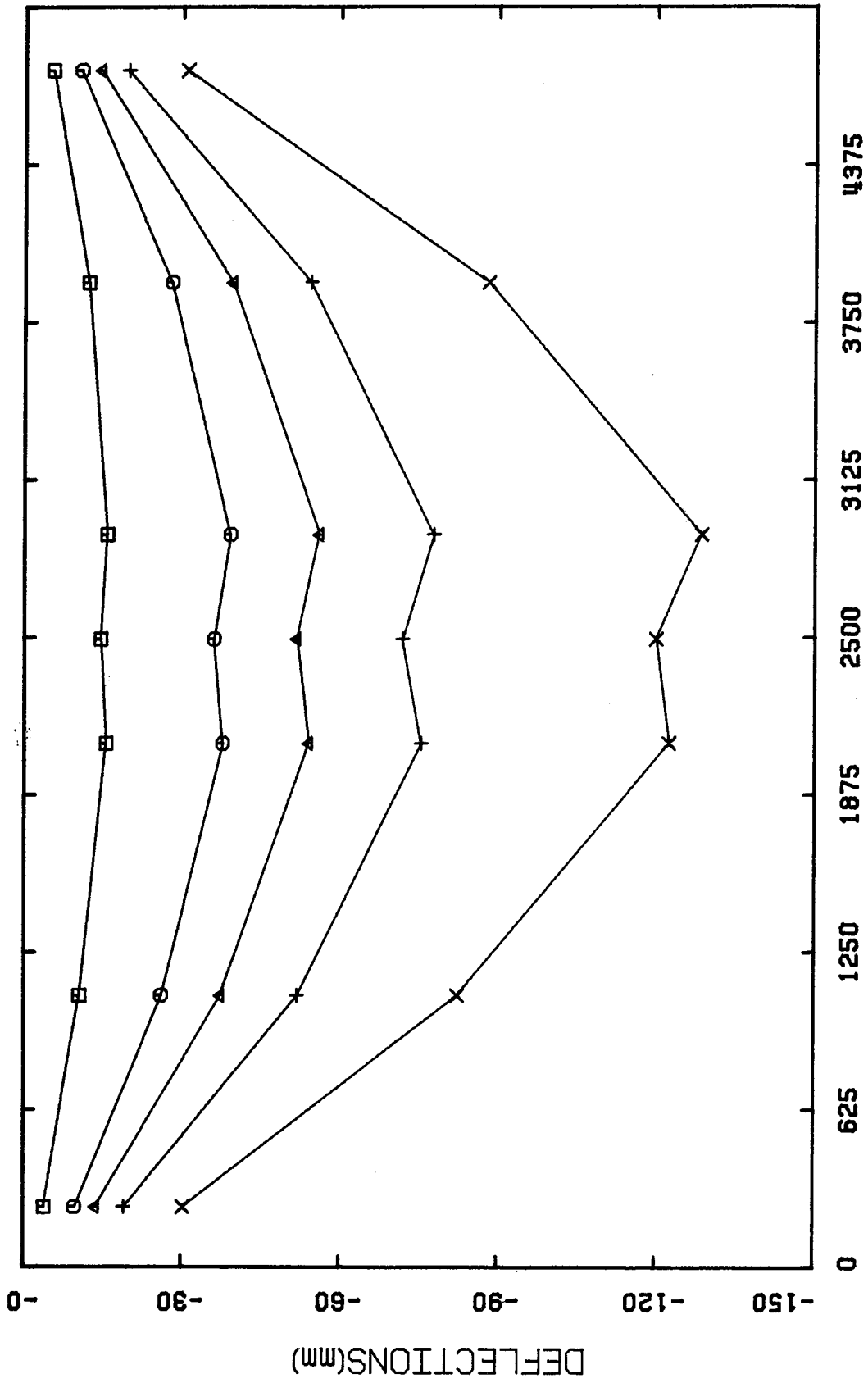

Figure 5.14 Deflected Shape of Specimen BCA1

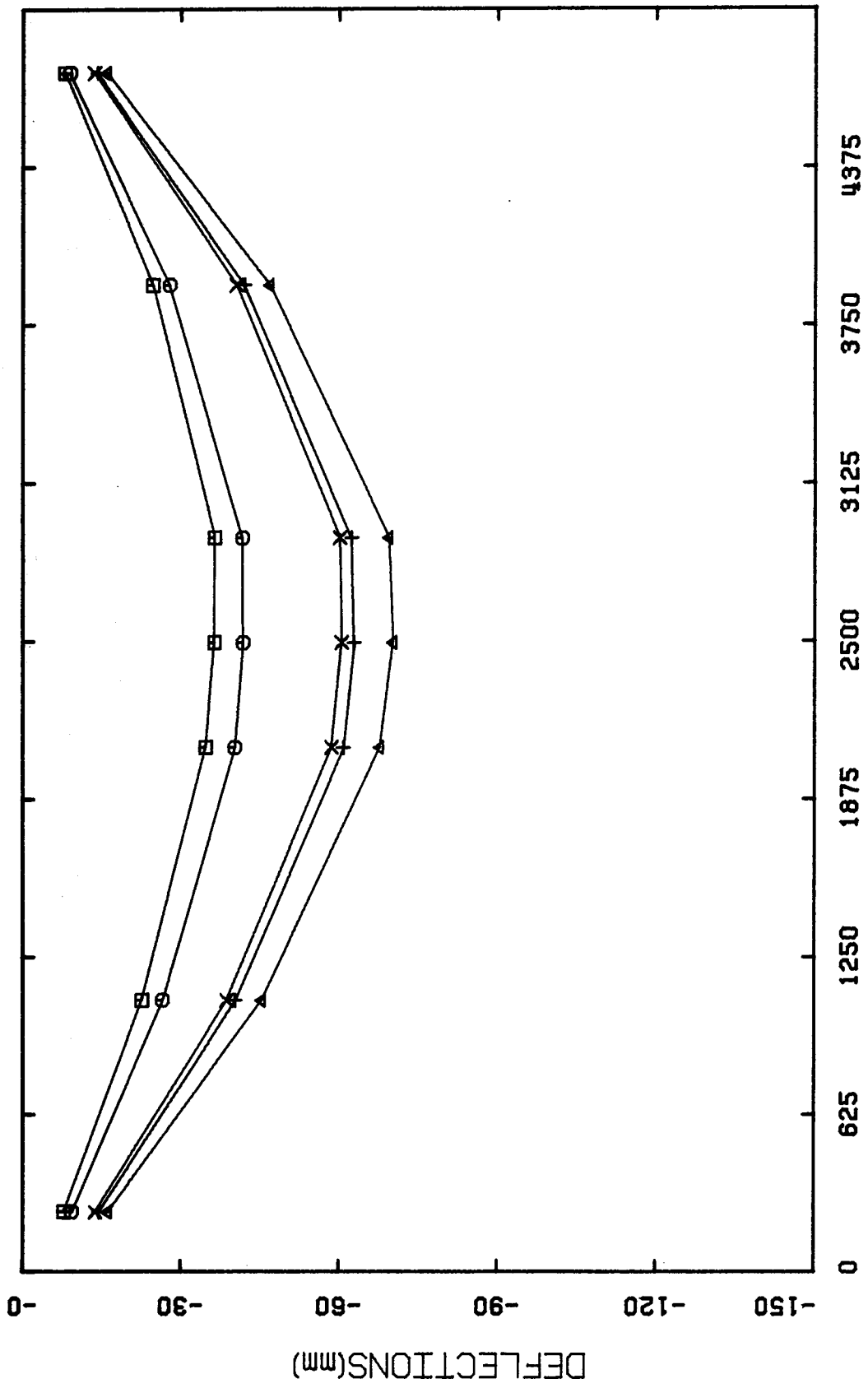

Figure 5.15 Deflected Shape of Specimen BCA2

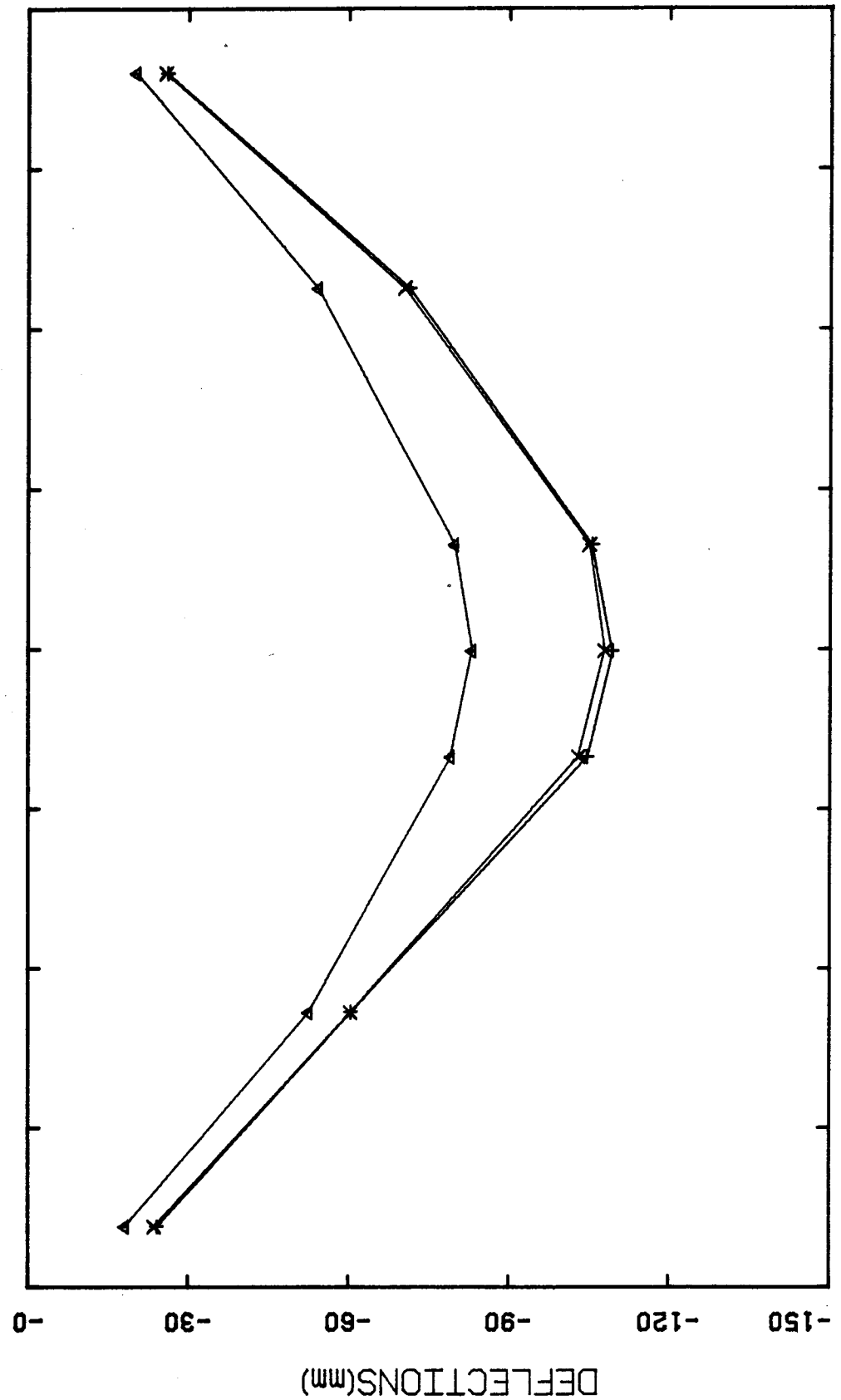

Figure 5.16 Deflected Shape of Specimen BCA3

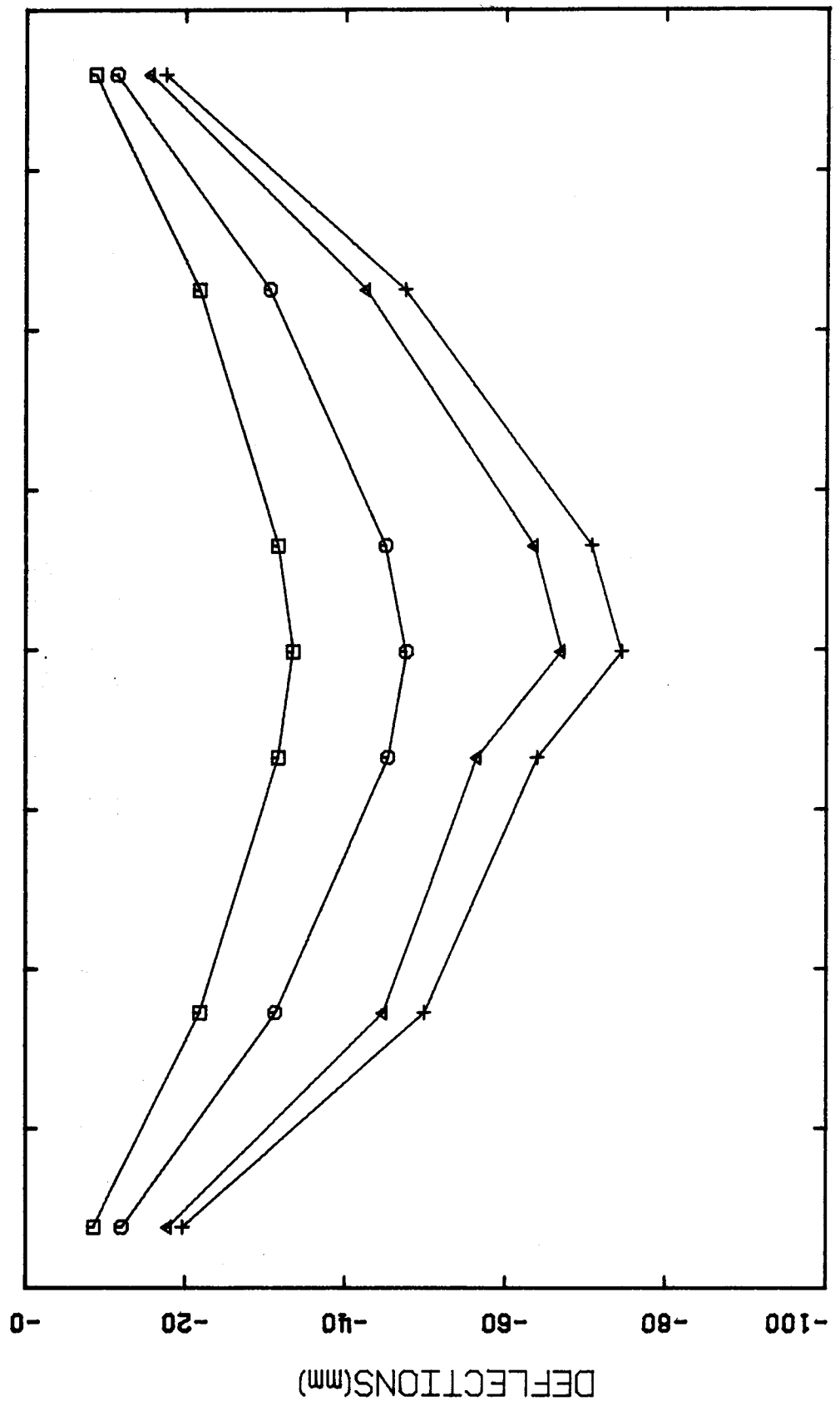

Figure 5.17 Deflected Shape of Specimen BCB1

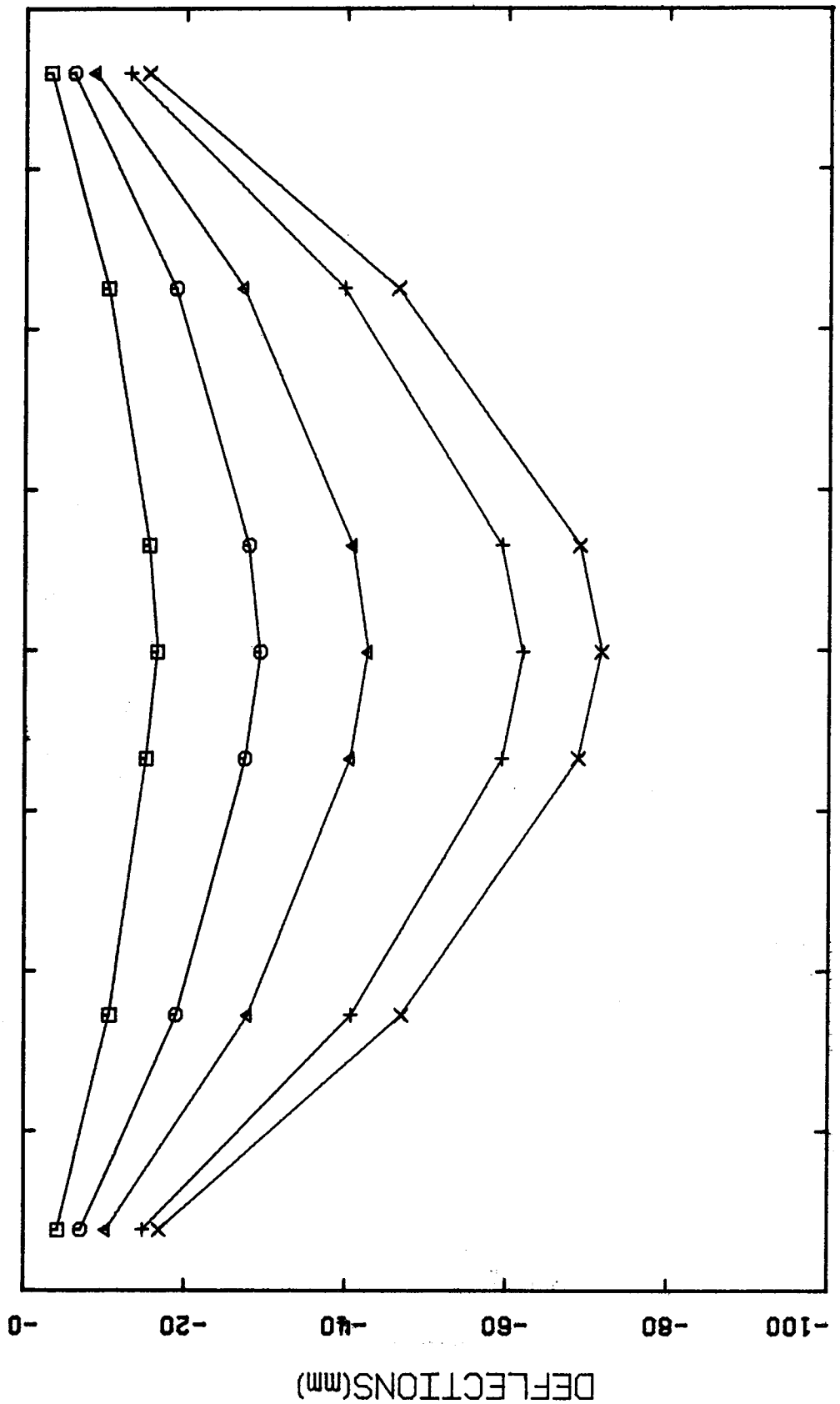

Figure 5.18 Deflected Shape of Specimen BCB2

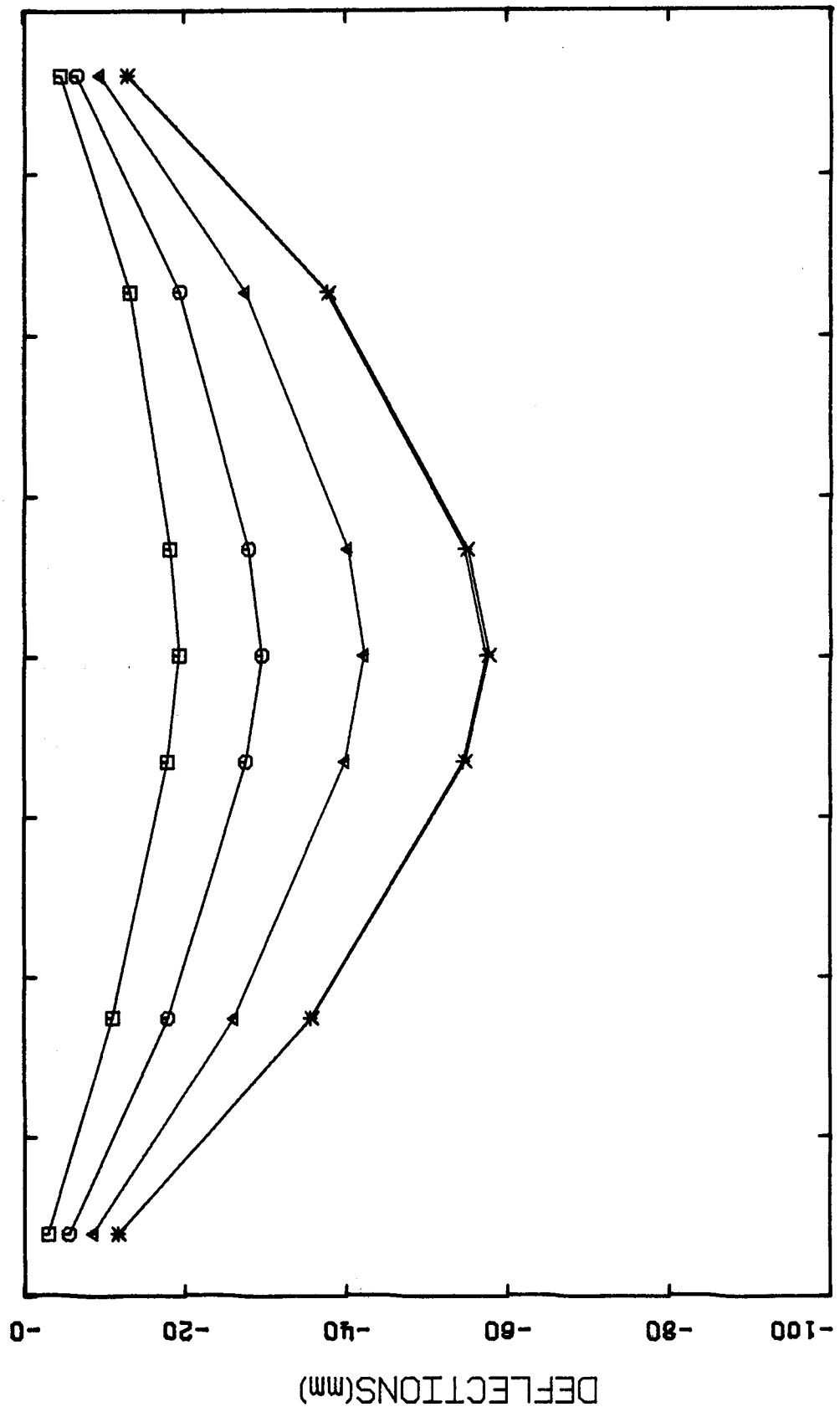

Figure 5.19 Deflected Shape of Specimen BCB3

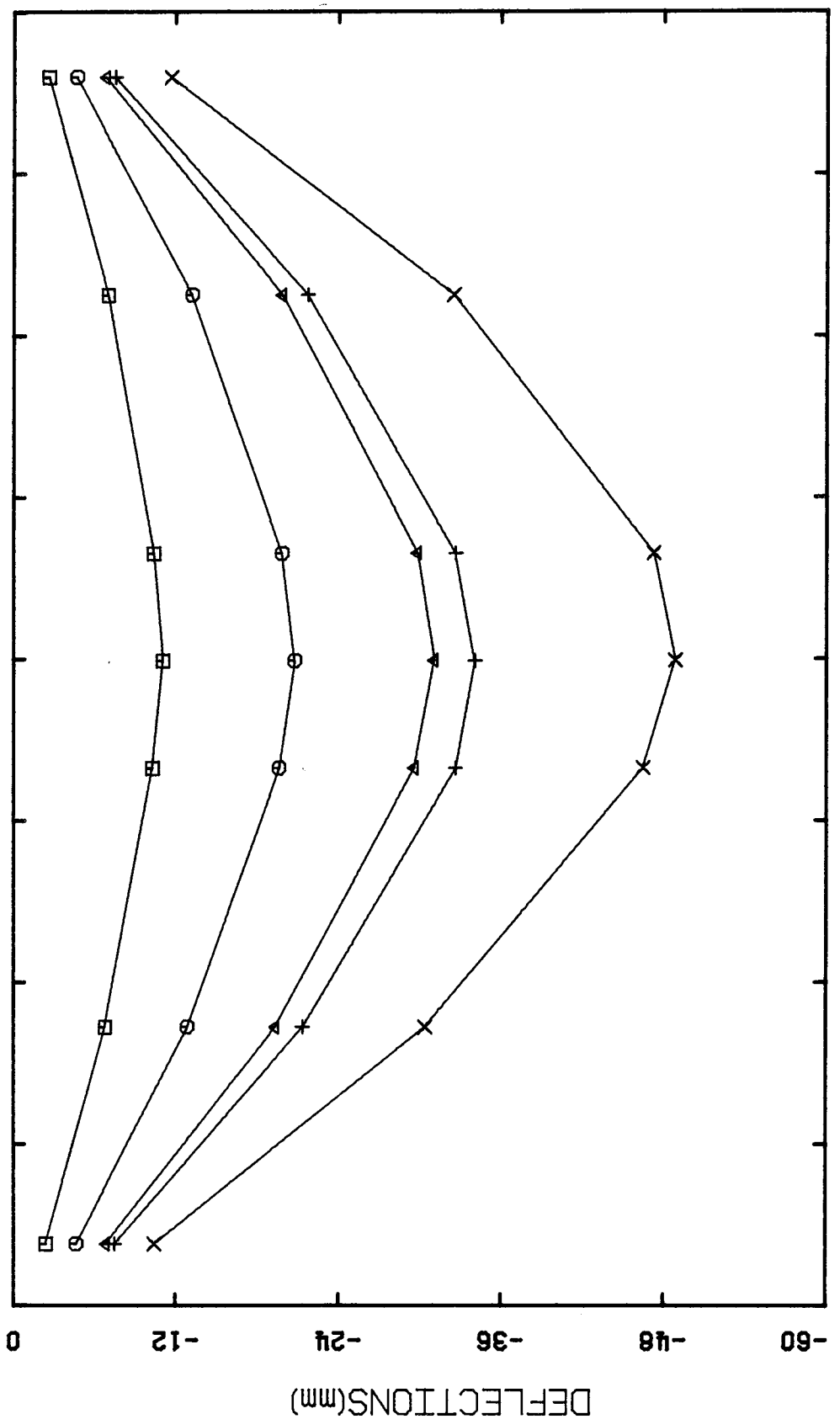

Figure 5.20 Deflected Shape of Specimen BCC1

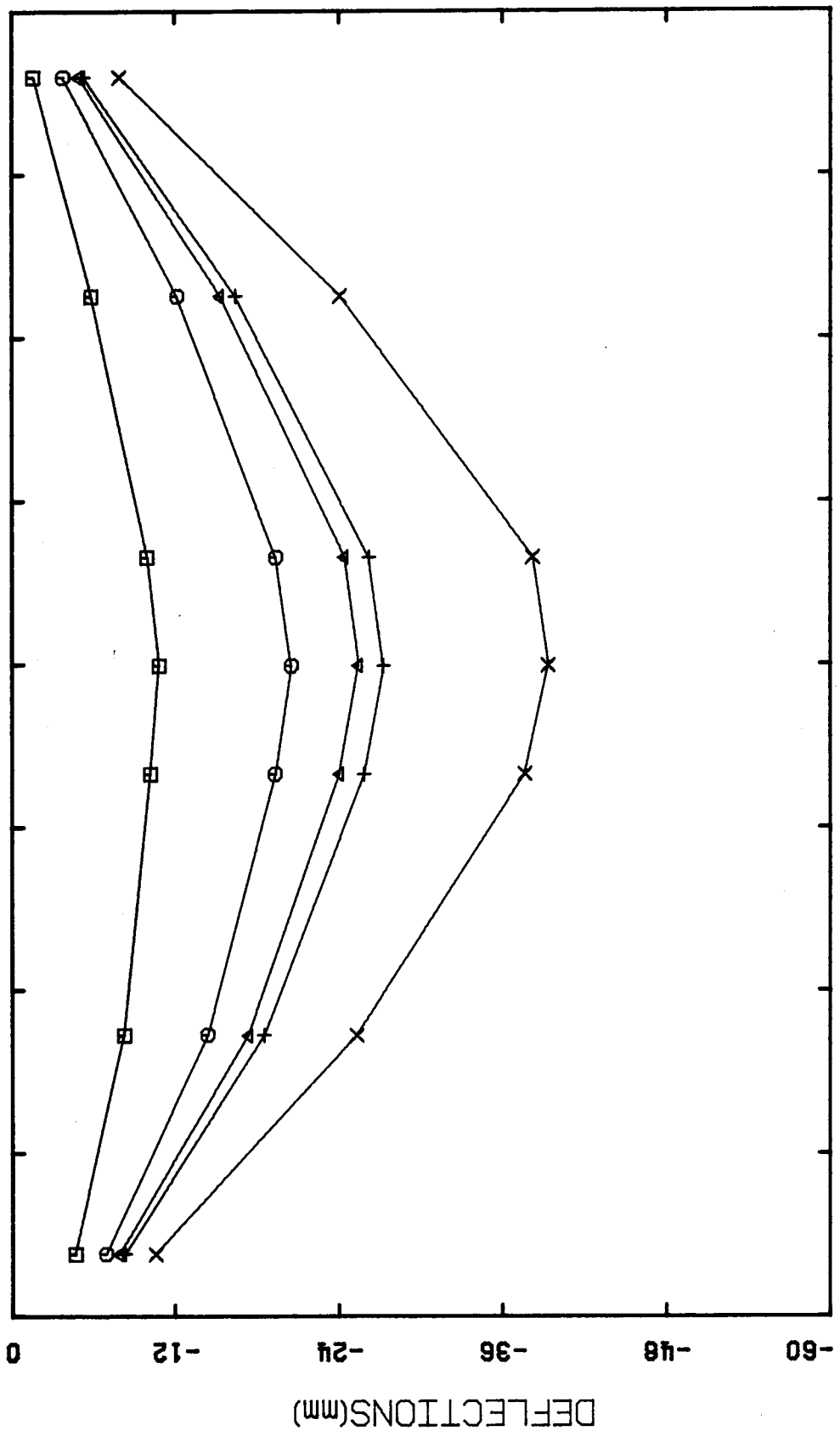

Figure 5.21 Deflected Shape of Specimen BCC2

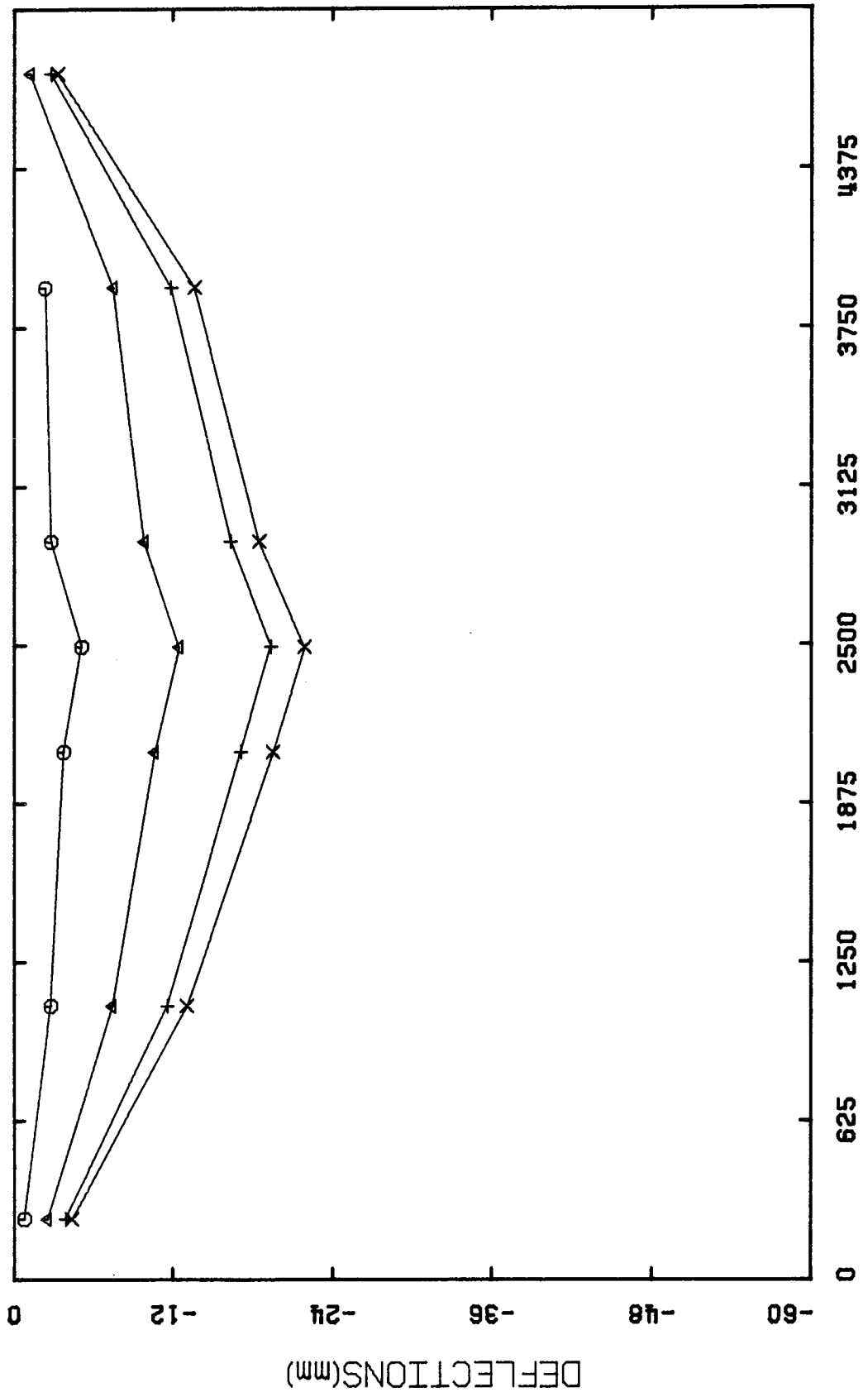

Figure 5.22 Deflected Shape of Specimen BCC3

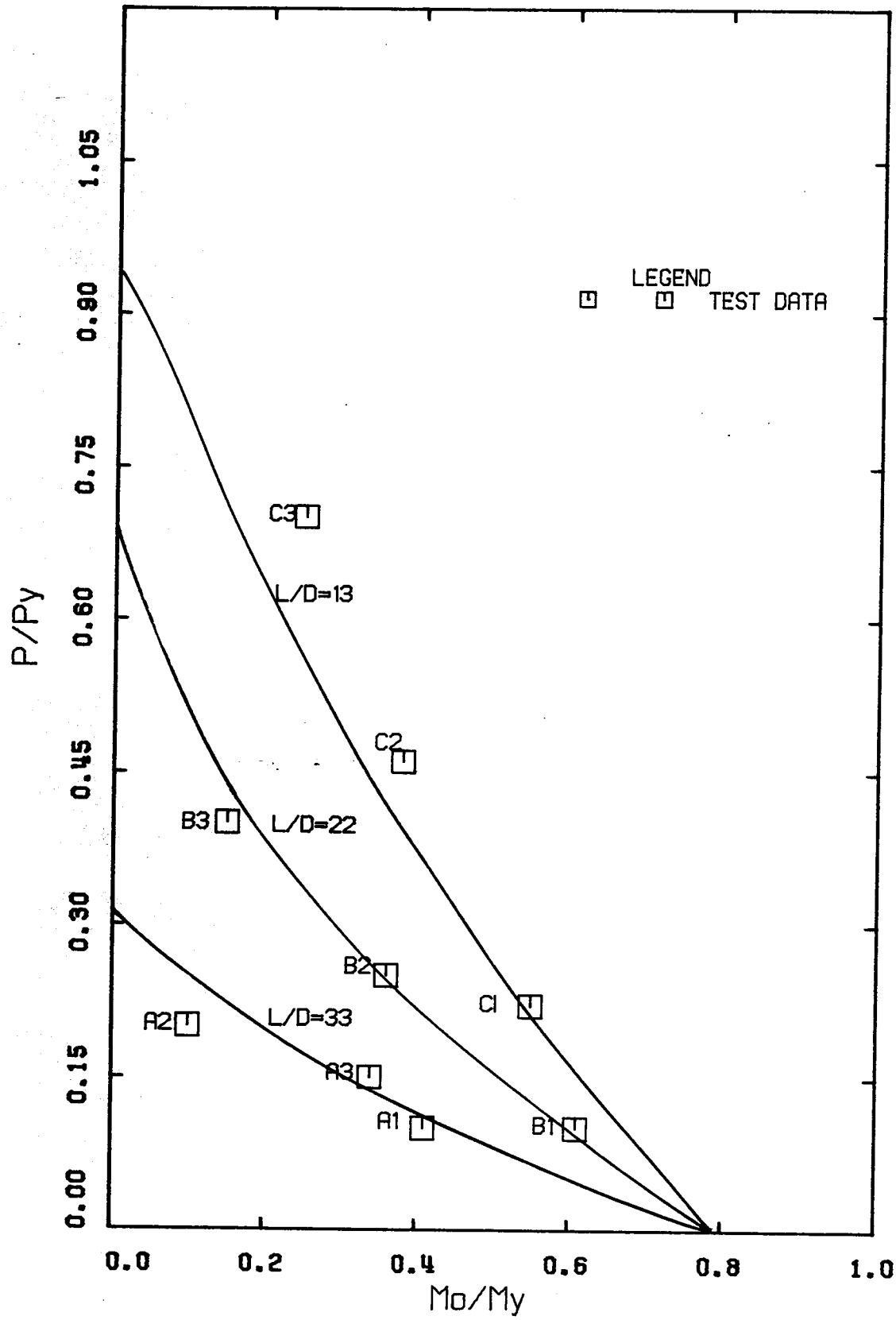

Figure 5.23 Interaction Curves Based on Undercapacity Factor of 0.7

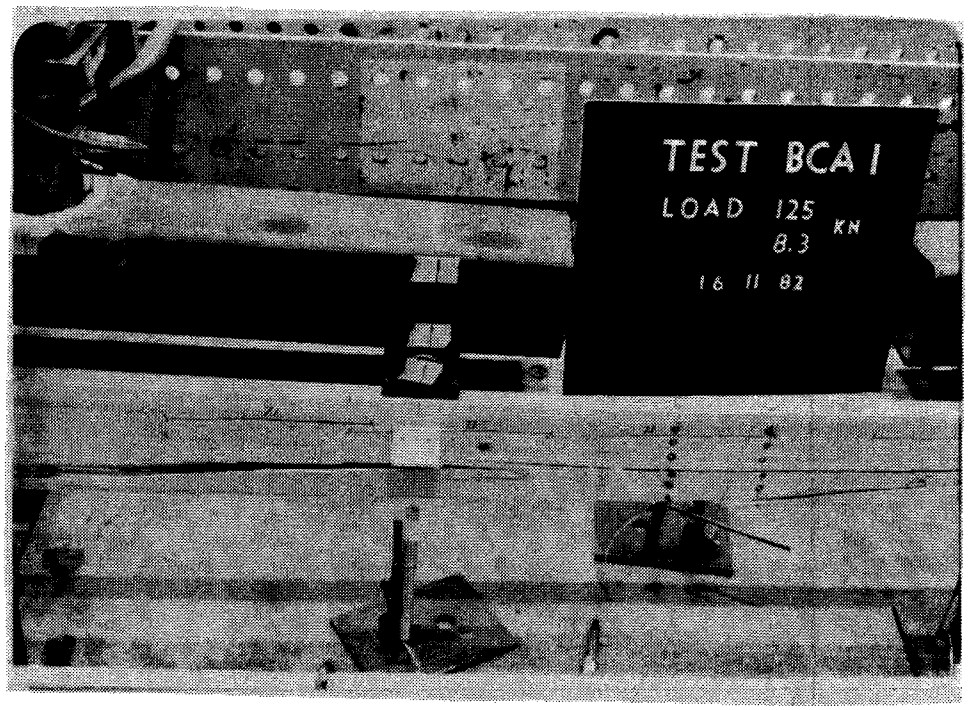

(a)

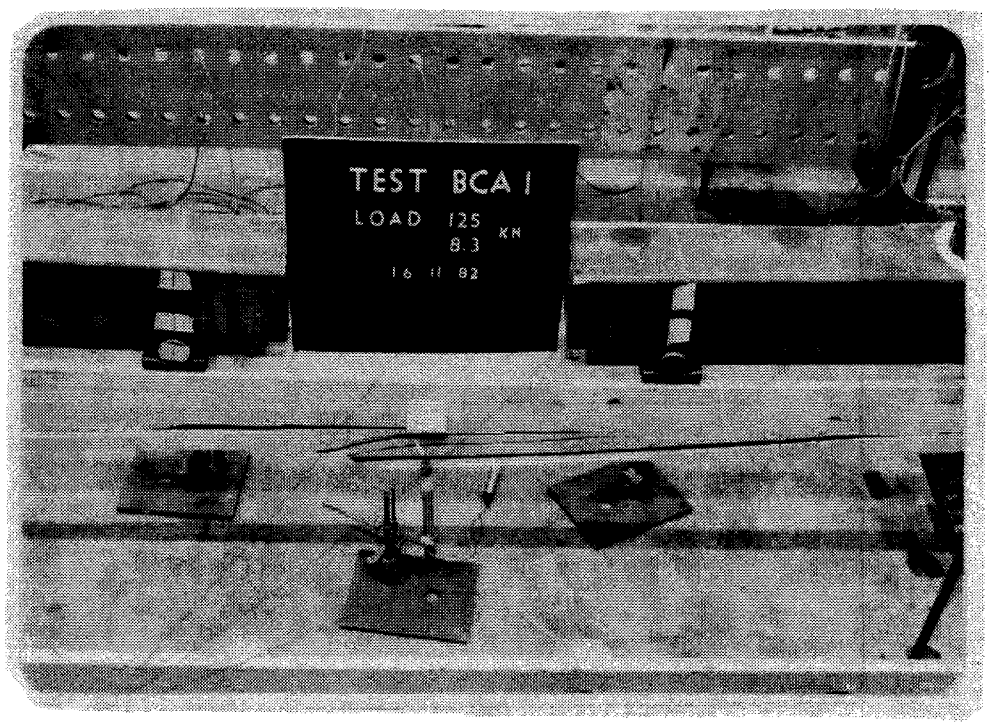

(b)

Plate 5.1 Failure of Specimen BCA1

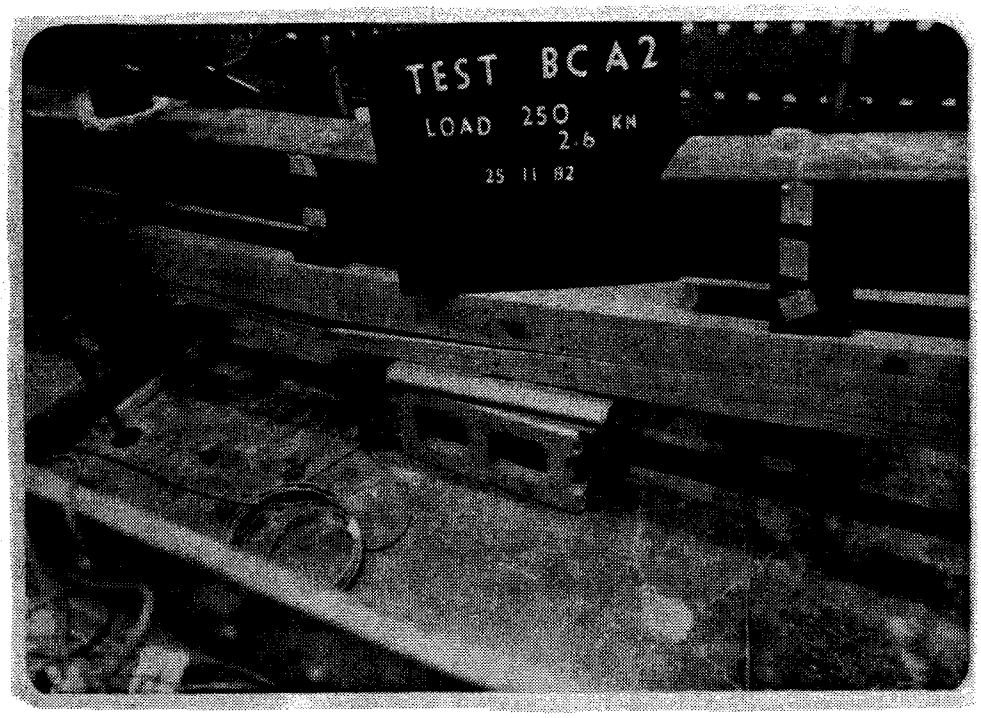

(a)

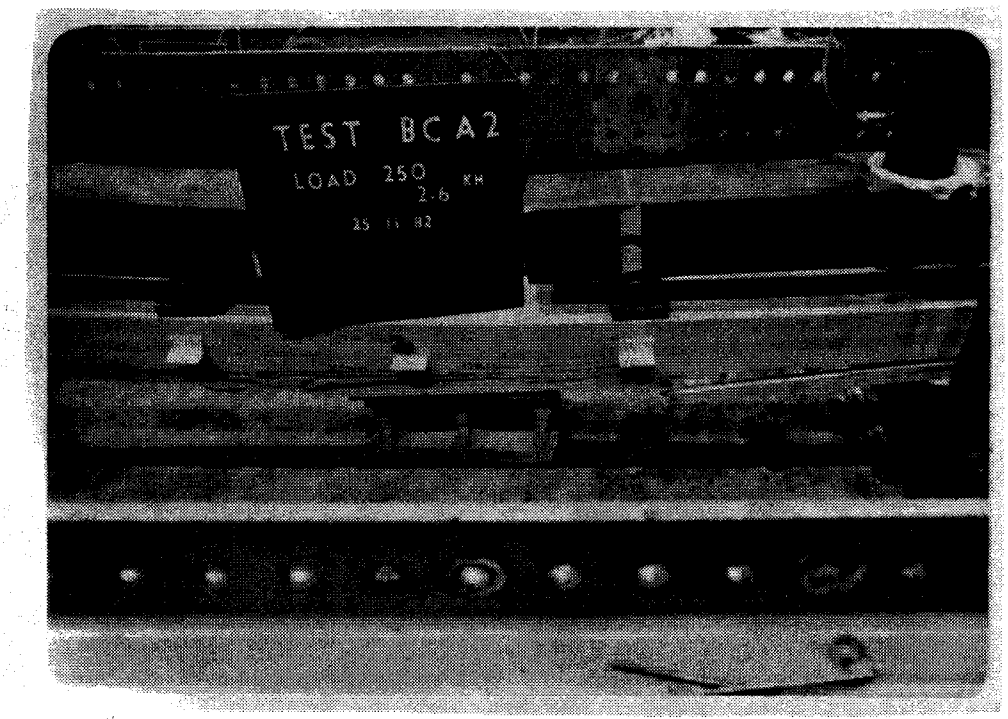

(b)

Plate 5.2 Failure of Specimen BCA2

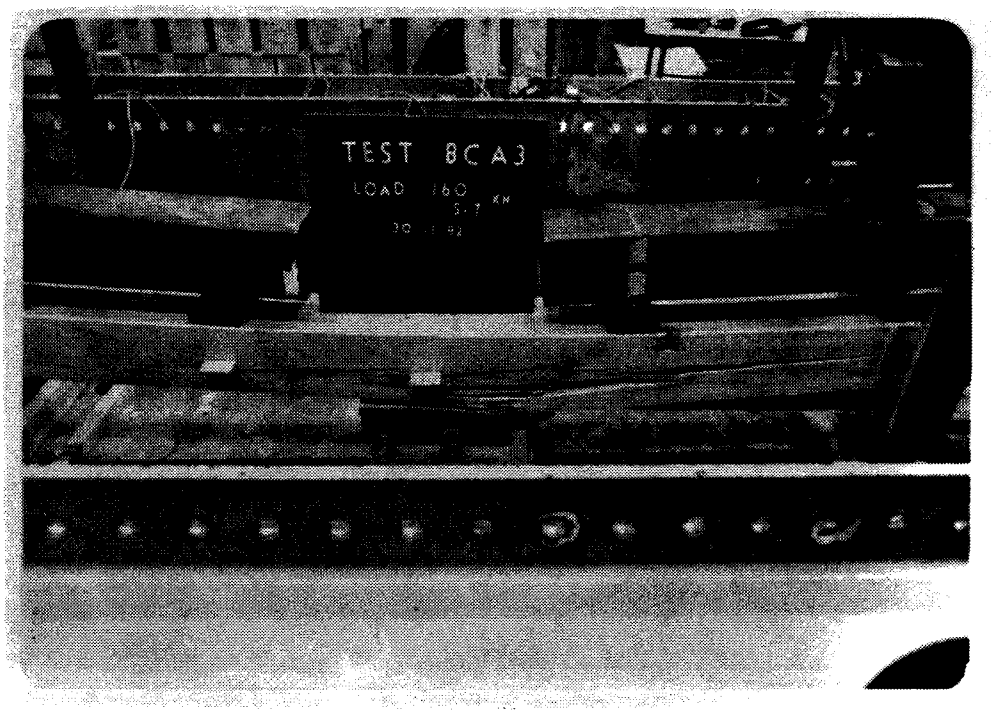

(a)

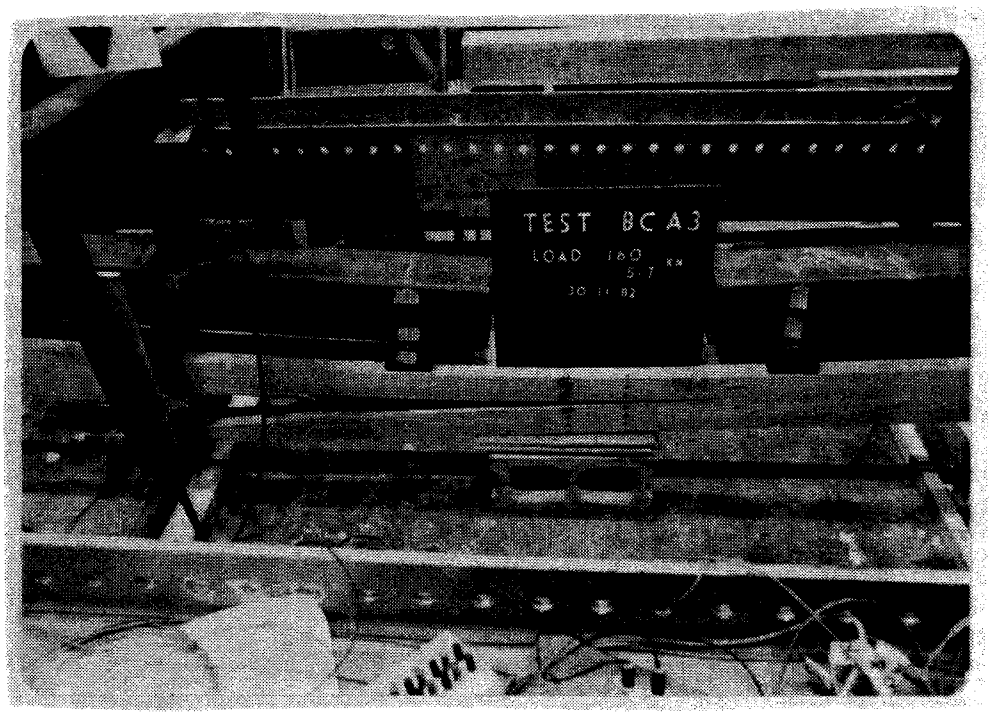

(b)

Plate 5.3 Failure of Specimen BCA3

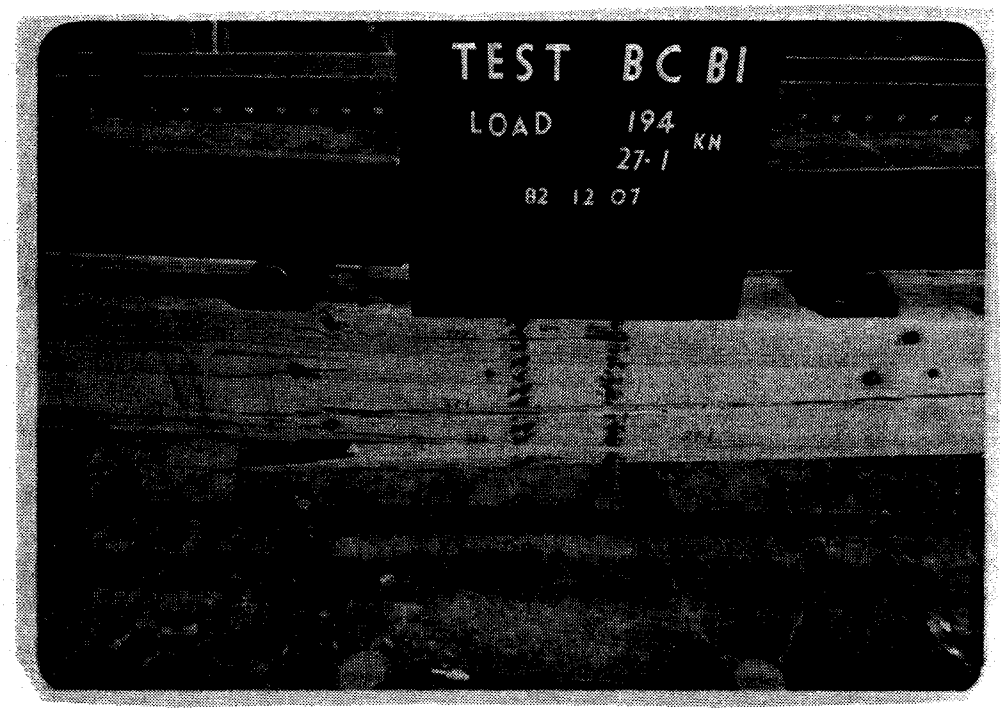

(a)

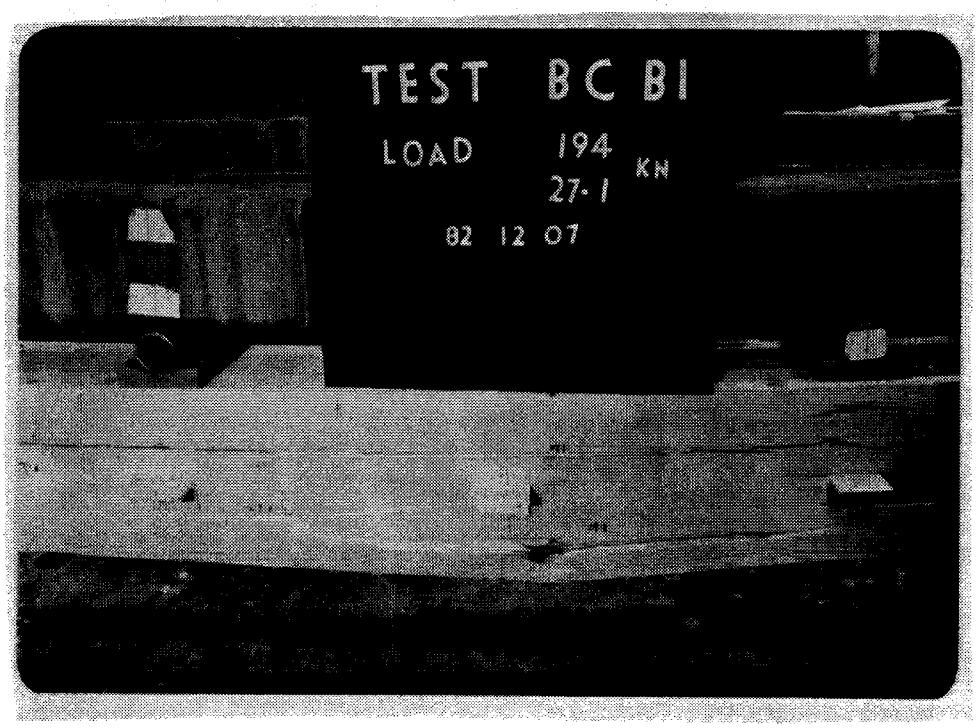

(b)

Plate 5.4 Failure of Specimen BCB1

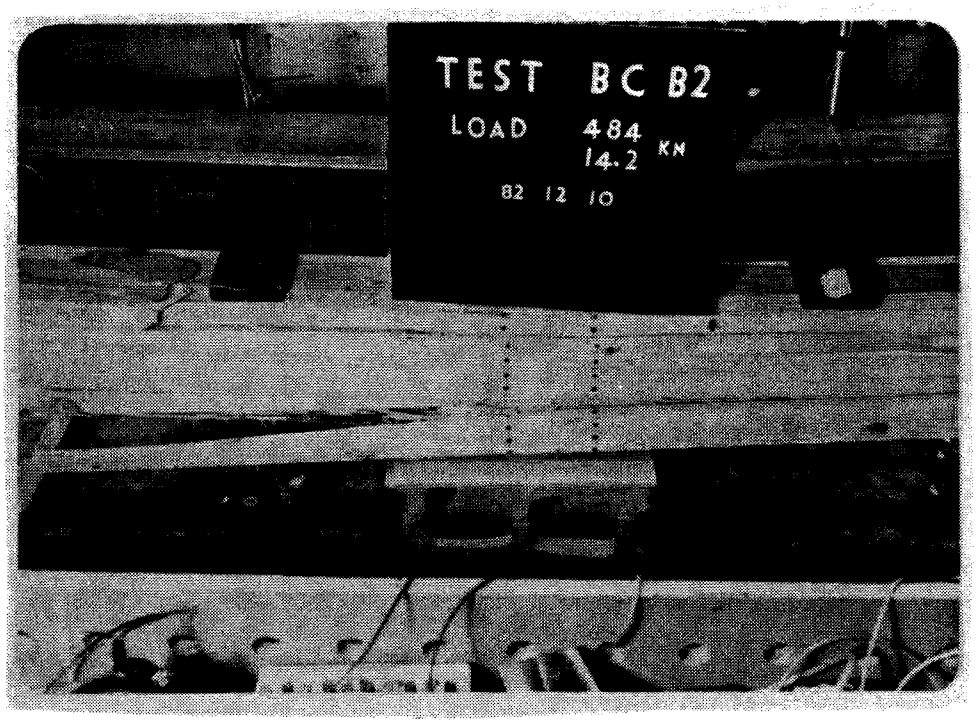

(a)

(b)

Plate 5.5 Failure of Specimen BCB2

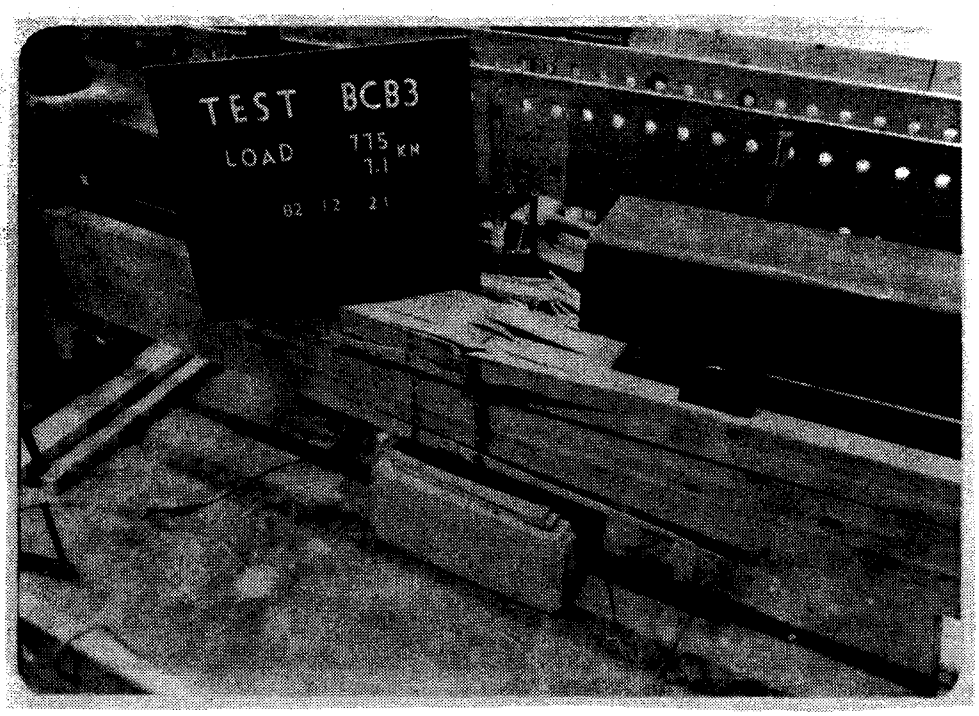

(a)

(b)

Plate 5.6 Failure of Specimen BCB3

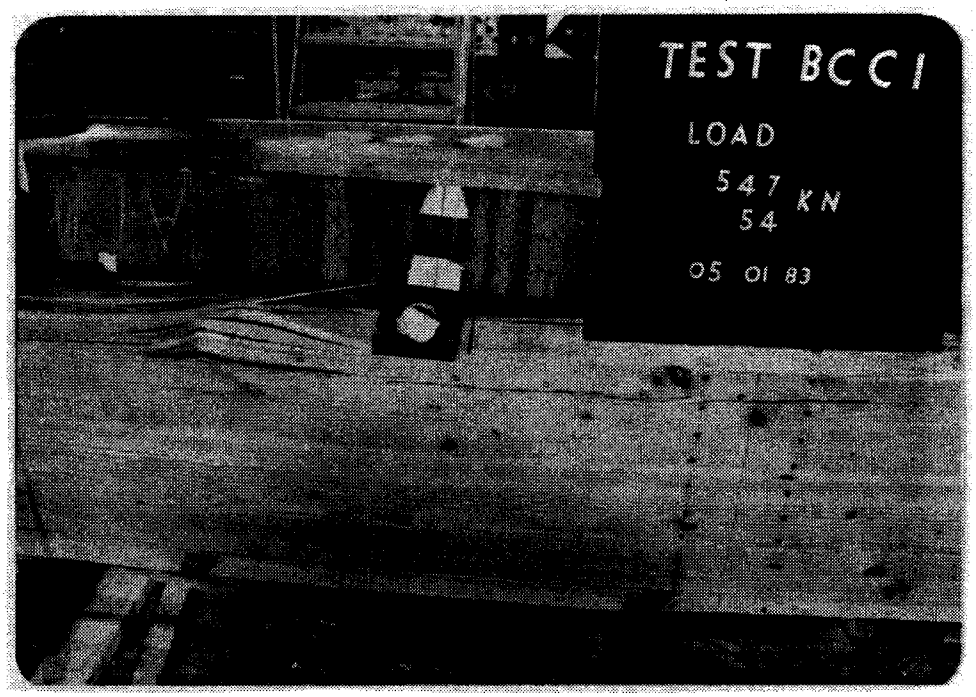

(a)

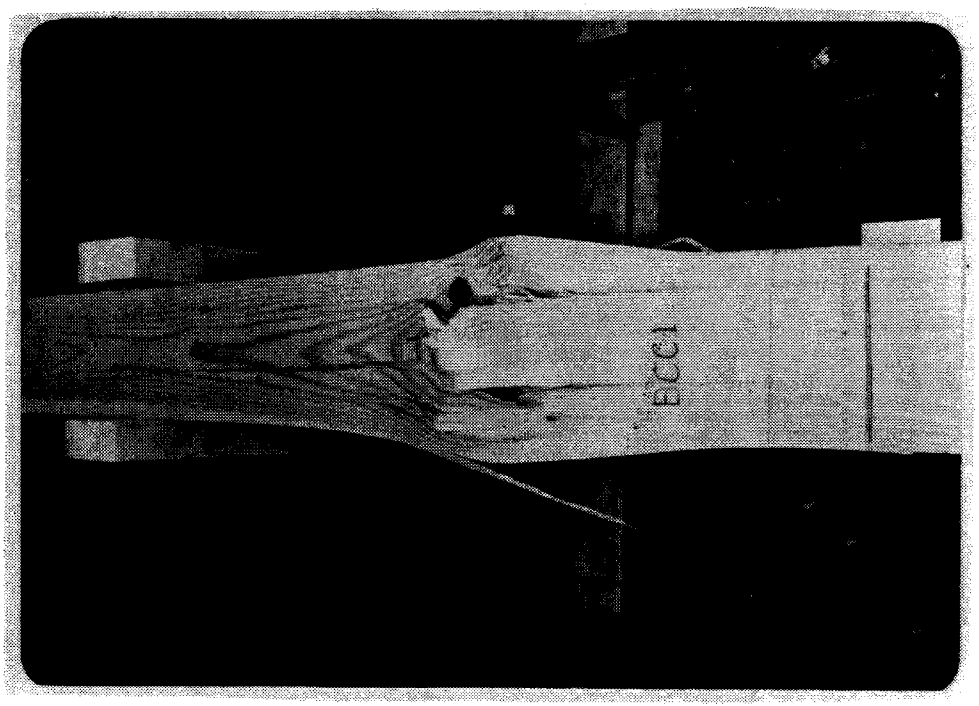

(b)

Plate 5.7 Failure of Specimen BCC1

(a)

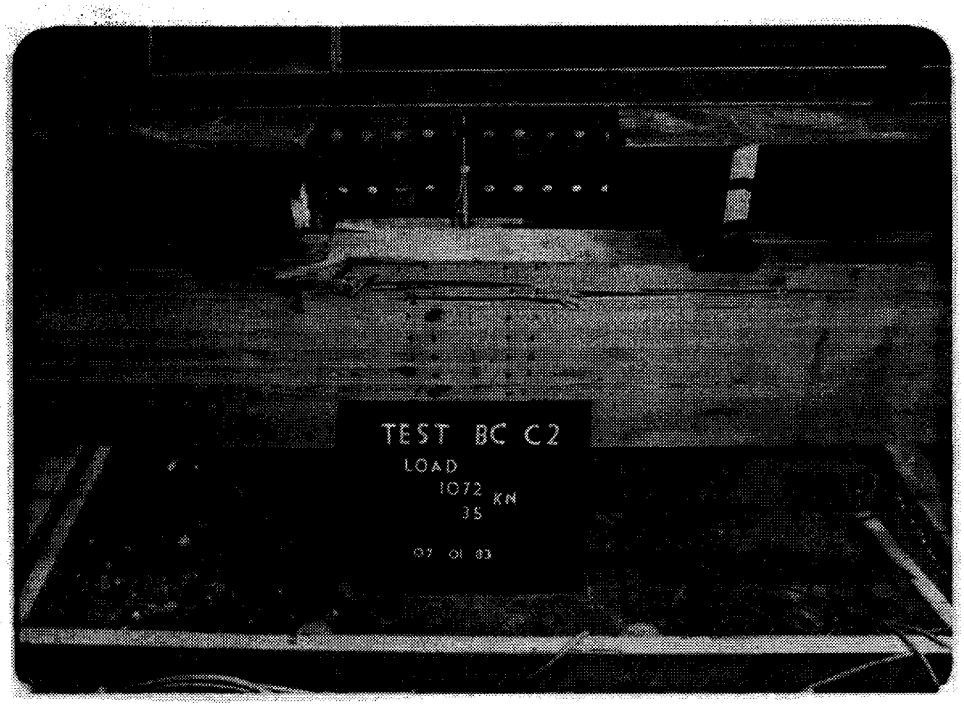

(b)

Plate 5.8 Failure of Specimen BCC2

(a)

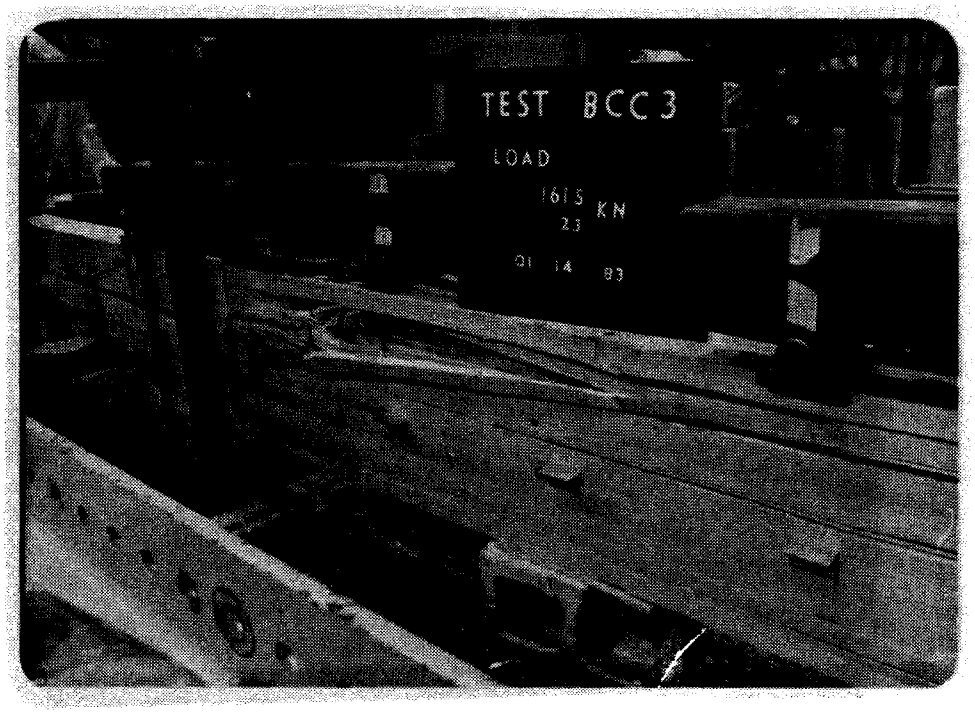

(b)

Plate 5.9 Failure of Specimen BCC3

6. CONCLUSIONS AND RECOMMENDATIONS

6.1 Observations and Conclusions

The following are the results of the theoretical and experimental investigation of timber beam-columns reported herein:

1. The theoretical interaction curves relating the bending moment,M, and the compressive axial force, P, depend on the amount of plasticity in the compression zone and the tension strain at failure.
2. The theoretical prediction based on sine wave deflected shape of beam-column gives the highest values of moments. The moment magnifier approach gives the smallest moment values. The Newmark's numerical integration method gives moment values intermediate between the other two methods.
3. The value of the tensile strain at failure is dependent on the type of material and the magnitude of the applied axial load.
4. The interaction curves obtained from the Newmark's numerical analysis pocedure and modified by an undercapacity factor of 0.7 are in good correlation with the test results.
5. The moment magnifier approach has potential as a design method if used with an appropriate undercapacity factor.
6. Insufficient specimens were tested to provide statistically significant data. The present program must

be viewed as a pilot study.

6.2 Recommendations for Further Study

The following recommendations should be considered in further investigations into the ultimate strength behaviour of timber beam-columns:

1. A number of tests should be conducted at each axial load level for each slenderness ratio.
2. A larger number of small-scale specimens, more closely related to each beam-column specimen should be tested in order to better define the material properties of each beam-column specimen.
3. During fabrication, care should be taken to ensure that obvious defects are not located at critical sections and in critical laminations.
4. The use of electrical resistance strain gauges to measure compression and tension strains should be considered.

References

1. CAN3-086-M80 Code for Engineering Design in Wood. Canadian Standards Association, Rexdale, Ontario, 1980.
2. Pearson, R.G. The Strength of Solid Timber Columns. Australian Journal of Applied Science, Vol. 5, No. 4, 1954, pp.363-403.
3. Wood, L.W. Formulae for Columns with Side Loads and Eccentricity. Report No. 1782, US Department of Agriculture, Forest Service, Forest Products Laboratory, Madison, Wisconsin, 1961.
4. Galambos, T.V. Structural Members and Frames. Prentice Hall, New York, 1968.
5. Hammond, W.C., Curtis, J.O., Sidebottom, O.M. and Jones, B.A.(Jr.) Collapse Loads of Wooden Columns with Various Eccentricities and End Restraints. Transactions, American Society of Agricultural Engineers, Vol. 13, No. 6, 1970, pp. 737-742.
6. Zakic, D.B. Inelastic Bending of Wood Beams. Journal of the Structural Division, American Society of Civil Engineers, Vol. 99, No. ST10, October, 1973, pp. 2079-2095.
7. Gurfinkel, G. Wood Engineering. Southern Forest Products Association, New Orleans, Lousiana, 1973.
8. Chen, W.F. and Atsuta, T. Theory of Beam Columns. Vol. 1. McGraw-Hill Book Company, 1976.

9. Zakic, D.B. Inelastic Behaviour of Wood Beam Columns. Journal of the Structural Division, American Society of Civil Engineers, Vol. 105, No. ST7, July, 1979, pp. 1347-1363.

10. Larsen, H.J. and Theilgaard, E. Laterally Loaded Timber Columns. Journal of the Structural Division, American Society of Civil Engineers, Vol. 105, No. ST7, July, 1979, pp. 1347-1363.

11. Malhotra, S.K. Analysis and Design of Timber Columns Subjected to Eccentric Loads. Proceedings, Canadian Society of Civil Engineering Annual Conference, May, 1982, pp. 117-132.

12. CSA Standard 0122-M1980. Structural Glued-Laminated Timber. Canadian Standards Association, Rexdale, Ontario, 1980.

13. CSA Standard 0177-M1981. Qualification Code for Manufacturers of Structural Glued-Laminated Timber. Canadian Standards Association, Rexdale, Ontario, 1981.

14. ASTM Standard D-198. Static Tests of Timbers. American Society for Testing and Materials, Philadelphia, Pa, 1982.

Appendix A - Program Listings

Appendix A1

Method 1

```
      C*************************************************
      C      THIS PROGRAMME COMPUTES INTERACTION DIAGRAM
      C      FOR WOOD BEAM-COLUMNS GIVEN VARIOUS MATERIAL
      C      PROPERTIES USING A SINGLE EQUATION.
      C      IT ALSO PLOTS THE OUTPUT.
      C*************************************************
            DIMENSION POVPY(40),EMOVMY(40)
      C
      C...PRINT TITLE AND READ INPUTS
            WRITE(6,2000)
            J=1
          1 READ(5,1000,END=999)ELOVD,ALPHA,EUC,EUT,FRAC
            M=0
            EYC=ALPHA*EUC
            ET=FRAC*EUT
            SRLIM=ET/EYC
      C
      C...PRINT PARAMETERS AND TABLE HEADS
            WRITE(6,2100)ELOVD,ALPHA,EUC,ET,SRLIM
            WRITE(6,2200)
      C
      C..COMPUTE THE DIFFERENT LOADS
            IF(ELOVD.LE.0.)GO TO 1
            PI=3.141593
            PISQ=PI**2
            ND=1
      C
      C...COMPUTE P/PY,SIGT/SIG.UC,MO/MY
         10 DO 100 I=5,105,5
            POVPY(ND)=FLOAT(I-5)/100.
            IF(POVPY(ND).EQ.1.)POVPY(ND)=0.999
            A=(1.-POVPY(ND))
            BE=2.*A*ALPHA-2.*ALPHA
            DISC=BE**2+4.*ALPHA*(2.*A-ALPHA)
            IF(DISC.LT.0.) GO TO 100
            DE=SQRT(DISC)
            SR=(BE+DE)/(2.*ALPHA)
            IF(SR.GT.SRLIM)SR=SRLIM
      C...CALCULATE MO/MY
            EMOVMY(ND)=3.*A-4.*A**2/(1.+SR)-(1.+SR)**2/(4.*A)
           **POVPY(ND)*12.*EUC*ALPHA*(ELOVD**2)/PISQ
      C
      C...OUTPUTTHE RESULTS
            IF(EMOVMY(ND).LT.0.)GO TO 150
            WRITE(6,2300)POVPY(ND),SR,EMOVMY(ND)
            ND=ND+1
        100 CONTINUE
            GO TO 200
        120 IF(POVPY(ND).LT.0.)GO TO 998
        150 POVPY(ND)=POVPY(ND)-0.001
            A=1.-POVPY(ND)
            BE=2.*A*ALPHA-2.*ALPHA
            DISC=BE**2+4.*ALPHA*(2.*A-ALPHA)
            IF(DISC.LT.0.) GO TO 999
            DE=SQRT(DISC)
            SR=(BE+DE)/(2.*ALPHA)
            IF(SR.GT.SRLIM)SR=SRLIM
      C...CALCULATE MO/MY
           !EMOVMY(ND)=3.*A-4.*A**2/(1.+SR)-(1.+SR)**2/(4.*A)
           **POVPY(ND)*12.*EUC*ALPHA*(ELOVD**2)/PISQ
            IF(POVPY(ND).LT.0.)GO TO 200
      C
      C...OUTPUT THE RESULTS
        180 WRITE(6,2300)POVPY(ND),SR,EMOVMY(ND)


        200 CALL PLOTIT(EMOVMY,POVPY,ND,J,1,1,3,0.0,0.25,
           *5.,0.,0.15,8.,6)
            J=J+1
      C...GO TO READ FRESH INPUTS
            GO TO 1
        998 WRITE(6,2400)POVPY(ND),EMOVMY(ND)
        999 J=0
            CALL PLOTIT(EMOVMY,POVPY,ND,J,1,1,3,0.0,0.25,
           *5.,0.,0.15,8.,6)
            STOP
      C
      C...
      C...FORMAT STATEMENTS
       1000 FORMAT(6F10.5)
       2000 FORMAT(///,23X,'INTERACTION CALCULATIONS FOR  WOOD'//
           *23X,'BEAM-COLUMNS- RECTANGULAR SECTIONS'//
           *34X,'WINTER1A'//
           *23X,'**********************************')
       2100 FORMAT(///10X,'L/D= ',F8.5,5X,'ALPHA= ',F8.5,//10X,'EUC= ',
           *F8.5,5X,'ET= ',F8.5,5X,'SRLIM= ',F8.5//)
       2200 FORMAT(10X,'P/PY',10X,'SIG.T/SIG.UC',9X,'MO/MY'//)
       2300 FORMAT(10X,F5.3,12X,F6.4,11X,F7.4//)
       2400 FORMAT(//10X,'NEGATIVE VALUE OF P/PY =',F10.6,
           *'AND M/MY = ',F10.6/)
            STOP
            END
End of file
```

Appendix A2

Method 2

```
C*****************************************************************
C...THIS PROGRAMME CALCULATES THE ULTIMATE STRENGTH OF TIMBER
C   BEAM-COLUMNS BY NEWMARK'S PROCEDURE. IT IS THE LATEST VERSION
C   OF WINTER4, MODIFIED FOR A FOUR POINT LATERAL LOADING SYSTEM.
C   IT CALCULATES THE FINAL DEFLECTION TO 5 PERCENT ACCURACY.
C
C
C
C
C
C*****************************************************************
C
      INTEGER C,Q,V
      COMMON W(10),WO(10),EMOMY(10),EMOMYT(10),PDEL(10),PHOPHY(10),
     *SLOPE(10),R(10),EY,ELOVD,POVPY,A,PHUPHY,EQOOY,EMOPY(10),
     *EMOVP(10),V,EMYOPY,NN,EMUT,EMOMYM(40),THETAO(40),POVPYM,JJ
      WRITE(6,2000)

      READ(5,950)(R(I),I=1,9)
    5 READ(5,900,END=999)ELOVD,ALPHA,EUC,EUT,FRAC
      EY=ALPHA*EUC
      ET=FRAC*EUT
      SRLIM=ET/EUC
      WRITE(6,2100)ELOVD,ALPHA,EY,EUC,ET,SRLIM
C
C
C...CALCULATE PURE AXIAL CAPACITY FROM COLN. CURVE
C
      CALL STAR
C
      CALL AXCAP
C
      CALL STAR
C
C     CALL PLOTIT(THETAO,EMOMYM,ND,NP,1,1,3,0.,  ,5.,0.,  ,8.,6)
C
   10 READ(5,1000,END=999)POVPY
C
C...CHECK FOR ANOTHER L/D FOR CONSIDERATION --- NEG. P/PY
C
      IF(POVPY.LT.0.)GO TO 5
C
   15 NP=NP+1
      OPCT=0.
      A=1.-POVPY
      BE=2.*A*ALPHA-2.*ALPHA
      DISC=BE**2+4.*ALPHA*(2.*A-ALPHA)
      IF(DISC.LT.0.)WRITE(6,2800)
      DE=SORT(DISC)
      SR=(BE+DE)/(2.*ALPHA)
      SRLIM=ET/EY
      IF(SR.GT.SRLIM)SR=SRLIM
      AOVD=(EUC*(1.-ALPHA))/(EUC+ET)
      PHUPHY=(1.+SR)/(2*(1.-AOVD))
      EMUT=3.*A-(2.*(A)**1.5)/SORT(PHUPHY)
      EMYOPY=1./(6.*ELOVD)
C...INITIALISE VARIOUS COUNTERS
      L=1
      M=0
      C=0
      V=0
      NP=0
      II=1
      JJ=1
      ND=0
      CALL STAR
C
      WRITE(6,2150)
C
C.. CALCULATE ASSUMED MOMENT
C
   20 CALL MOMENT
C
C...CHECK IF IN FINER M/MY SECTION
C
      IF(C.GT.0)GO TO 550
C
   30 CALL ELADEF
C..
C.. CALCULATE THE PDELTA EFFECT  AND ADD THE EFFECT
C
   50 DO 70 I=1,9
      PDEL(I)=POVPY*WO(I)/EMYOPY
      EMOMYT(I)=EMOMY(I)+PDEL(I)
   70 CONTINUE
C
C...CALCULATE PHI AND DEFLECTION FROM M-P-O RELATIONS
C
      CALL PHIDEF
C
C...CORRECT THE DEFLECTIONS
C
       CALL CORDEF
C
      L=L+1
C
C...CHECK IF CONVERGENCE
C
      TOLER=0.
      DO 100 J=2,8
      IF(WO(J).EQ.0)GO TO 100
      DIF=ABS(W(J)-WO(J))
      OPCT=DIF/WO(J)
  100 TOLER=TOLER+ABS(OPCT)
      IF(TOLER.LE.0.210.OR.L.GT.5)GO TO 300
C
C...CHECK IF MAXIMUM CURVATURE EXCEEDED
      IF(PHOPHY(NN).GT.PHUPHY)GO TO 500
C
C...OTHERWISE USE NEW DEFLECTION ESTIMATE
C
      DO 200 K=1,9
  200 WO(K)=W(K)
```

```
114             OPCT=0.
115             GO TO 50
116         300 IF (TOLER.LE.0.210)GO TO 400
117             CALL STAR
118             WRITE(6,2200)EMOMY(5)
119             CALL STAR
120     C
121     C...CHECK IF MAX. M/MY(AT POINT 5) IS LESS THAN 0.10
122             IF(EMOMY(5).LT.0.1)GO TO 10
123             IF(C.GT.0) GO TO 10
124             GO TO 500
125     C...CALCULATE THETAO FOR CONVERGENCE ACCORDING TO CHEN AND ATSUTA
126         400 THETAO(II)=4.*W(3)
127             NIT=L-1
128             EMOMYM(II)=EMOMY(5)
129             WRITE(6,2300)POVPY,NIT,EMOMYM(II),THETAO(II),TOLER
130     C
131     C..CHECK FOR NEGATIVE THETAO
132     C
133             IF (THETAO(II).LT.0.)GO TO 10
134     C
135         450 ND=ND+1
136             II=II+1
137             IF(EMOMY(5).GE.EMUT)WRITE(6,2500)EMUT
138             IF(EMOMY(5).GT.EMUT)GO TO 10
139     C
140     C...REPEAT CALCULATION FOR OTHER M/MY VALUES
141     C
142             IF(C.GT.0)GO TO 550
143     C...REINITIALISE COUNTER
144             L=1
145             OPCT=0.
146             GO TO 20
147     C
148     C...USE FINER FRACTIONS OF M/MY BEFORE DIVERGENCE
149     C...REINITIALISE COUNTER AGAIN
150     C...CHECK IF MAX. M/MY IS LESS THAN 0.1
151     C
152         500 IF(EMOMY(5).LT.0.1)GO TO 10
153             IF(C.GT.0)GO TO 550
154             L=1
155     C
156     C...TAKE BACK MOMENT CALCULATION ONE STEP
157     C
158             V=V-4
159             C=C+1
160             GO TO 20
161         550 DO 600 Q=1,9
162             EMOMY(Q)=EMOMY(Q)+0.01
163             IF(EMOMY(Q).LT.0.)GO TO 10
164         600 CONTINUE
165     C
166     C...CONITNUE FOR ANOTHER SET OF ITERATIONS IN FINER FRACTIONS
167     C
168
169             C=C+1
170             IF(C.GE.10)GO TO 10
171             OPCT=0.
172             GO TO 30
173     C
174     C...FORMAT STATEMENTS
175     C
176           900 FORMAT(5F10.5)
177           950 FORMAT(10F8.6)
178          1000 FORMAT(F10.5)
179          2000 FORMAT(25X,'WOOD ULTIMATE STRENGTH  BY',
180                *'NEWMARKS METHOD  -  WINTER4C',///)
181
182          2100 FORMAT (//10X,'L/D= ',F10.3,5X,'ALPHA= ',F10.5,5X,'EY= ',
183                *F10.5,//10X,'EUC= ',F10.5,5X,'ET= ',F10.5,5X,'SRLIM= ',F10.5)
184          2150 FORMAT(//10X,'P/PY',10X,'NIT',10X,'M/MY',10X,'THETAO',
185                *10X,'TOLERANCE')
186          2200 FORMAT(12X,'DIVERGENCE OF DEFLS. AFTER 5 ITERATIONS',
187                *'AT MAX. M/MY= ',F7.4)
188          2300 FORMAT(/10X,F4.3,10X,I3,9X,F5.3,8X,F10.8,9X,F6.4)
189          2500 FORMAT(/'**********MO IS GREATER THAN ULTIMATE,MUL = ',F10.7)
190          2600 FORMAT(/'***********NEGATIVE DISC. IN SIGT/SIGUC')
191           999 STOP
192               END
193     C
194     C*****************************************************************
195     C...SUBROUTINE TO CALCULATE PURE AXIAL CAPACITY FROM COLN CURVE
196     C*****************************************************************
197               SUBROUTINE AXCAP
198               INTEGER C,Q,V
199               COMMON W(10),WO(10),EMOMY(10),EMOMYT(10),PDEL(10),PHOPHY(10),
200              *SLOPE(10),R(10),EY,ELOVD,POVPY,A,PHUPHY,EODOY,EMOPY(10),
201              *EMOVP(10),V,EMYOPY,NN,EMUT,EMOMYM(40),THETAO(40),POVPYM,JJ
202     C
203     C... ENTER L/D VALUE SEPARATING SHORT FROM LONG  COLUMN
204     C.. .NOTE THE ASUMPTION OF SIGUC=SIGY IN CALCULATION
205     C
206               SUOVSY=1.00
207               K=21
208     C
209     C...CHECK SLENDERNESS RANGE
210     C
211               IF(ELOVD.LE.K)GO TO 100
212               POVPYM=3.141593**2/(12.*ELOVD**2*EY)
213               GO TO 200
214           100 POVPYM=SUOVSY*(1.-(ELOVD/K)**4/3.)
215     C
216           200 WRITE(6,1000)ELOVD,POVPYM
217
218          1000 FORMAT(//'*********FOR L/D= ',F6.3,'   MAX. AXIAL STRENGTH',
219                *' RATIO, PU/PY= ',F6.3//)
220               RETURN
221               END
222     C
223     C*************************************************************
224     C...SUBROUTINE TO CALCULATE MOMENT FOR ALL SEGMENTS
225     C*************************************************************
226               SUBROUTINE MOMENT
```

```
      INTEGER C,Q,V
      COMMON W(10),WO(10),EMOMY(10),EMOMYT(10),PDEL(10),PHOPHY(10),
     *SLOPE(10),R(10),EY,ELOVD,POVPY,A,PHUPHY,EOOOY,EMOPY(10),
     *EMOVP(10),V,EMYOPY,NN,EMUT,EMOMYM(40),THETAO(40),POVPYM,JJ
      V=V+2
      EOOOY=FLOAT(V-2)/10000.
      DO 100 I=1,9
      EMOMY(I)=6.*R(I)*EOOOY*ELOVD
      EMOPY(I)=EMOMY(I)*EMYOPY
      IF (EMOMY(I).LT.0.)GO TO 999
  100 CONTINUE

      RETURN
  999 WRITE(6,1000)
 1000 FORMAT(//10X,'NEGATIVE MOMENT VALUE')
      RETURN
      END
C
C
C*************************************************************
C... SUBROUTINE  TO CALCULATE ESTIMATED DEFLECTION - ELASTIC
C*************************************************************
      SUBROUTINE ELADEF
      INTEGER C,Q,V
      COMMON W(10),WO(10),EMOMY(10),EMOMYT(10),PDEL(10),PHOPHY(10),
     *SLOPE(10),R(10),EY,ELOVD,POVPY,A,PHUPHY,EOOOY,EMOPY(10),
     *EMOVP(10),V,EMYOPY,NN,EMUT,EMOMYM(40),THETAO(40),POVPYM,JJ
C
C.. CALCULATE DEFLECTION USING EIGHT DIVISIONS
C
      THETA=SQRT(POVPY*12.*EY)*ELOVD

      DO 100 I=1,9
      EMOVP(I)=EMOPY(I)/POVPY
      BETA=FLOAT(I-1)*THETA/8.
      WO(I)=EMOVP(I)*(((1.-COS(THETA))/SIN(THETA))*SIN(BETA)
     *+COS(BETA)-1.)
  100 CONTINUE
      RETURN
      END
C
C*********************************************************************
C... SUBROUTINE TO CALCULATE CURVATURE AND DEFLECTION FROM M-P-O RELATIONS
C*********************************************************************
      SUBROUTINE PHIDEF
      INTEGER C,Q,V
      COMMON W(10),WO(10),EMOMY(10),EMOMYT(10),PDEL(10),PHOPHY(10),
     *SLOPE(10),R(10),EY,ELOVD,POVPY,A,PHUPHY,EOOOY,EMOPY(10),
     *EMOVP(10),V,EMYOPY,NN,EMUT,EMOMYM(40),THETAO(40),POVPYM,JJ
C
C...CALCULATE VARIOUS CURVATURES
C
      DO 100 NN=1,9
      B=3.*A-EMOMYT(NN)
      IF (B.EQ.0.) GO TO 100
      PHOPHY(NN)=(4.*A**3)/(3.*A-EMOMYT(NN))**2
      IF(PHOPHY(NN).GE.0..AND.PHOPHY(NN).LE.A)PHOPHY(NN)=EMOMYT(NN)
      IF(PHOPHY(NN).GT.PHUPHY)GO TO 400
  100 CONTINUE
C
C...CALCULATE SLOPES
C
      SLOPE(1)=PHOPHY(1)
      DO 200 J=2,9
      M=J-1
      SLOPE(J)=SLOPE(M)+PHOPHY(J)
  200 CONTINUE
C...CALCULATE DEFLECTION ESTIMATES
      W(1)=0.
      DO 300 K=2,9
      L=K-1
      W(K)=W(L)+SLOPE(L)
  300 CONTINUE
      RETURN
  400 IF(JJ.GT.2)RETURN

      WRITE(6,2000)EMOMY(5),EMUT
      JJ=JJ+1
 2000 FORMAT(//10X,'MAX. CURVATURE EXCEEDED AT   ',
     *' M/MY= ',F7.4,'; BUT ULT. MOMENT= ',F7.4)
      RETURN
      END
C
C*****************************************
C...SUBROUTINE TO CORRECT THE DEFLECTIONS
C*****************************************
C
      SUBROUTINE CORDEF
      INTEGER C,Q,V
      COMMON W(10),WO(10),EMOMY(10),EMOMYT(10),PDEL(10),PHOPHY(10),
     *SLOPE(10),R(10),EOOOY,ELOVD,EMOPY(10),
     *EMOVP(10),V,EMYOPY,NN,EMUT,EMOMYM(40),THETAO(40),POVPYM,JJ
      ERRT=W(9)
C
C.. APPLY CORRECTION APPROPRIATELY
C
      DO 100 I=1,9
      W(I)=-(W(I)-FLOAT(I-1)/8.*ERRT)
C
C.. CONVERT TO DEFLECTIONS IN TERMS OF L
C
      W(I)=W(I)*2.*EY*ELOVD/(64.)
  100 CONTINUE

      RETURN
      END
C
C**********************
      SUBROUTINE STAR
C**********************
C
      WRITE(6,2000)
 2000 FORMAT(//5X,'*********************************************',
```

```
     340           *'*************************************************************',
     341           *'*************'//)
     342            RETURN
     343            END
End of file
```

Appendix A3

Method 3

```
      C...THIS IS THE MOMENT MAGNIFIER VERSION OF THE
      C    INTERRACTION DIAGRAM(METHOD 3).
      C
      C    IT CALLS PLOTIT TO PLOT THE INTERACTION DIAGRAM.
      C
      C
            DIMENSION POVPY(40),EMOVMY(40)
      C     REAL*8 TITLE(11)/'L/D=0.05','L/D=3','L/D=5','L/D=8','L/D=10',
      C    *'L/D=12','L/D=15','L/D=18','L/D=20','L/D=23','L/D=25'/
      C       READ(5,500)(TITLES(I),I=1,12)
      C       READ(5,500)(TITLES(I),I=13,16)
      C       READ(5,500)(TITLES(I),I=17,20)
      C  500 FORMAT(12A4)
      C...PRINT TITLE AND READ INPUTS
            WRITE(6,2000)
            J=1
          1 READ(5,1000,END=999)ELOVD,ALPHA,EUC
            M=0
            EYC=ALPHA*EUC
      C
      C...PRINT PARAMETERS AND TABLE HEADS
            WRITE(6,2100)ELOVD,ALPHA,EUC
            WRITE(6,2200)
      C
      C..COMPUTE THE DIFFERENT LOADS
            IF(ELOVD.LE.0.)GO TO 1
            PI=3.141593
            PISQ=PI**2
            ND=1
      C
      C
         10 DO 100 I=5,105,5
            POVPY(ND)=FLOAT(I-5)/100.
      C...CALCULATE MO/MY
            POVPE=POVPY(ND)*12.*EUC*ALPHA*(ELOVD**2)/PISQ
            EMOVMY(ND)=(1.-POVPE)*(1.-POVPY(ND))
      C
      C...OUTPUTTHE RESULTS
      
            IF(EMOVMY(ND).LT.0.)GO TO 150
            WRITE(6,2300)POVPY(ND),EMOVMY(ND)
            ND=ND+1
        100 CONTINUE
        120 IF(POVPY(ND).LT.0.)GO TO 200
        150 POVPY(ND)=POVPY(ND)-0.001
      C...CALCULATE MO/MY
            EMOVMY(ND)=(1.-POVPE)*(1.-POVPY(ND))
            IF (EMOVMY(ND).LT.0.)GO TO 200
      C
      C...OUTPUT THE RESULTS
      C
        160 WRITE(6,2300)POVPY(ND),EMOVMY(ND)
      C 200 CALL CGPL(EMOVMY,POVPY,EMOVMY,ND,J,1,1,3,0,0.0,0.25,
      C     *5.0,0.0,0.15,8.,TITLES,6)
        200 CALL PLOTIT(EMOVMY,POVPY,ND,J,1,1,3,0.0,0.25,
           *5.,0.,0.15,8.,6)
      C       CALL CGPEPS(0.0,0.0,TITLE(J),8,0.1,0.75)
            J=J+1
      C...GO TO READ FRESH INPUTS
      C     GO TO 1
        998 WRITE(6,2400)POVPY(ND),EMOVMY(ND)
        999 J=0
            CALL PLOTIT(EMOVMY,POVPY,ND,J,1,1,3,0.0,0.25,
           *5.0,0.0,0.15,8.,6)
      C  999 CALL CGPL(EMOVMY,POVPY,EMOVMY,ND,0,1,1,5,0,1.0,2.0,
      C     *20.,0.,1.,20.,6)
            STOP
      C
      C...
      C...FORMAT STATEMENTS
         1000 FORMAT(3F10.5)
         2000 FORMAT(///,23X,'INTERACTION CALCULATIONS FOR  WOOD'//
           *23X,'BEAM-COLUMNS- RECTANGULAR SECTIONS'//
           *34X,'WINTERS(METHOD 3)'//
           *23X,'**********************************')
         2100 FORMAT(///10X,'L/D= ',F8.5,5X,'ALPHA= ',F8.5,//10X,'EUC= ',
           *F8.5//)
         2200 FORMAT(10X,'P/PY',10X,'MO/MY'//)
         2300 FORMAT(10X,F5.3,12X,F6.4,11X,F7.4//)
         2400 FORMAT(//10X,'NEGATIVE VALUE....  P/PY =',F10.4,
           *'AND M/MY = ',F8.4//)
            STOP
            END
End of file
```

Index

RECENT STRUCTURAL ENGINEERING REPORTS

Department of Civil Engineering

University of Alberta

81. *Tests of Wall Segments from Reactor Containments* by S.H. Simmonds, S.K. Rizkalla and J.G. MacGregor, October 1979.

82. *Cracking of Reinforced and Prestressed Concrete Wall Segments* by J.G. MacGregor, S.K. Rizkalla and S.H. Simmonds, October 1979.

83. *Inelastic Behavior of Multistory Steel Frames* by M. El Zanaty, D.W. Murray and R. Bjorhovde, April 1980.

84. *Finite Element Programs for Frame Analysis* by M. El Zanaty and D.W. Murray, April 1980.

85. *Test of a Prestressed Concrete Secondary Containment Structure* by J.G. MacGregor, S.H. Simmonds and S.H. Rizkalla, April 1980.

86. *An Inelastic Analysis of the Gentilly-2 Secondary Containment Structure* by D.W. Murray, C. Wong, S.H. Simmonds and J.G. MacGregor, April 1980.

87. *Nonlinear Analysis of Axisymmetric Reinforced Concrete Structures* by A.A. Elwi and D.W. Murray, May 1980.

88. *Behavior of Prestressed Concrete Containment Structures - A Summary of Findings* by J.G. MacGregor, D.W. Murray, S.H. Simmonds, April 1980.

89. *Deflection of Composite Beams at Service Load* by L. Samantaraya and J. Longworth, June 1980.

90. *Analysis and Design of Stub-Girders* by T.J.E. Zimmerman and R. Bjorhovde, August 1980.

91. *An Investigation of Reinforced Concrete Block Masonry Columns* by G.R. Sturgeon, J. Longworth and J. Warwaruk, September 1980.

92. *An Investigation of Concrete Masonry Wall and Concrete Slab Interaction* by R.M. Pacholok, J. Warwaruk and J. Longworth, October 1980.

93. *FEPARCS5 - A Finite Element Program for the Analysis of Axisymmetric Reinforced Concrete Structures - Users Manual* by A. Elwi and D.W. Murray, November 1980.

94. *Plastic Design of Reinforced Concrete Slabs* by D.M. Rogowsky and S.H. Simmonds, November 1980.

95. *Local Buckling of W Shapes Used as Columns, Beams, and Beam-Columns* by J.L. Dawe and G.L. Kulak, March 1981.

96. *Dynamic Response of Bridge Piers to Ice Forces* by E.W. Gordon and C.J. Montgomery, May 1981.

97. *Full-Scale Test of a Composite Truss* by R. Bjorhovde, June 1981.

98. *Design Methods for Steel Box-Girder Support Diaphragms* by R.J. Ramsay and R. Bjorhovde, July 1981.

99. *Behavior of Restrained Masonry Beams* by R. Lee, J. Longworth and J. Warwaruk, October 1981.

100. *Stiffened Plate Analysis by the Hybrid Stress Finite Element Method* by M.M. Hrabok and T.M. Hrudey, October 1981.

101. *Hybslab - A Finite Element Program for Stiffened Plate Analysis* by M.M. Hrabok and T.M. Hrudey, November 1981.

102. *Fatigue Strength of Trusses Made From Rectangular Hollow Sections* by R.B. Ogle and G.L. Kulak, November 1981.

103. *Local Buckling of Thin-Walled Tubular Steel Members* by M.J. Stephens, G.L. Kulak and C.J. Montgomery, February 1982.

104. *Test Methods for Evaluating Mechanical Properties of Waferboard: A Preliminary Study* by M. MacIntosh and J. Longworth, May 1982.

105. *Fatique Strength of Two Steel Details* by K.A. Baker and G.L. Kulak, October 1982.

106. *Designing Floor Systems for Dynamic Response* by C.M. Matthews, C.J. Montgomery and D.W. Murray, October 1982.

107. *Analysis of Steel Plate Shear Walls* by L. Jane Thorburn, G.L. Kulak, and C.J. Montgomery, May 1983.

108. *Analysis of Shells of Revolution* by N. Hernandez and S.H. Simmonds, August 1983.

109. *Tests of Reinforced Concrete Deep Beams* by D.M. Rogowsky, J.G. MacGregor and S.Y. Ong, September 1983.

110. *Shear Strength of Deep Reinforced Concrete Continuous Beams* by D.M. Rogowsky and J.G. MacGregor, September 1983.

111. *Drilled-In Inserts in Masonry Construction* by M.A. Hatzinikolas, R. Lee, J. Longworth and J. Warwaruk, October 1983.

112. *Ultimate Strength of Timber Beam Columns* by T.M. Olatunji and J. Longworth, November 1983.